TRANSLATIONAL CONTROL OF LIPID HOMEOSTASIS IN THE CELL CYCLE OF BUDDING YEAST

A Dissertation

by

NAIRITA MAITRA

Submitted to the Office of Graduate and Professional Studies of
Texas A&M University
in partial fulfillment of the requirements for the degree of

DOCTOR OF PHILOSOPHY

Chair of Committee,	Dorothy Shippen
Committee Members,	Michael Polymenis
	Hays Rye
	Vytas Bankaitis
Head of Department,	Jean-Philippe Pellois

May 2021

Major Subject: Biochemistry

Copyright 2021 Nairita Maitra

ABSTRACT

Proper coordination between cell growth and division relies heavily on several metabolic processes such as lipid metabolism. Lipids play indispensable roles both as key signaling molecules and in membrane biogenesis. Moreover, *de novo* lipid synthesis is essential to executing the faithful progression of cell cycle events. Our lab discovered that the translational efficiency of the critical lipogenic enzymes acetyl coenzyme A carboxylase (*ACC1*) and fatty acid synthase (*FAS*) peaked in mitosis. We also reported that the abundance of significant lipid species was higher late in the cell cycle. Overall, all the evidence suggested that lipid synthesis impinged on the later phases of the cell cycle. However, it is not known if and how lipid biogenesis can promote any specific cell cycle event.

In this thesis, I report that increased lipogenesis promotes nuclear division. I mutated inhibitory elements, upstream open reading frames (uORFs), in the 5' leaders of *ACC1* and *FAS1* of budding yeast. Translation of *ACC1* and *FAS1* is de-repressed in the absence of the uORFs. The protein level of Fas1p is elevated almost 4-fold, with no significant changes in the mRNA level. Furthermore, the uORF mutant produces more lipids and accelerates the nuclear division.

Accurate lipid trafficking is also vital for the proper timing of mitotic events. I used a temperature-sensitive mutant of Sec14p (*sec14-1*), a phosphatidylinositol transfer protein (PITP), to investigate the roles of lipid trafficking in the cell cycle. Even at the permissive temperature, *sec14-1* cells suffer from a perturbed cell cycle. The mutant

cells are bigger, grow slowly, and are delayed in the G2/M phase. Nuclear division is severely delayed in *sec14-1* cells. However, de-repressing the translation of *ACC1* and *FAS1* corrects the cell cycle phenotypes of *sec14-1* cells. These results provide a context to probe connections among membrane trafficking, lipogenesis, and cell division.

In summary, I have identified a unique gain-of-function mutant of fatty acid synthesis. My work shows that translational control of lipogenesis is a critical input in the cell cycle. It is not merely required for mitosis, but it can actively promote nuclear division, a key landmark of the eukaryotic cell cycle.

DEDICATION

I dedicate this thesis to my parents, Babita Maitra and Parag Kumar Maitra, who have always supported me incessantly and my 18-year-old self, who did not give up on the dream.

ACKNOWLEDGEMENTS

I want to thank my advisor, Dr. Michael Polymenis, for his mentorship and encouragement throughout my Ph.D. journey. I am grateful for the trust he showed in me and allowed me to be part of his research quest. He provided me with immense freedom to explore new things. I cannot thank him enough for his motivation, willingness to share his knowledge, patience with my "goofiness," and making his laboratory a nurturing environment for "budding" scientists. His productive feedback and guidance led me to reach the finish line of my Ph.D. journey.

I want to acknowledge Dr. Dorothy Shippen, Dr. Vytas Bankaitis, and Dr. Hays Rye for serving as my committee members and for all their insights and enriching my research with productive feedback. I am incredibly thankful to Dr. Bankaitis for sharing his expertise on the lipid projects and providing the required reagents and yeast strains. I would like to recognize Dr. Heidi Blank for her mentorship, advice, and guidance in my research. I have learned many things from her, starting from running a western gel to the nitty-gritty of yeast genetics. It helped me to broaden my scientific outlook. I want to thank Staci Hammer for all her contribution to my work and my lab-floor mates, Jasmine, Neha, and Ishita, for always having my back.

I will immensely be indebted to all my seniors and friends of the Bengali community in College Station, especially Isita di, Shyamalendu da, and Sagnika, for all their selfless help during these five years. They made the stay at College Station

enjoyable and comfortable. Special thanks to Sagnika for her dear friendship throughout my graduate career.

I want to acknowledge my parents Babita Maitra and Parag Kumar Maitra, for their unconditional love and support. They contributed to my growth, and I am grateful to have them in my life. My heartfelt thanks to Sayan, who has been by my side throughout the graduate school tenure, encouraged me, persisted that I moved forward, and always looking out for me. I am glad to find a life-long best friend in him.

Finally, I am grateful to all my close friends and loving family, classmates, and Biobio staff and advisors for their support and care. I want to thank everyone who touched my life with kindness and respect in my graduate school journey. Lastly, I want to thank all the frontline workers who have been risking their lives since last year to keep us safe. Hopefully, we can soon see the light at the end of this dark tunnel.

CONTRIBUTORS AND FUNDING SOURCES

Contributors

This work was supervised by a dissertation committee of Professor Michael Polymenis [advisor], Professor Dorothy Shippen, Professor Hays Rye of the Department of biochemistry and biophysics, and Professor Vytas Bankaitis of the Department of molecular and cellular medicine.

The study presented in Chapter 2 was done in collaboration with the laboratory group of Bankaitis Lab, with contributions from group members led by Kristin Baetz at the University of Ottawa; Brian Kennedy at Buck institute for research on aging; and Wenshe Liu at the Department of chemistry, Texas A&M University. Jin Huang, Carl J. Mousley, Louis Dacquay, and Michael Kennedy designed the genetic, transcriptomic, biochemical experiments. I designed and performed all the cell cycle experiments. Guillaume Drin and Neale D Ridgway carried out the lipid extraction and transfer assays. Chong He performed the replicative lifespan experiments. Ashutosh Tripathi analyzed the structural modification of the protein.

The lipidomic data (figure 14) presented in Chapter 3 were done at the West Coast Metabolomics Center at the University of California at Davis. Part of the elutriation experiments was conducted by Staci Hammer. Clara Kjerfve made some essential strains for the study. I performed all the rest of the experiments presented in this chapter.

Funding sources

Graduate study was supported in part by the Excellence Fellowship from the Texas A&M Agrilife, the teaching assistantship from Texas A&M University, and the National Institute of Health (NIH) grant [R01GM123139] to Michael Polymenis. The contents of this dissertation are solely the responsibility of the student and do not necessarily represent the official views of NIH.

TABLE OF CONTENTS

Page

LIST OF FIGURES

Page

LIST OF TABLES

Page

CHAPTER II

INTRODUCTION*

History of the cell cycle

'The dream of every cell is to become two cells' – Francois Jacob.

Every cell goes through a series of ordered events called the cell cycle that generates two cells from one. The cell cycle mainly comprises events where the cell grows, duplicates its content, and eventually segregates the components into two cells. The replica of the cellular components is inherited by the daughter cell from the pre-existing cell, *'Omnis cellula e cellula'* (Rudolf Virchow, 1855).

The existence of all life forms on this planet depends on cell division. Duplication and transmission of genetic and cellular content through the cell cycle are key to forming a new organism. For a single cell organism, cell division generates an entirely new individual. In a multicellular organism, cell division gives rise to different cell types, from a founder single cell to managing the body's various functions. Cell division is also necessary to replace damaged and dead cells in tissues and organs and, therefore, often holds therapeutic roles. The accuracy with which cell cycle events are

* Part of this chapter (pg. 38 - pg. 41) is reprinted with permission from 'Lipid biosynthesis: When the cell cycle meets protein synthesis?' by Heidi M. Blank, **Nairita Maitra**, & Michael Polymenis (2017). Cell cycle, 16(10), 905-906

executed facilitates the survival of the living organisms. An unregulated cell cycle leads to uncontrolled cell duplication, which causes proliferative diseases such as cancer.

Theodor Schwann and Matthias Schleiden established the cell theory tenets that cells are the basic unit of life, and all life forms, be it animals or plants, are made up of cells. However, scientists were struggling to answer how cells are born. Robert Remak and Rudolf Virchow later postulated that all cells arrive from their preexisting form, denouncing the idea of spontaneous generation of life. It became the third tenet of cell theory, and the existence of the cell cycle was realized.

Briefly, the cell cycle is divided into distinct phases. S phase is when DNA is replicated, M phase represents the period when the segregation of the duplicated chromosomes occurs. Eventually, the cell cycle ends with cytokinesis, producing two new cells (Figure 1A). The two phases of S and M are separated by gap phases G1 and G2. G1 occurs between M and S phases, whereas G2 occurs between S and M phases. The duration of each of these phases can vary over a broad range across different cell types and for the same cells proliferating at different conditions. DNA duplication in the S phase serves as a molecular landmark of cell cycle progression. The M phase can also be vividly characterized, starting with the nuclear membrane fragmentation (or not in the case of fungi) to the equatorial lining of the condensed chromosomes and later segregation of the chromosomes to the opposite poles, eventually yielding two new nuclei. Mitosis is followed by cytokinesis, where the cytoplasm physically divides into two new cells.

The transition from one phase to another in the cell cycle is regulated by a class of serine/threonine-protein kinases, namely, the cyclin-dependent kinases (CDKs). CDKs were proposed to be the "cell cycle engines" driving the cells forward in the cell cycle. Different CDKs trigger the onset of S or M phases. The cyclins regulate the catalytic activity of the CDKs. Initially discovered in marine invertebrates, cyclins are proteins that fluctuate in levels in the cell cycle (Evans et al., 1983). Depending on the cell cycle stage, specific cyclins bind to the CDKs. For instance, in *Saccharomyces cerevisiae,* Cln1p, Cln2p, and Cln3p are G1 cyclins facilitating the G1/S transition while Clb1p, Clb2p, Clb3p, and Clb4p are the G2 cyclins triggering the transition of G2/M phases. Cdc28p (Cdk1) in all cases acts as the catalytic subunit of the Cdk complex (Figure 1B) (Surana et al., 1991).

S. cerevisiae has 5 genes encoding CDKs, namely *CDC28, PHO85, KIN28, SSN3,* and *CTK1*. *CDC28* or *CDK1* is the key one (Mendenhall & Hodge, 1998), advancing the cell cycle. A gene analogous to *CDC28*, in the fission yeast, is *cdc2+*(Dorée & Hunt, 2002). Cdk activity is mainly regulated by four mechanisms, cyclin binding, Cdk inhibitor binding, activation by phosphorylation, by the Cdk activating kinase (CAK), and inhibition by phosphorylation (Mendenhall & Hodge, 1998). Cyclins bind to the CDKs with the help of their cyclin box of approximately 100 amino acid residues to regulate the activity. All the cyclins temporally oscillate during the cell cycle, controlling the cell cycle transitions (Nasmyth, 1996).

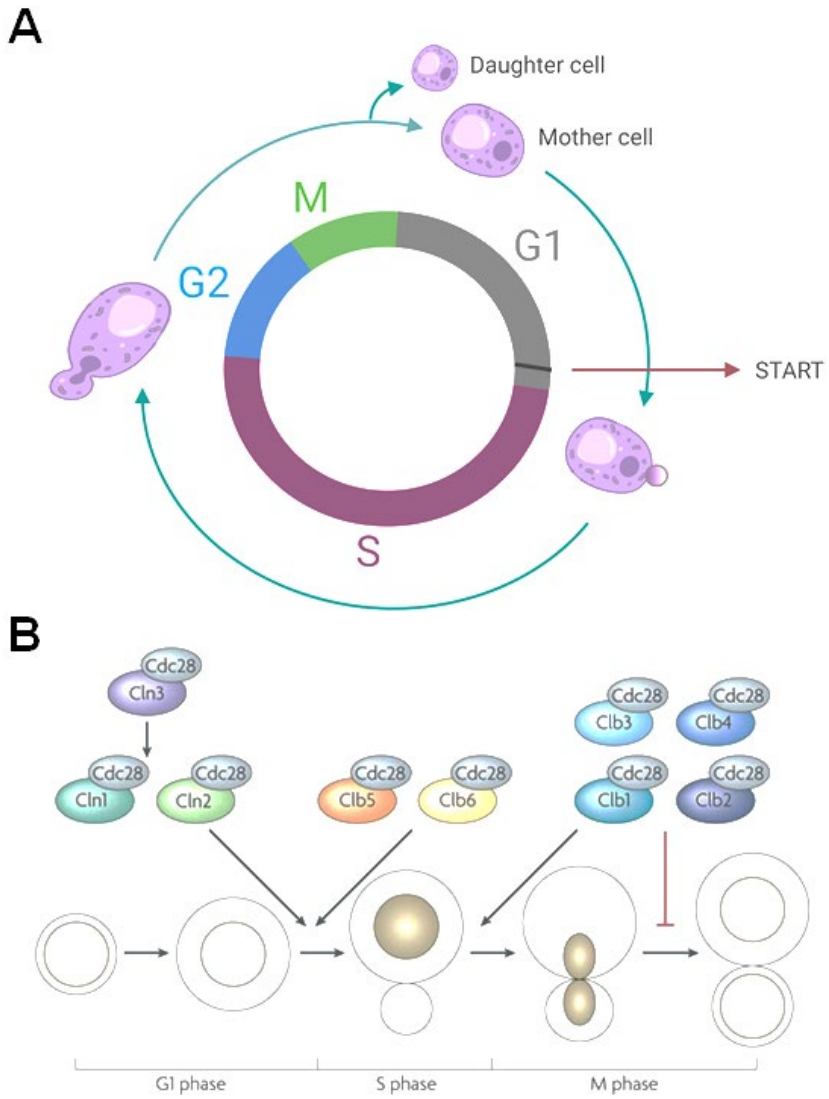

Figure 1 Schematic representation of the cell cycle progression

A. General schematic of the cell cycle progression and different morphological changes in the budding yeast related to the cell cycle. Unbudded cells grow during G1. Budding occurs after the cell reaches START. DNA synthesis initiates in the S phase. The bud continues to grow through G2 and mitosis (M). Eventually, the daughter cell buds out from the mother cell during cytokinesis. Budding yeast undergoes asymmetrical division yielding larger mother cells and smaller daughter cells. B. Budding yeast cyclins activate a single cyclin-dependent kinase (Cdc28). The G1-phase cyclins (Cln1, Cln2, and Cln3) promote bud emergence, spindle pole body duplication (not shown), and activation of the B-type cyclins. The S-phase cyclins (Clb5, Clb6) advance DNA replication (shaded nucleus), and the M-phase cyclins (Clb1, Clb2, Clb3, and Clb4) promote spindle formation and the initiation of mitosis. Mitotic cyclins inhibit mitotic exit and cell division. Following cytokinesis, a mother and daughter cell is generated. Figure 1B is adapted from the publication 'Multiple levels of cyclin specificity in cell-cycle control', reprinted with permission (Bloom & Cross, 2007)

Much of our current understanding of the cyclin/CDK regulation originated from different avenues of research carried out for roughly the past fifty years, including in the labs of Lee Hartwell, Paul Nurse, and Tim Hunt. In early 2000, their work on the elucidation of the cell division cycle genes was awarded the Nobel Prize.

Genetic dissection of the cell cycle from the Hartwell lab led to the identification of randomly generated conditional, temperature-sensitive mutants of budding yeast. The mutants were screened individually by time-lapse photomicroscopy (Hartwell et al., 1970). Cell division control (*cdc*) mutant cell populations were arrested with the same cellular morphology in the cell cycle at the restrictive temperature (Biggins et al., 2020; Hartwell et al., 1970). Hartwell and colleagues could distinguish the different mutants that could not execute a cell cycle event based on their morphology. A mutant incapable of progressing beyond a specific cell cycle point would keep growing until they could not anymore and would be stuck at that stage, and all the cells of the mutant population would look the same. On the contrary, cells of the mutants lacking a non-cell cycle function would be arrested at various points in the cell cycle when shifted to the non-permissive temperature.

Hartwell's lab utilized the genetics of the most straightforward eukaryotic system, budding yeast. Because of its morphology, budding yeast has an additional advantage. It is easy to score the cell cycle stages by looking at the cells under the light microscope. Budding yeast cells are small, round when they are born, and as they progress through the cell cycle, they form a bud. The buds on the surface of the mother cell are the early form of the daughter cell and the primary readout of the commitment

step, START (Figure 1A) (Hartwell et al., 1974; Hartwell & Unger, 1977) (restriction point in mammalian cell (Pardee, 1974)). Budding indicates that cells are committed to complete at least one round of DNA replication, and no mating factor can stop them now. The size of the bud strongly correlates with the stages of the cell cycle progression. The size ratio of the bud to the mother cell progressively increases in the cell cycle, and the ratio is the visual marker of the cell's position in the cell cycle.

Hartwell discovered >30 *cdc* mutants and categorized them based on their properties, e.g., *cdc24* cells in budding, *cdc7* cells in DNA replication. However, cells mutant in *CDC28* (*cdc28-1*) when shifted to non-permissive temperatures were arrested early in the cell cycle with unbudded morphology. DNA replication stopped, and no duplication of spindle pole bodies (SPB; centrosomes in a human cell) was observed. The results led to the idea of *CDC28* as the 'one regulator to rule them all.' *CDC28* was later discovered as the master regulator of the cell cycle, controlling different cell cycle events, starting from bud emergence to DNA replication and SPB duplication. Lee Hartwell proposed that Cdc28p ensures the faithful execution of the commitment step, START. Cdc28p participates in every crucial point during the cell cycle. The different cyclin-Cdc28p complexes phosphorylate many substrates to perform different cell cycle functions (Figure 1B). In the 1970s, while Lee Hartwell was working exclusively in budding yeast to decipher the regulators of the cell cycle, Paul Nurse was seeking the cell cycle controller in the fission yeast. Paul Nurse employed a similar kind of screen in the fission yeast, *Schizosaccharomyces pombe*. He identified *cdc* mutant cells whose shape is abnormally elongated when shifted to the restrictive temperature. He

successfully discovered twenty-seven such *cdc* mutants encoded by fourteen different genes, participating in different fission yeast cell cycle stages (Nurse et al., 1976). One of the mutants was *cdc2.* Gain-of-function mutants in the same gene were identified as *wee2* in another screen. These *wee2* mutants were dividing at a smaller size than the wild type. At the same time, other *cdc* mutants were found to be arrested at mitosis but *wee2* altered the timing of mitosis. As a result, it was later clear that the gene product of *cdc2* or *wee2* was not a mere requirement for mitosis, but it is a master regulator (Nurse & Thuriaux, 1980). This mutant behaved like the *cdc28* mutant of budding yeast, both blocking cells at commitment steps (at G2/M in fission yeast, G1/S in budding yeast) . Later on, it was found the function of the gene product of *CDC28* can complement the *cdc2* mutant of fission yeast (Beach et al., 1982), proving for the very first time that START and regulation of mitosis are catalyzed by similar enzymes from budding to fission yeast, probably in all eukaryotes. It was found to hold for human cells too. A human homolog of *cdc2* was cloned by complementation (Lee & Nurse, 1987). Hence, regulating the cell cycle is very much conserved from unicellular yeasts to multicellular humans.

When Lee Hartwell and Paul Nurse were busy unraveling the cell cycle's molecular mechanism, away from the cell cycle world, Tim Hunt was studying the regulation of mRNA translation in sea urchins (Nasmyth, 2001). Hunt and his colleagues were determining the change in the protein synthesis pattern in the eggs of sea urchin upon fertilization, and at the same time, quantifying the protein level. They incorporated radioactive methionine [^{35}S] in the newly synthesized proteins and separated them in

SDS-polyacrylamide gels. Interestingly, one protein was identified to be oscillating periodically with the cell cleavage. Later it was shown that oscillation was due to the degradation of the protein. Tim Hunt coined the name for the protein, 'cyclin' (Evans et al., 1983). Similar events were witnessed in other sea urchins. In clams, two such proteins were detected, cyclin A and cyclin B. Temporal rise and fall of cyclins were found to coordinate with the timing of several cell cycle events. For instance, the formation and disassembly of the mitotic spindle, condensation, and decondensation of chromosomes, even the breakdown and formation of nuclei required cyclins.

Meanwhile, in the cell cycle world, scientists were performing nuclear transplantation and cell fusion experiments. The study aimed to seek answers for what happens when cells at two different cell cycle stages are fused. Mitosis was found to be dominant over any other cell cycle stages. Whenever cells from the M phase were fused with cells of any other phases, G1, G2, or S, the mitotic events were always triggered, e.g., chromosome condensation (Johnson & Rao, 1970). Similar results were deduced from experiments on maturing frog oocytes (Masui & Markert, 1971). Cytoplasm from stimulated frog oocytes was transferred into unstimulated oocytes, which caused the onset of meiosis in the recipient eggs. The factor responsible for triggering the meiosis in the unstimulated eggs was called the 'maturation promoting factor' or MPF. Later, with the discovery of the 'cyclins' from the Hunt lab, scientists speculated that cyclins might be the constituents of the MPF. In 1988, MPF was purified from *Xenopus* oocytes (Labbé et al., 1988). It required the heterodimer of one molecule of Cdc2p and one molecule of cyclin B for its activity.

Many labs contributed to further elucidating the role of cyclins. They deduced that the cyclins are the critical regulatory subunit of CDKs and their degradation is necessary for cell cycle progression. The Ruderman lab cloned the first cyclin gene, cyclin A, from clams and found it to promote entry into mitosis (Swenson et al., 1986). From Marc Kirshners's lab, Andrew Murray showed that cyclin degradation is imperative for Cdk1 inactivation and required to exit mitosis, but cyclin was required for the transit from metaphase to anaphase (Murray et al., 1989). Although cyclins are required for the regulation of CDKs, any one of them is not essential in most organisms because there are several other cyclins performing overlapping and redundant functions. Hartwell's *cdc* screen identified essential genes that were unable to execute their function at higher temperature. Hence, cyclins were never detected in his *cdc* screen. Nevertheless, cyclin B was identified to be *cdc13* in Paul Nurse's mutant screen in the fission yeast (Nasmyth, 2001).

So far, the discussion has led us to understand the key molecules that regulate the cell division and necessary to exit the division and enter the next cell cycle faithfully. However, a fundamental question still needs to be addressed- How do cells decide when to divide? The G1 to S transition commits the cells to another round of division. If cells have not grown enough, they will not initiate DNA synthesis. How does growth dictate the cell's decision to divide? This is a subject that still lacks understanding. How do cells couple growth with division?

Coordination of cell growth and division

Cell size homeostasis

Cell growth and division are fundamental and separate processes. For all living organisms, general cellular parameters, cell size, and macromolecular composition remain constant during successive cell division cycles (Lloyd, 2013; Björklund, 2019). Hence, these physiological phenomena suggest the existence of a tight coupling between cell growth and division. In a proliferating culture, coordination between growth and division is achieved by sensing the cell size and conveying the signal to cell division components. However, if cell division is blocked, cells do not stop growing (Johnston et al., 1977); instead, they attain an abnormally large size. Strong coordination ensures that the subsequent generations of cells are not progressively smaller or larger. Despite the importance of the coupling between growth and division, our understanding of the molecular mechanism is unclear and sometimes hotly debated.

Cell growth helps maintain the proper size of an individual cell or organism and controls the body shape, symmetry, and proportion. The earliest observation about cell size was made almost 100 years ago by Theodor Boveri and colleagues when they deduced a positive correlation between cell size and ploidy in sea urchins. They observed that the increase in the ploidy in the embryo affected the number of divisions, and after the larval stage, sea urchin cells with more DNA were proportionally larger (Jorgensen & Tyers, 2004; Amodeo & Skotheim, 2016). The correlation between cell size and the DNA content was later found to hold for other multicellular organisms, e.g., mouse, human cells, etc. (Epstein, 1967). The coupling is consistent in unicellular

eukaryotes such as budding yeast (Mortimer, 1958; Mayer et al., 1992) and prokaryotic cells.

Every cell type under a given condition exhibits a characteristic cell size. Cells born abnormally large or small will go back to their physiological size after a few cell divisions. Several models describe how cell size homeostasis is maintained. The models include 'sizer,' 'timer,' and 'adder' models (Figure 2). The sizer model argues that the cells need to reach a critical size before undergoing division. However, the timer model proposes that cells will grow for a specific time before dividing. Hence this model suggests that cells have a mechanism to measure time. Lastly, the adder model offers that cells add a constant mass during each cell cycle irrespective of their size (Fantes et al., 1975). Based on these models, we can predict how many cell divisions are needed before a cell can return to its normal cell size. In case of an adder situation, the cells will return to the normal size range after a few divisions. On the other hand, according to a sizer model, an abnormally small cell will continue growing until it has reached a specific size, and the size homeostasis will be maintained within one generation (Vuaridel-Thurre et al., 2020). Both fission and budding yeast have sizers to dictate their growth and division. In fission yeast, a significant sizer acts at the G2/M transition. On the other hand, in budding yeast, daughter cells and mother cells have different cell cycles. While daughter cells spend more time in G1 before they grow enough to transit to DNA replication, mother cells are already big enough and do not spend much time in the G1 phase. Hence, the growth of the daughter cells follows a sizer mechanism that

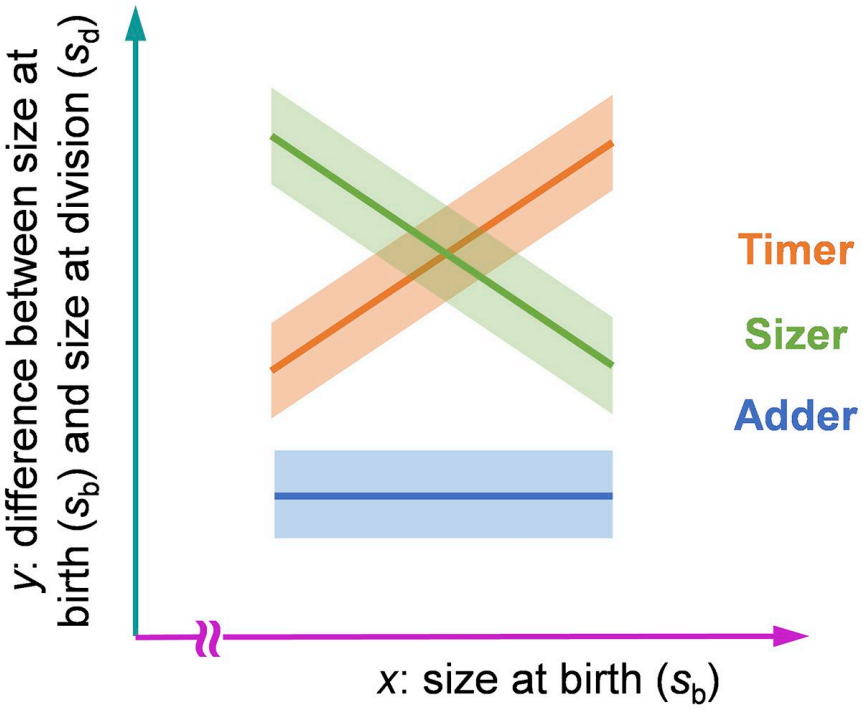

Figure 2 The three models of cell size control

Size control behaviors of growing cells are assessed by measurements of size at birth and division. The graph shows a plot of size grown over the cell cycle ($y = s_d - s_b$) *vs* size at birth ($x = s_b$). A sizer shows a slope of −1. An adder has a slope close to 0. A timer has a slope of +1. The figure is obtained from the publication 'Controlling cell size through sizer mechanisms' reprinted with permission (Facchetti et al., 2017).

operates mainly in the G1 phase, and an adder mechanism exists for the mother cells (Di Talia et al., 2007).

Budding yeast and animal cells spend most of their time in the G1 phase compared to the other cell cycle phases. Moreover, the cells of a proliferating culture can be arrested in the G1 phase by limiting growth factors or removing nutrients. On the contrary, overexpression of growth factors such as the PI3K pathway can shorten the G1 phase (Jorgensen & Tyers, 2004). Thus, G1 specific events are responsible for maintaining the physiological coupling between growth and division (Polymenis & Schmidt, 1999). Indeed, the size-control predominantly occurs during the earlier stage in the cell cycle, specifically during the G1 to S transition (Di Talia et al., 2009). How cells decide to enter the S phase has always been a question of interest, especially in the cancer field. A balance between growth and division determines the proliferation rate of the cells.

G1/S transition

Coordination of growth and division is best characterized in the budding yeast. They are the favored model organism for several reasons: easy genetic tools, simpler regulatory architecture, and straightforward cellular geometry (Mitchison, 2003). Budding yeasts divide asymmetrically, with the daughter cell being smaller than the mother cell. The cells remain in G1 until the commitment point, START (Hartwell & Unger, 1977). Activation of G1/S cyclin-Cdk complexes allows irreversible passage through START, followed by spindle pole body (SPB), or centrosome, duplication, and DNA replication initiation. The G1 cyclins, especially Cln3p in budding yeast and cyclin D in vertebrates,

trigger passage through START. Cln3p was not thought to oscillate in the cell cycle. However, there are emerging studies that indicate an opposite scenario. Cln3p peaks in mid G1, almost 7-10-fold (Lucena et al., 2018; Thorburn et al., 2013; Zapata et al., 2014). It was proposed that G1 cyclins increase in abundance in response to growth signals. Hence, it seems G1 cyclins are the ones that respond to the environmental signals and facilitate the cells to coordinate their growth with the decision to undergo START and commit to a round of DNA replication.

Approximately two hundred genes are turned on at the G1/S transition, including cyclins (G1/S cyclins Cln1p and Cln2p, and the S cyclins Clb5p and Clb6p) (Johnson & Skotheim, 2013). Two major regulatory proteins SBF (SCB binding factor) and MBF (MCB-binding factor), control the expression of most of those genes. SBF and MBF are heterodimers with DNA binding motifs, recognizing specific DNA sequences. In early G1, Whi5p, a transcriptional repressor, is bound to SBF and inhibits G1 specific transcription. However, Cln3-Cdc28p when reaches a threshold level, phosphorylate Whi5p and promotes its dissociation from SBF and its nuclear export (Bloom & Cross, 2007) (Figure 3A). Once MBF and SBF are turned on, they initiate the expression of *CLN1* and *CLN2*. Cln1p and Cln2p bind to Cdc28p and stimulate expression of the G1/S specific genes and ensure that cells pass through the commitment step. Furthermore, the Cln1,2-Cdc28p complex phosphorylates the Cdc28p inhibitor Sic1p, marking it for degradation (Yang et al., 2013). Sic1p inhibits Cdk complexes with Clb5p and Clb6p. However, once the complex of Cln1,2-Cdc28p surpasses a threshold level, they cause phosphorylation of Sic1 at multiple sites, and cause its degradation (Figure 3B).

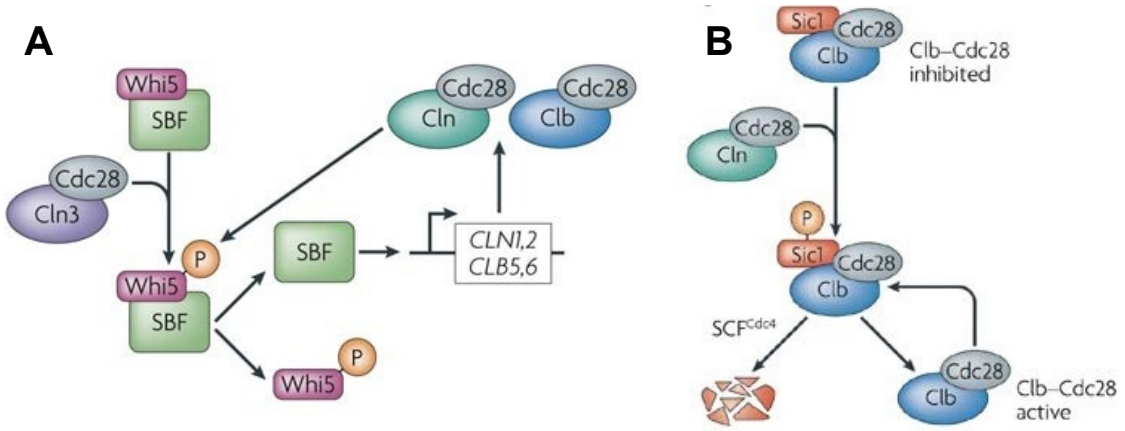

Figure 3 Schematic representation of pathways involved in G1/S transition

A. The transcription repressor Whi5 inhibits the activity of the SBF transcription factor. Phosphorylation of Whi5 by Cln3–Cdc28 induces the nuclear export of Whi5 and activates SBF, which induces the transcription of the genes that encode Cln1, Cln2, Clb5 and Clb6. B. Sic1 inhibits the activity of Clb–Cdc28 complexes. Cln–Cdc28 phosphorylates Sic1, which promotes SCFCdc4-mediated ubiquitylation and subsequent degradation of Sic1, allowing for Clb–Cdc28 activation and S-phase entry. Clb–Cdc28 complexes also phosphorylate Sic1 to induce its proteolysis. P, phosphate. The Figure is adapted from the publication 'Multiple levels of cyclin specificity in cell-cycle control', reprinted with permission (Bloom & Cross, 2007)

Cell size regulators

We often stumble upon the obvious question: which molecule mediates the physiological link between growth and division, and size control. In a dividing cell, proteins are the major macromolecules, comprising almost 46% of the dry mass (Lange & Heijnen, 2001). As a result, cell cycle researchers started considering protein synthesis as a primary indicator of cell growth. Scientists can track the amount of radiolabeled amino acid in a newly synthesized protein or the intensity of a fluorophore tagged to the protein of interest. In fission yeast, Paul Nurse and colleagues thought Pom1p and Cdr2p kinases could act as sizers or 'rulers' (Moseley et al., 2009), and similarly, it was FtsZ and DnaA in bacteria (Robert, 2015). However, definitive evidence is still lacking. For instance, Pom1p, which serves as cell polarity kinase and a dose-dependent inhibitor of mitotic entry, could allow the cells to sense the elongation. Although the deletion of Pom1p and Nif1p (another size altering gene) can modulate the cell size, these genes are not direct size sensors (Wood & Nurse, 2013).

Cell size regulation in budding yeast was proposed to involve Cln3p, a key regulator of G1 progression, a function tightly linked to cell size control. Several studies indicate that Cln3p oscillates and peaks in the mid G1 before START. No molecular mechanism is available to explain the higher amplitude of Cln3p levels before START. However, evidence of an upstream open reading frame (uORF) mediated translational control of *CLN3* can be found, which would potentially modulate levels of Cln3p under different nutrient conditions (Polymenis & Schmidt, 1997; Blank et al., 2018).

Despite its role in the coordination of growth and division, Cln3p cannot fully explain the coupling. Cells lacking Cln3p are still viable with a longer G1 and bigger critical size. Other signals feed into the cell cycle machinery to facilitate the cell's commitment to division. Alternatively, recent work has shown that the concentration of Whi5p, the inhibitor of G1/S cyclins, is gradually diluted as the cells transit from daughter to mother cells. Thus, small cells have more Whi5p (Rb in human cells (Zatulovskiy et al., 2020)) in their nucleus than their bigger counterparts (Schmoller et al., 2015), and this is how they know if they are big enough to undergo division. However, there are several unresolved questions centered around the 'dilution model.' For example, it is still not clear the molecular mechanism of the dilution. Moreover, some reports defy the dilution model completely (Dorsey et al., 2018; Litsios et al., 2019). Furthermore, a recent study shows that the size compensation effect in G1 can also happen from mutations in genes with no direct link to G1/S transition (Soifer et al., 2016). Nonetheless, these observations suggest an extensive regulatory mechanism that cells might use to coordinate growth with division.

While cell growth and proliferation in yeast cells are controlled by nutrient availability, animal cells are provided with a constant food supply. Their decision to divide is regulated by several mitogens and complex signaling pathways (Lloyd, 2013). However, in either case, dividing cells must assess both internal and external environments, and at the same time, maintain size homeostasis.

Lipids must be synthesized anew during the cell cycle. The requirement of lipids in the cell cycle (discussed later) suggests that *de novo* lipid synthesis is involved in the

coupling between growth and division. Moreover, recently Vadia et al. predicted that fatty acid synthesis could be a potential determinant of cell size (Vadia et al., 2017). Not only cell envelope, other membranous organelles (e.g., nuclear envelope) also depend on the availability of fatty acid synthesis. *De novo* fatty acid synthesis dictates the structural integrity of the organelles, including the plasma membrane, and can actively promote certain cell cycle events (Chapter 3). Metabolic inputs are crucial for the coordination of growth and division and carrying out cell cycle transitions.

To study the coordination between growth and division and different molecules participating in the coordination, one needs cells that progress synchronously in the cell cycle. This brings us to the next topic, where some popular ways to synchronize dividing cells will be discussed.

Synchronization of cells

An exponentially growing cell culture provides information on the steady-state level of macromolecules, e.g., protein, RNA, etc. (Cooper, 2003). However, we need a different approach to determine the level of molecules that oscillate in the cell cycle or assay organelles that undergo dynamic morphological rearrangement as a function of the cell cycle, e.g., nuclear division. It is imperative to collect the culture of cells in the same phase of the cell cycle and follow them as they transition to another phase together, in a synchronous culture. Single-cell experiments provide valuable information, but we often need more than one cell for analytical purposes, such as studying the protein level or

ribosomal content. Hence, we require methods to enrich cells in a specific cell cycle phase and assay for the molecule or organelle of interest during the cell cycle.

There are naturally synchronous model systems, e.g., the eggs of the sea urchin (the same model system where the cyclins were detected for the first time). Both fertilization and the subsequent cleavage divisions in the sea urchin are synchronous, providing a way to study the effects of the cell cycle (Nasmyth, 2001). Sea urchins and eggs from *Xenopus laevis* are an instrumental model system to study the synchronous embryonic cell cycles. However, in somatic cell cycles, we need methods to obtain synchrony either by imposing blocks or selecting a population of cells in the same cell cycle phase.

Block and release methods

In the block and release methods, a drug or conditional allele is introduced to cause a reversible block of the cell cycle, leading to the cells' arrest at a particular cell cycle stage. On removal of the block, when cells are returned to a permissive growth condition, or the drug is removed, the arrest is lifted, and the cells progress synchronously in the cell cycle. However, it should be noted that blocking cell division does not arrest the growth of the cell. Even if the cells are halted at a specific cell cycle stage, they will still grow, uncoupling growth from division. Hence, special measures must be taken to avoid experimental artifacts. Nonetheless, arrest and release (block and release) methods have provided us with immense knowledge of the molecular mechanism of the cell cycle and have several advantages. The process is cheap, fast, and easy to perform. Other benefits of this method include high yield and the potential to

induce synchronization almost in all cells. The conditional mutants (cell division cycle or *cdc* mutants) isolated from Hartwell's screen can be used in block and release methods of synchronization.

Cell division cycle *(cdc*) mutant genes are temperature sensitive. They grow well at a permissive temperature. In contrast, when shifted to a non-permissive temperature, the cells can proceed until they reach the cell cycle point when the function of the mutant gene is required. It takes one or two consecutive cycles to get all the cells arrested simultaneously in the cell cycle. The cells at this point remain viable but have stopped progressing in the cell cycle. Particularly in budding yeast, this method yields highly uniform cells of similar morphology and can be observed under a light microscope. However, the rise of temperature can induce stress responses (Folch-Mallol et al., 2004; Verghese et al., 2012). Depending on the type of arrest, one can use different *cdc* mutants. To arrest at G1, *cdc28* is most popularly used (Reed, 1980). Similarly, *cdc36*, *cdc37*, *cdc39* mutants can also induce G1 arrest. Some *cdc* mutants, such as *cdc19*, *cdc25*, *cdc33,* and *cdc35,* can arrest even before *cdc28* arrest. Other *cdc* mutants stop the cells at a specific stage of the cell cycle, for, e.g., *cdc24* blocks budding, *cdc31* prevents spindle pole body duplication, *cdc7* arrests at S-phase, *cdc16, cdc23*, *cdc27* and *cdc20* can induce metaphase arrest, etc. (Juanes, 2017). Another widely used *cdc* mutant is *cdc15,* which encodes for a protein kinase and is required to exit mitosis. This temperature-sensitive *cdc* mutant, when shifted to a higher temperature, blocks the cells in mitosis, specifically in late anaphase with cells having a large bud. The advantage of using the *cdc15* mutant is that synchrony is exceptional after

the 'release.' Almost 90% of the cells disassemble their mitotic spindle within 15mins (Amon, 2002). Although these *cdc* mutants were initially discovered in budding yeast, they are also available in other organisms except for most animal systems (Fitch et al., 1992).

Cell cycle researchers have also used chemicals to induce synchrony within the cell population. These chemicals mostly behave as inhibitors of specific cell cycle phases. For example, they can inhibit spindle formation or alter nucleotide concentration to block DNA replication (S-phase arrest). Arresting DNA replication is one of the prevalent ways to induce synchrony in the cell cycle of mammalian cells. The use of a high concentration of thymidine (2mM) changes the nucleotide pool and decreases the concentration of dCTP. As a result, DNA replication cannot be completed, and the cells halt at S phase (Hyland et al., 2000). Thymidine is administered in two phases to achieve G1 arrest. This is known as the double thymidine block. Following the first exposure for 12 h, cells at the G1/S boundary will enter the S phase, and before they can enter the next S-phase, the second administration of thymidine will arrest the cells in the late G1 phase (Harper, 2005).

Apart from thymidine, there are examples of other compounds that can arrest cells in the S phase, e.g., hydroxyurea (HU). Cells depend on ribonucleotide reductase (RNR) to produce deoxynucleotide triphosphates (dNTPs). HU inhibits RNR reversibly and affects DNA synthesis, and in turn, arrests the cells at S phase (Slater, 1973; 1974). At a high concentration of HU, cells of budding yeast accumulate with medium-sized buds and unreplicated DNA. Other inhibitors can specifically arrest M-phase by

perturbing spindle formation. Nocodazole is a well-known inhibitor that depolymerizes microtubules. The addition of nocodazole leads to spindle assembly failure and, as a result, cells get stuck in mitosis (Alfaro-Aco & Petry, 2015; Jaspersen & Winey, 2004; Kilmartin, 2014).

Another chemical to induce synchrony in yeast cells is made by the budding yeast themselves. The alpha factor is a 13 amino acid peptide pheromone produced by one of the mating cells of budding yeast (Mat alpha) and halts the cell cycle progression of the opposite mating cells (Mat A) in the G1 phase (Hartwell, 1973). Cells arrested with alpha-factor exhibit one spindle body with 1C DNA content and adopt a pear-shaped structure called a shmoo. Shmoo formation is a clear indication of G1 arrest and can be observed under the microscope. It is a popular strategy to synchronize haploid yeast cells. However, alpha-factor can only be used to arrest Mat A cells. Moreover, the pheromone can be easily degraded by a protease, Bar1p (Juanes, 2017). Additionally, alpha-factor causes morphological changes and significantly alters the cell's transcriptional program during the G1 phase (Amon, 2002; Spellman et al., 1998; Cho et al., 1998).

The inhibitors inducing the cell cycle arrest, can profoundly alter cellular physiology. A significant proportion of cells often do not re-enter the cell cycle, even if the drug is removed or permissive growth conditions are provided. Hence a more effective method that does not perturb the normal cell cycle progression is preferable. Much of the physiological alteration caused by the inhibitors can be avoided by using a selection method.

Selection methods

The selection methods enable us to select for a fraction of cells present in the same cell cycle stage based on physical properties, e.g., cell morphology. One of the popular approaches is to select for mitotic cells detached from the culture flask (Terasima & Tolmach, 1963). Mitotic cells become round and lose their adherence to the surface of the flask. A gentle shake can dislodge these cells resulting in almost 95% of cells being in M phase (Urbani et al., 1995). This method provides a relatively pure synchronous culture without perturbing cellular physiology. However, this mitotic shake off strategy is limited to adherent cells such as HeLa or CHO cells (Banfalvi, 2008).

The work presented here employs a different approach: a biophysical method called centrifugal elutriation to select for a synchronous population of yeast cells. This technique relies on sedimentation based on cell size. Cell size correlates with cell cycle progression in the budding yeast. At an early stage, yeast cells are small and round. However, as they progress, their size increases. Large cells with buds represent mitotic cells, whereas small unbudded cells represent G1 or daughter cells. Like the mitotic shake-off method in mammalian cells, centrifugal elutriation does not disturb the normal cell cycle progression maintaining the coupling between growth and division. Although elutriation can select synchronous cells during all the cell cycle stages, S, G2, and M phases, tight synchrony can only be achieved in the early G1 cells (Banfalvi, 2008). Nonetheless, centrifugal elutriation is still considered one of the best ways to select unperturbed synchronous cell fractions.

The centrifugal elutriation machine's basic set up comprises a large chamber connected to a spinning rotor and a pump capable of forcing fluid into the chamber. Cells growing in suspension are the ideal candidates for elutriation. During the process, cells are loaded in the machine, and two opposing forces act on them, namely the centrifugal force and the pump's fluid force. While the centrifugal force tends to sediment the cells at the bottom, the fluid force pushes the cells towards the chamber exit. The balance of the two forces makes the large budded cells migrate towards the highest centrifugal force (bottom of the rotor), and the small cells are brought to the top of the chamber (Manukyan et al., 2011; Amon, 2002). At an optimum speed of the rotor and the pump, cells are pushed out of the chamber based on their size. Smallest and unbudded cells exit the chamber first. As the cells are not under the effect of inhibitors or genetic manipulation, the G1 cells obtained by the elutriation method considered the 'true G1' cells as experimentally feasible (Amon, 2002).

Small unbudded G1 cells collected by centrifugal elutriation progress in a highly synchronous manner and allow studying the early stages of the cell cycle accurately. However, there are certain disadvantages to using this method. Experimental set up requires large and expensive centrifugation equipment. It is a time-consuming and labor-intensive experiment. Care must be taken to avoid introducing any stress to the cell fractions, altering the cells' normal physiology. Moreover, the synchrony is dispersed after the first cell cycle, and the yield of G1 cells is low. However, to enrich the number of cells in the G1 phase or at a particular cell size (cell cycle stage), it is possible to perform multiple elutriations. In each elutriation, cells progress in the cell cycle up to a

certain point before being harvested at the desired cell size. In the end, cells collected at about the same sizes but from different elutriation experiments are pooled together. A cell size series progressing through the entire cell cycle can thus be created with enough cells obtained at each point in the cell cycle stage.

How do we confirm cell synchronization?

To assess the degree of synchronization, we commonly use two methods – determining budding index and DNA content (Manukyan et al., 2011; Foltman et al., 2016). The simplest way of monitoring the cell cycle position in the budding yeast is to observe the number and size of the buds using a phase-contrast microscope. G1 cells are small and unbudded. The presence of tiny buds represents the onset of the S phase. In G2/M phases, buds are larger and become almost the size of the mother. The percent of budded cells in the population determines the budding index of the synchronous culture and the cell cycle stage indicator. Additionally, DNA content can be studied by flow cytometry to determine the cell cycle position. DNA of the individual cell is stained with a dye, either propidium iodide or sytox green (Forsburg & Rhind, 2006; Green et al., 2009; Givan, 2001; Zhang & Siede, 2004; Haase & Lew, 1997). The fluorescence distribution of DNA is plotted as a histogram consisting of two peaks. The first peak represents 1C or unreplicated DNA (the G1 phase) and the second peak is of replicated DNA or 2C content representative of the G2/M phase. The valley between 1C and 2C DNA peak is occupied by the fraction of cells undergoing chromosome replication indicative of the S phase. Moreover, immunofluorescent studies of microtubules can be used to determine

the cell cycle stages. Finally, the stage-specific study of gene transcripts is also useful in confirming mitotic cell cycle positions (Spellman et al., 1998; Futcher, 1999).

Translational control

It has been known for several decades that protein synthesis is required for cell cycle progression. However, the rate of protein synthesis from specific transcripts does not solely depend on the concentration of those transcripts. The translational efficiency of transcripts also plays a critical role in determining the rate of protein synthesis off these transcripts. Discrepancies between the protein synthesized and mRNA content are evidence of translational control (Figure 4). Translational control modulates the expression of a gene. In response to physiological and pathological conditions, protein levels can be rapidly altered by translational control. Stress response often triggers translational control of certain genes to provide a rapid response (Spriggs et al., 2010; Holcik & Sonenberg, 2005).

Eukaryotic mRNA translation is divided into three main stages- initiation, elongation, and termination. Among all the stages, initiation is the rate-limiting step (Barbosa et al., 2013). During initiation, the 40S ribosomal subunit is recruited to the m^7G-capped 5' end of the eukaryotic mRNA by translation initiation factors (Sonenberg & Hinnebusch, 2009). The 40S subunit, along with the initiation factors, forms a 43S pre-initiation complex (PIC). The 43S PIC consists of the eukaryotic initiation factors (eIFs) 3, 1, 1A, and 5 and a ternary complex with methionine loaded tRNA.

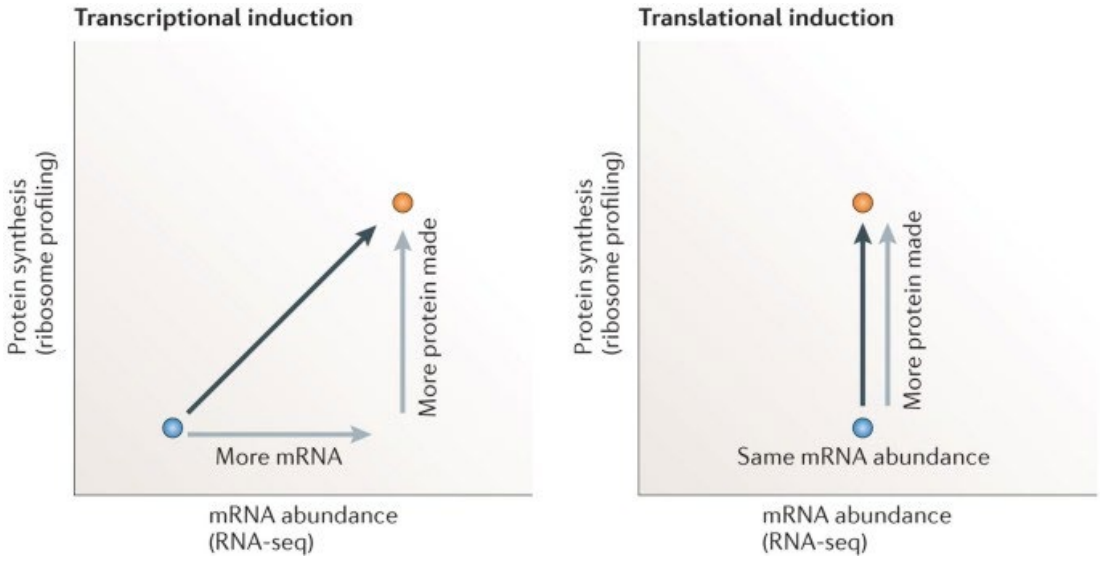

Figure 4 Plot of Transcriptional and translational control

Matched ribosome profiling and mRNA sequencing (RNA-seq) data distinguish between alternative modes of gene expression regulation. Transcriptional induction results in matched increases in mRNA abundance, as measured by RNA-seq, and protein synthesis, as measured by ribosome profiling. Translational induction manifests as an increase in ribosome-bound mRNA measurements without a corresponding change in mRNA abundance. The image is reprinted with permission from the publication 'Ribosome profiling: new views of translation, from single codons to genome scale' (Ingolia, 2014)

eIF4 complex executes multiple functions with the aid of its different proteins. eIF4E physically interacts with the m^7G-cap. eIF4A is a helicase that helps to unwind the secondary structure of the mRNA. eIF4G is a scaffold protein providing support to eIF4E, eIF4A and eIF3. Simultaneous interaction between eIF4E, poly(A) binding protein, and eIF4G facilitates circularization of the transcript. The 3' UTR comes close to the 5' UTR, letting the 3' UTR binding proteins regulate the translation initiation (Gebauer & Hentze, 2004). During the initiation process, the PIC starts scanning the mRNA in the 5' to 3' direction in search of the start codon in an ATP-dependent reaction. Once the pre-initiation complex encounters the start codon, AUG, the translation initiation factors are released, and the 60S ribosomal subunit joins the 40S subunit. A translational competent 80S ribosome is formed.

Structural features and regulatory sequences of the transcript determine its translation fate. These include the cap structure and the poly(A) tail modifications, internal ribosome entry sequences, upstream open reading frame (uORF), secondary or tertiary RNA structures such as hairpins, etc., and specific binding sites (Gebauer & Hentze, 2004). Furthermore, translational initiation factors such as eukaryotic translation initiation factors (eIF) 4E and eIF2 can affect translation (Sonenberg & Hinnebusch, 2009). In principle, these regulations can activate or repress translation. However, the regulatory mechanisms so far discovered are mostly inhibitory. In this dissertation, the focus will be mainly on the uORF mediated translational control.

uORFs are a sequence of an initiation codon in frame with a termination codon either upstream or downstream of the main AUG (Barbosa et al., 2013). The presence of

an upstream start codon in the 5' leader can let PIC initiate translation. Sometimes, a non-cognate start codon present in the 5'UTR is also selected by the PIC for translation initiation (Hinnebusch et al., 2016). In either case, translation from the uORF attenuates translation from the main open reading frame. uORFs are conspicuously common in many oncogenes and genes involved in cellular growth and differentiation (Morris & Geballe, 2000). General principles by which uORFs regulate translation are beginning to be understood. How the ribosome recognizes the uORFs dictates how they will modulate the translation of the main ORF. They engage the scanning ribosomes, and fewer ribosomes reach the main ORF. The translation is significantly reduced. Indeed, a study reports that uORFs are correlated with 30-80% reduced protein expression from the downstream ORF (Calvo et al., 2009).

Translation of *GCN4* provides a classic example of uORF mediated regulatory control (Figure 5). *GCN4* encodes a protein that induces amino acid synthesis during starvation. Translation of *GCN4* is inhibited under normal physiological conditions when amino acids are abundant. However, during starvation, *GCN4* translation is de-repressed. There are four uORFs in the 5'leader of *GCN4* that regulate the translation of Gcn4p. Translation of the first uORF allows translation of *GCN4* quite efficiently. It is an example of translation occurring by reinitiation, whereby a ribosome after terminating the synthesis of a peptide, stays on the transcript. After translation termination, the 60S ribosome subunit dissociates at the stop codon of the first *GCN4*

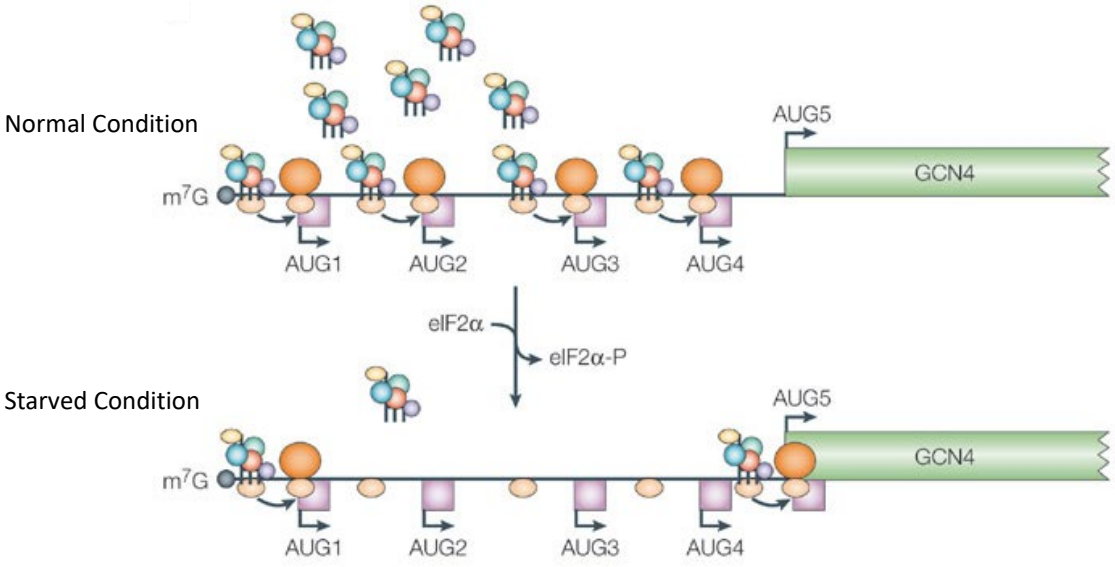

Figure 5 Translation of yeast *GCN4* is regulated by upstream open reading frames (uORFs)

When the ternary complex is abundant, ribosomes initiate at uORF1 and resume scanning to reinitiate at uORF2, uORF3 or uORF4. However, ribosomes that terminate at these latter uORFs cannot resume scanning, thereby decreasing the probability of initiation at the *GCN4* ORF. By contrast, during amino-acid starvation, increased levels of eIF2α phosphorylation lower the abundance of the ternary complex and reinitiation at uORF2–4 becomes less frequent, which allows scanning ribosomes to reach the *GCN4* ORF. The figure is adapted from the publication 'Translational control in stress and apoptosis' and reprinted with permission (Holcik & Sonenberg, 2005).

uORF. However, the 40S ribosome subunit is still bound to the mRNA and can start scanning.

Work from Hinnebusch and colleagues predicts that the 40S ribosome can resume scanning and initiate translation at the *GCN4* ORF upon acquiring the essential initiation factors. The probability of forming the PIC increases as the 40S moves further away from uORF1. The longer it takes to scan the 5'UTR, the translation of *GCN4* becomes more feasible. *GCN4* translation is regulated by the availability of the scanning complex at the right time. Under rich growth conditions, the initiation factors are abundant. The chances of forming the PIC is high. Hence, re-initiation at any one of the 3 proximal uORFs is possible, thus, attenuating the translation of *GCN4*. However, under stress conditions, due to the low abundance of the required factors, the 40S subunit can hang around a bit more on the mRNA before forming the PIC and resuming the initiation. By the time the initiation factors are available, the 40S subunit has bypassed uORFs 2-4 and it can reinitiate translation from the *GCN4* ORF (Hinnebusch, 2005). A similar translational regulation is observed to control the expression of the transcription factor *ATF4* (Figure 5) (Vattem & Wek, 2004). *ATF4* encodes for a protein involved in the mammalian starvation response. Genome-wide studies of the 5'UTRs revealed that 50% of the mammalian genes possess uORFs in their 5' leader. However, the peptides translated from the uORFs are less abundant and are highly unstable (Vanderperre et al., 2013). Other examples of uORF mediated translational control found in budding yeast are for modulating the expression of *ROK1* (Jeon & Kim, 2010),

YAP1 and *YAP2* (Vilela et al., 1998), *ACC1*, *FAS1*, and *MPS1* (Blank et al., 2017*;* 2020*;* Maitra et al., 2021).

Ribosome profiling has emerged as a critical tool to analyze translation directly (Ingolia et al., 2009). Microarrays and RNA seq can provide mRNA abundance, but do not indicate if a specific mRNA region is being translated. However, these methods can be adapted to profile ribosome-protected mRNA (Ingolia, 2014). In this technique, cycloheximide-treated cells are subjected to nuclease digestion. Cycloheximide inhibits the 80S ribosome translocation step of the translation process, impeding the movement of the scanning ribosomes. The ribosomes physically enclose 28-30 nucleotides of the transcript and shield those regions from nuclease activity. The exact location of the ribosome can be inferred from these protected regions. High throughput sequencing is used to characterize the pool of ribosome footprints.

The ribosomes occupy not all parts of the mRNA. Ribosomes are usually found in the coding sequence and absent from the 3' untranslated region. Thus, ribosome profiling can determine the exact position of the transcript that is being translated. Furthermore, ribosome profiling contains information on footprint density, which varies across different genes and single mRNA. Footprint density can estimate the level of synthesis of the encoded proteins (Ingolia, 2014). Nonetheless, ribosome profiling data can be utilized to determine ribosome occupancy at the uORF present in the 5' UTR. Such studies can inform on the translation of the uORFs. Ribosome profiling data have confirmed the occurrence of such translation both in human and yeast cells (Arribere & Gilbert, 2013; Pelechano et al., 2013; Blank et al., 2017).

Transcripts undergoing periodic fluctuations through the cell cycle have been identified in the landmark work of Spellman et al. and Cho et al. Eight hundred genes were identified in the studies of Spellman et al. while Cho et al. were able to characterize oscillations of 416 transcripts (Spellman et al., 1998; Cho et al., 1998). Until recently, there were few if any mRNAs known to have altered translational efficiency during the cell cycle. The earliest evidence for cell cycle-specific translational control came from the isolation of conditional mutants in yeasts, which turned out to be translational factors. Later, other examples of cell cycle genes under translational control were discovered, including the G1 cyclin Cln3p (Polymenis & Schmidt, 1997). In mammalian cells, however, the first example of translational control can be dated back to 1996. The Reed lab discovered variation in the amount of a Cdk inhibitor, $p27^{kip1}$. It was irrespective of its mRNA content. Further investigation revealed that the posttranscriptional regulation of $p27^{kip1}$ was achieved by translational control (Hengst & Reed, 1996).

Our lab played a significant role initially identifying almost 17 (Blank et al., 2017) and more recently 130 (Blank et al., 2020) transcripts that are under periodic translational control in an unperturbed cell cycle of budding yeast. These studies unravel the molecular basis of the requirement of protein synthesis for cell division.

Ribosome profiling studies on animal cells report on extensive cell cycle-dependent translational control. Chemicals such as selective CDK inhibitors were used in these studies to induce cell cycle arrest and generate synchronous cell culture (Stumpf et al., 2013; Tanenbaum et al., 2015). The studies are further discussed in the next

section in much more detail. Chemically induced synchronization provides a wealth of knowledge on translational control of mRNAs in the animal cell. However, it is to be noted that arrested cells never stop growing. Protein synthesis is an integral component of cell growth. Therefore, to investigate translational control in the cell cycle requires actively growing cells, progressing synchronously in the cell cycle. Blank et al. utilized centrifugal elutriation to obtain non-arrested and synchronous G1 cells (Blank et al., 2017). They identified mRNAs of lipogenic enzymes to be under periodic translational control during the cell cycle (*ACC1*, *FAS1*, *FAS2*, *PCT1*). The study revealed a fundamental link between lipid synthesis and protein synthesis during the cell cycle and hinted at the cell cycle-specific role of lipid synthesizing enzymes during cell division.

Fatty acids, lipids, and the cell cycle

The cell cycle enables exact duplication of cellular and molecular components. Membranous and non-membranous organelles get doubled in their numbers and are equally distributed to the new cells during cell division. Lipids maintain energy homeostasis and act as a signaling molecule in a dividing cell (Storck et al., 2018). They are structurally diverse. Some lipids are amphipathic molecules, with a polar head and hydrophobic fatty acid tails linked to the head by an ester bond, while Cholesterol and sphingolipids are hydrophobic containing a sterol and sphingosine backbone respectively. Lipids are an essential structural component of the membrane and need to be precisely synthesized to facilitate the transitions of the cell cycle. Unregulated lipid accumulation creates pathological storage of lipid droplets. Increased number of lipid

droplets leads to a poor prognosis for many cancers (Accioly et al., 2008). Several studies are emerging to dissect the significance of lipids and their regulation during the cell cycle.

Both in eukaryotic and prokaryotic cells, lipid composition is linked to the cell cycle (Furse & Shearman, 2018). Cells regulate lipid composition to maintain a constant membrane curvature elastic energy. HeLa cells can modify their membrane stored elastic energy throughout the cell cycle, altering two different types of lipids in the S and G2 phases of the cell cycle (Hague et al., 2013). The lipid composition of the plasma membrane plays a significant role in stabilizing the central positioning of the myosin-based contractile ring to promote fidelity of cell division in the fission yeast (Snider et al., 2017). Essential lipids of the plasma membrane phosphatidylcholine and phosphatidylethanolamine are differentially regulated in the cell cycle of the mammalian cells (Sanchez-Alvarez et al., 2015).

Lipids are not merely a building block of the cell surface membrane. Research in the Polymenis lab has shown that enhanced lipogenesis does not alter the cell size or their ability to grow (Blank et al., 2017). Hence, apart from being the main constituents of the membrane, lipids most likely participate in other cell cycle-dependent roles. Lipid synthesis is necessary to maintain the changing cellular morphology during the cell cycle, for example, in nuclear envelope remodeling (in fungi).

Recently, the Marcotte lab (UT Austin) and our lab collaboratively set out to study the abundance of biomolecules during the cell cycle. Our teams utilized the technique of centrifugal elutriation to obtain un-arrested synchronously dividing budding

yeasts. Analysis by mass spectrometry of different metabolites extracted from the yeast cells at various stages of the cell cycle revealed that the lipid repertoire was significantly enriched during the later phases of the cell cycle. Along with phospholipids and triglycerides, the ergosterol biosynthetic pathway enzymes peaked predominantly in mitosis (Blank et al., 2020). Lipid metabolism is significantly upregulated in the later cell cycle phases. These findings are consistent with our previous genome-wide study showing that mRNAs encoding the critical enzymes of fatty acid synthesis *(ACC1*, *FAS*) peaked late in the cell cycle (Blank et al., 2017).

Fatty acids are the building blocks of all the lipids that exist in the cell. Two critical enzymes participating in the *de novo* synthesis of fatty acids are acetyl CoA carboxylase (*ACC1*) and fatty acid synthase (*FAS*). Acc1p carboxylates acetyl CoA to make malonyl-CoA (W. Al-Feel et al., 1992), which serves as the FAS substrate. In the subsequent catalytic reactions facilitated by the two subunits of FAS (α-subunit Fas2p, β-subunit Fas1p), two carbons are added to malonyl CoA (Figure 6). The cascade of reactions continues for seven to eight cycles, synthesizing 16 or 18 carbon fatty acids, respectively (Klug & Daum, 2014) (Figure 6).

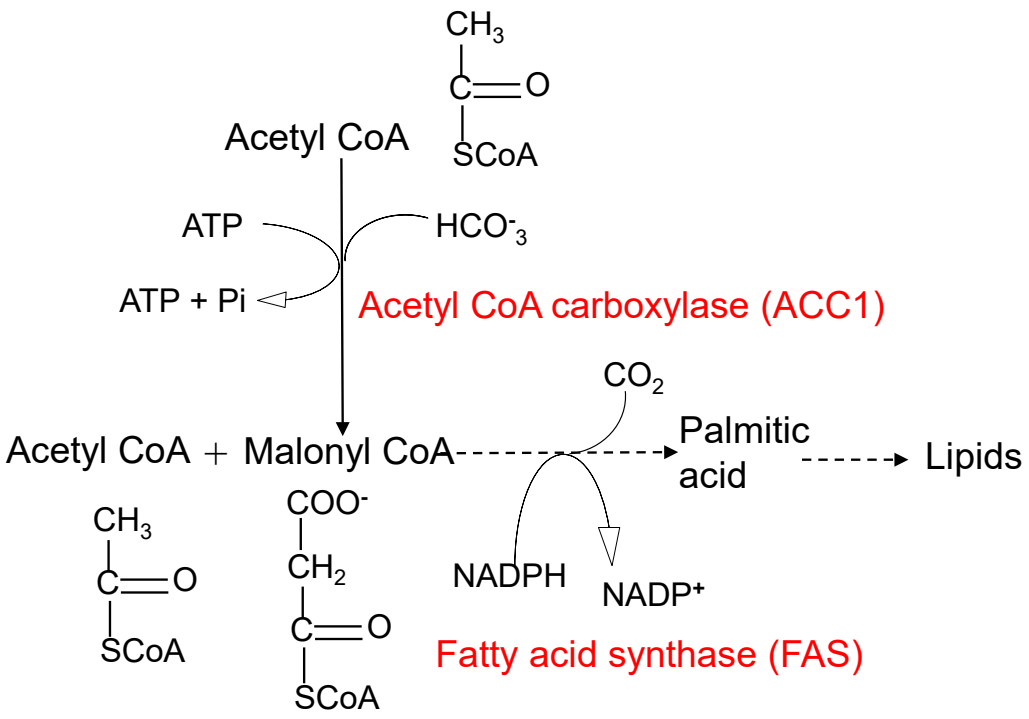

Figure 6 Schematic representation of the *de novo* fatty acid synthesis pathway

Acetyl CoA carboxylase (ACC1) is the first rate-limiting enzyme of the pathway, followed by fatty acid synthase (FAS). Acetyl CoA serves as the two carbon subunits for each cycle of the pathway. The pathway cycles 7-8 times before producing 16-18 carbon fatty acid synthesis. Fatty acids are distributed in the cytosol as free fatty acids (FFA) or are incorporated into phospholipids. Every lipid synthesis needs de novo fatty acid synthesis.

Lipid biosynthesis: When the cell cycle meets protein synthesis?

Cells must tightly coordinate the levels of many of their proteins to navigate accurately and safely the transitions of the cell cycle. For cells to grow and divide, proteins and lipids must be synthesized anew in every cell cycle. The amount, composition, and localization of the lipid repertoire are dynamic in dividing cells (Atilla-Gokcumen et al., 2014). However, little is known about how cells regulate their lipid content during a cell cycle. Genome-wide studies in yeast (Blank et al., 2017) and human cells (Stumpf et al., 2013; Tanenbaum et al., 2015) revealed surprising control mechanisms at the translational level of lipid metabolism in the cell cycle.

To find transcripts under translational control, ribosome profiling employs deep sequencing to quantify all pieces of mRNAs in the cell bound to translating ribosomes (Ingolia et al., 2012). Our lab used budding yeast collected at specific sizes via centrifugal elutriation to examine by ribosome profiling a cell size series spanning the entire cell cycle (Blank et al., 2017). The synchrony achieved is free of possible arrest-induced artifacts and preserves as much as possible the normal coordination of growth and division. A striking result was that translation of mRNAs encoding the core enzymes of lipid biogenesis, acetyl-CoA carboxylase (*ACC1*) and fatty acid synthase (*FAS1* and *FAS2*), was upregulated in mitosis (Blank et al., 2017). A short upstream open reading frame (uORF) adjusts the translation of *ACC1*, leading to >10-fold increase late in the cell cycle, and also represses translation of *ACC1* in poor media (Blank et al., 2017).

Human cells arrested at different points along the cell cycle were also subjected to ribosome profiling (Stumpf et al., 2013). The cells in the studies of Stumpf and colleagues (Stumpf et al., 2013) were not released from their arrest, leaving open the possibility of artifacts. Nonetheless, translation of mRNAs encoding enzymes of lipid metabolism was regulated, with most peaking in mitosis (Stumpf et al., 2013). The human cells examined by Tanenbaum and colleagues were arrested in the G2 phase with a small-molecule inhibitor of the cyclin-dependent kinase CDK1 (Tanenbaum et al., 2015). Washing the inhibitor away enabled the arrested cells to progress synchronously through mitosis and enter the next G1. It is not clear if the cells in this experiment attained their normal degree of coupling between growth and division since the arrest period was 18 h and the cells were released for only 45 or 225 min (Tanenbaum et al., 2015). Despite these limitations, Tanenbaum and colleagues interrogated progress through a key cell cycle phase, mitosis, during which animal cells were thought to repress overall protein synthesis (Tanenbaum et al., 2015). Most (> 90%) of the mRNAs they identified were repressed translationally in mitosis (Tanenbaum et al., 2015). Under the same conditions, demonstrating the varying nature of transcript-specific translational control, some mRNAs had *increased* translational efficiency (Tanenbaum et al., 2015). Among them was *FASN*, encoding human fatty acid synthase, whose translational efficiency was increased by >2-fold in mitosis compared with the G2 phase (Tanenbaum et al., 2015). But mitotic upregulation of lipid metabolism need not come about only through translational control. *De novo* fatty acid synthesis and upregulation of human

acetyl-CoA carboxylase (ACACA) through post-translational control were essential for completion of mitosis (Scaglia et al., 2014).

There could be many reasons why cells need new lipids late in the cell cycle. The most obvious need would arise from the sudden increase in the outer cell surface upon exit from mitosis, which approaches ≈40% for spherical cells. However, yeast cells with perturbed lipid homeostasis are still able to increase their exterior surface during mitosis, (Blank et al., 2017) arguing for more specialized roles for lipids in the eukaryotic cell cycle. A comprehensive lipidomic study by Atilla-Gokcumen and colleagues demonstrated extensive changes in lipid composition and localization during the cell cycle in human cells, especially along the midbody before cell separation (Atilla-Gokcumen et al., 2014). These investigators found 23 lipid biosynthetic enzymes essential for cytokinesis, including enzymes of sphingolipid metabolism and fatty acid elongases (Atilla-Gokcumen et al., 2014). Finally, the nuclear membrane goes through dramatic rearrangements during cell division, from complete breakdown and reassembly in animal cells, to massive expansion during the closed mitosis of many fungi. *De novo* lipid biogenesis is needed for the development of the nuclear membrane in yeast. Reduced function of Polo-like kinase, acetyl-CoA carboxylase or fatty acid synthase was proposed to lower phosphatidic acid levels, reducing the ability of cells to increase the area of their nuclear membrane (Walters et al., 2014).

Overall, the studies discussed so far point to the emerging role of lipid metabolism in underpinning cell cycle landmarks and the ability of cells to progress through cell cycle transitions. Interest in the area is high, extending to therapeutic

applications, with inhibitors of fatty acid synthase in Phase 1 clinical trials for the management of advanced stage solid tumors (ClinicalTrials.gov Identifier: NCT02223247). Translational control expands the ways that cells control their lipid composition and it may link two fundamental aspects of cell growth in volume and surface, synthesis of proteins and lipids. Future work will connect specific lipids and the enzymes that make them with their corresponding structural or signaling roles in the cell cycle, e.g., nuclear envelope remodeling during mitosis as a function of lipogenesis.

Role of fatty acids/lipids in nuclear envelope remodeling

The nucleus was discovered by Antoine Von Leeuwenhoek when he was observing red blood cells of salmon fish under his microscope. Later, the term ‘nucleus’ was coined by Robert Brown in 1831. Since then, many scientists like Robert Brown or Franz Bauer, and others have advanced the field of nuclear biology by elucidating the structure and function of the nucleus. Being larger in size, the nucleus was the only organelle that could be visualized through the early microscopes. Hence, the nucleus became a morphological marker to observe and monitor during the cell cycle.

The nucleus is usually round to oval during the vegetative state of the cell (interphase). From its formation, the nuclear envelope starts expanding as it progresses through the cell cycle, reaching its maximum size at the G2/M transition. Throughout the cell's life, nuclear size scales with the cell size maintaining a constant nucleocytoplasmic ratio (N/C) in budding and fission yeast (Neumann & Nurse, 2007; Webster et al., 2009).

The ratio is crucial for cell cycle progression of yeast cells. Any anomaly in the ratio can perturb the cell's healthy physiology.

Chromosomes that carry hereditary material reside in the nucleus. The earlier history of our understanding of the cell cycle was synonymous with chromosome segregation because chromosome segregation could be visualized under the microscope. The nucleus adapts a different morphology during mitosis to accommodate the dynamic chromosome segregation. In mammalian cells, the nuclear membrane disassembles completely during mitosis, while in other eukaryotes, such as budding yeast, the nucleus remains intact throughout the cell cycle. The major components of a nucleus are a) nuclear envelope (NE), b) nucleoplasm, c) nucleolus, d) chromosomes, along with other structural entities residing in the nucleus. Each of these components has its share of function to maintain the integrity of the nucleus and the genome residing in the nucleus. For this dissertation, much of the focus will be on the NE.

The NE, a hallmark of eukaryotic cells, is a highly organized double-membrane lipid bilayer structure separating the nucleus from other cytoplasmic organelles (Figure 7). It comprises the outer nuclear membrane (ONM) that is continuous with the endoplasmic reticulum (ER) facing the cytoplasm and the inner nuclear membrane (INM) encircling the nucleoplasm. Apart from providing a physical barrier to the genome, the NE also facilitates the selective bidirectional transport of proteins, RNA, and ribonucleic complexes through the nuclear pore complexes (NPCs) (Hoelz et al., 2011). NPCs are the proteinaceous complexes embedded within the envelope fusing the INM and ONM at many sites.

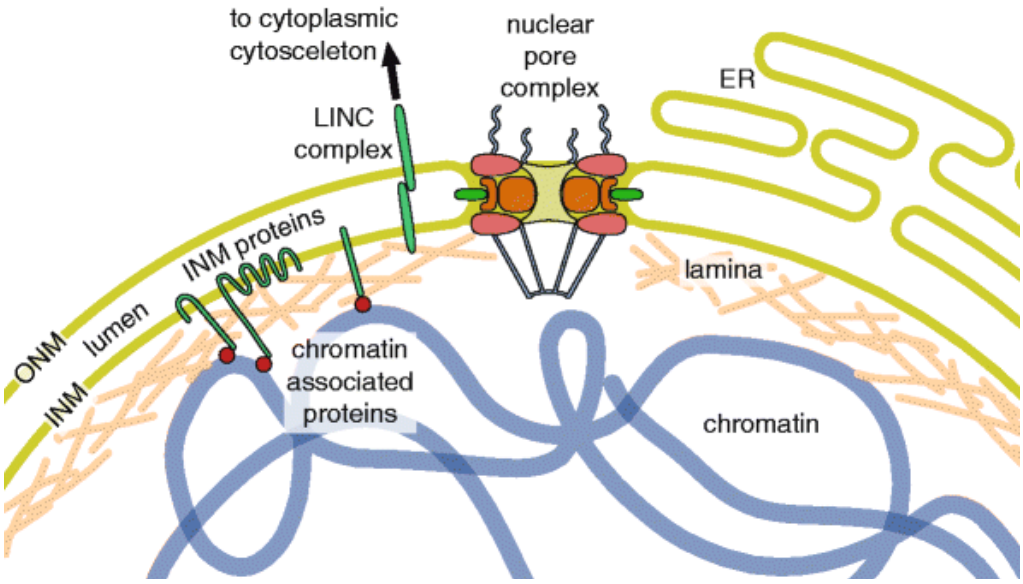

Figure 7 Nuclear Envelope

The two-membrane sheets of the nuclear envelope are separated by a lumenal space and are continuous with the bulk endoplasmic reticulum (*ER*) network. The outer nuclear membrane (*ONM*) and the inner nuclear membrane (*INM*) are fused at nuclear pores, where nuclear pore complexes are integrated to regulate bidirectional transport between the cytoplasm and the nucleoplasm. The INM is distinctly characterized by a set of integral membrane proteins that connect the nuclear envelope to chromatin by interacting directly or indirectly via chromatin-associated proteins and the nuclear lamina. The nuclear lamina is additionally connected to the cytoplasmic cytoskeleton by the interaction of LINC complex proteins of the ONM and INM across the NE lumen. The figure is adapted from the publication ‘ Building a nuclear envelope at the end of mitosis: coordinating membrane reorganization, nuclear pore complex assembly, and chromatin de-condensation’ reprinted with permission (Schooley et al., 2012).

More than 500 individual proteins and 30 different nucleoporins (Nups) assemble to form the NPCs, among which the majority of the Nups have phenylalanine-glycine (FG) repeats to establish the permeability barrier (Ungricht & Kutay, 2017; Hetzer, 2010). Although small hydrophobic molecules can passively pass through the NPC, the hydrophilic molecules need nuclear export/import signals recognized by the specific receptors. Defects in the nucleocytoplasmic transport or altered expression of nuclear transport factors cause several diseases, including cancer. Apart from the Nups, several other proteins are embedded in the INM or the ONM, involved in gene regulation and chromosomal organization.

The NE is further structurally supported by the peripheral meshwork of intermediate filaments called lamins underlying the INM. The lamins provide rigidity to the nucleus's structural framework and contribute to chromatin organization and nuclear processes (Arnone et al., 2013). Mutations in lamin A/C cause different laminopathies in human beings, mostly muscular dystrophy or neuropathies. In humans, alterations in nuclear morphology are attributes of aging (e.g., progeria) and several cancers (Scaffidi & Misteli, 2006; Méndez-López & Worman, 2012). Furthermore, in cancer cells, lack of nuclear stiffness often enables the formation of metastases, facilitating their penetration into tissues (Dahl et al., 2008). Although lamins are absent in yeast, there is some evidence on lamin-associated proteins, which are functionally essential to maintain the shape and structure of the nucleus (Meseroll & Cohen-Fix, 2016). When metazoan nuclear lamin proteins were expressed in yeast, they localized to the nuclear periphery, indicating the existence of a conserved role of certain lamin-interacting factors (Smith &

Blobel, 1994) in yeast. Nonetheless, proper nuclear morphology is vital for the cellular functions such as gene expression regulation and chromatin organization regulation.

The NE undergoes dramatic rearrangement during mitosis. Every cell type adopts a different strategy to enable the access of the duplicated chromosomes by the microtubules. Metazoan cells go through 'open mitosis' (Figure 8), where the NE, the NPCs, the nuclear lamins, and other associated proteins disperse early in mitosis (prophase). As a result, the barrier between the nucleus and the cytoplasm is lost. The lack of nuclear compartmentalization facilitates the microtubules that emanate from cytoplasmic centrosomes to access the chromosomes and promote its segregation. After the chromosomes have accurately segregated, the NE starts reassembling around the full complement of chromosomes in the daughter cells, which marks the end of mitosis (telophase). The mechanism ensures the formation of a single nucleus for each daughter cell after mitosis.

NE breakdown during open mitosis is prompted by phosphorylation of many NE proteins, the inner nuclear membrane integral proteins, nuclear lamins, and nuclear pore complex. Phosphorylated NE proteins disrupt the protein complexes and dissociate the link between the nuclear membranes and the chromosomes (Güttinger et al., 2009; Ungricht & Kutay, 2017; Liu & Pellman, 2020). These events are accompanied by the absorption of the nuclear membrane into the endoplasmic reticulum (Yang et al., 1997). In telophase, membranes and NPCs, and NE proteins are recruited, encircling the

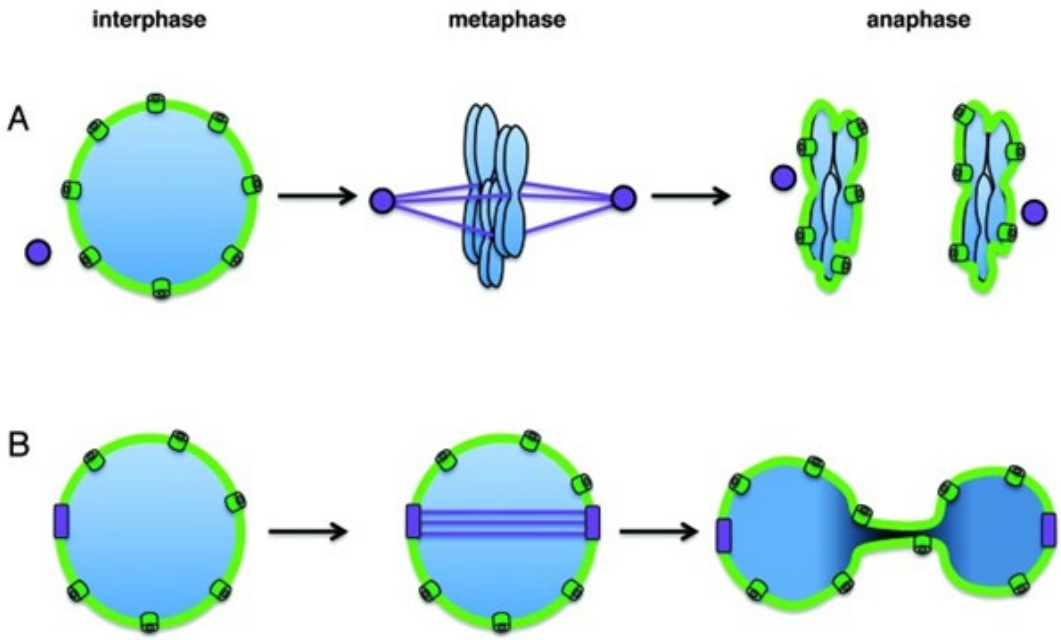

Figure 8 The nuclear envelope during different types of mitosis

(A) Open mitosis. During interphase, the chromatin (blue) is contained within the nuclear envelope (light green). As cells enter mitosis, the nuclear envelope disassembles, allowing spindle microtubules (purple lines) nucleated by centrosomes (purple spheres) to align the chromosomes on the metaphase plate. The nuclear envelope reforms in late anaphase, following chromosome segregation. (B) Closed mitosis. Shown is mitosis as it occurs in S. cerevisiae. The spindle pole body (purple) is embedded in the nuclear envelope throughout the cell cycle. After spindle pole body duplication, an intranuclear spindle is formed (*S. cerevisiae* chromosomes do not condense enough to visualize individual chromosomes or a metaphase plate). During anaphase, the nucleus elongates and the nuclear envelope expands as the sister chromatids move away from each other. The image is reprinted with permission from the publication 'The dynamic nature of the nuclear envelope: lessons from closed mitosis' (Arnone et al., 2013).

newly segregated chromosomes. Moreover, recruitment is enabled by the dephosphorylation of the nuclear envelope proteins by different phosphatases (Liu & Pellman, 2020). Resealing of the nuclear membrane is primarily facilitated by the endosomal sorting complex required for transport (ESCRT)-III. During late anaphase, ESCRT-III recruits ATPase and Vps4p to the reassembling NE. Along with spastin, these proteins coordinate the closure of NE and coordinate spindle disassembly (Vietri et al., 2015; Vietri & Stenmark, 2018).

In the exact opposite spectrum of the metazoan mitosis is the 'closed mitosis' (Figure 8) carried out by budding and fission yeasts. The centrosome equivalent in these yeasts is called the spindle pole body (SPB). They serve as the microtubule-organizing center (MTOC) for the mitotic spindles and duplicate only once every cell cycle. SPBs are either permanently embedded in the nuclear envelope (budding yeast (Jaspersen & Winey, 2004)) or get integrated into the nuclear envelope before mitosis (fission yeast (Ding et al., 1997)). Since the SPB is already assembled within the NE, they can easily access the duplicated chromosomes. NE breakdown becomes unnecessary. However, the NE must elongate in coordination with chromosome movement and segregation. SPB duplication leads to intra-nuclear spindle formation that primarily facilitates nuclear expansion (Meseroll & Cohen-Fix, 2016). The NE expands during anaphase when the sister chromatids start moving apart (Arnone et al., 2013). It expands through the bud neck, and due to the narrowness, the nucleus adopts an hour-glass structure (Meseroll & Cohen-Fix, 2016). After the chromosome segregation, the NE divides by an unknown

mechanism yielding two new nuclei around the newly segregated chromosomes, both in the mother cell and daughter cell (Meseroll & Cohen-Fix, 2016).

'Closed mitosis' seems to be an economical solution for chromosome segregation. The nucleus remains intact throughout the cell cycle, and the mixing of nuclear and cytoplasmic material can be circumvented. Furthermore, cells do not need to reseal the NE after mitosis, and the risk of leaving behind some chromosome material is minimized. However, other issues must be resolved, for instance, the timing of the nuclear expansion, cell cycle events that serve as the cue for nuclear expansion, etc. Witkin *et al*. found that nuclear expansion during closed mitosis in budding yeast results from cell cycle cues, which signal mitotic entry and is independent of spindle elongation. Fission yeast also expand the NE independent of the spindle elongation during mitosis (Castagnetti et al., 2010). Furthermore, studies from Campbell et al. showed that the nuclear membrane has distinct domains that respond differently to increased phospholipid synthesis and restrain the NE expansion around the bulk DNA. There are unknown tethering factors present throughout the NE to facilitate this differential expansion (Campbell et al., 2006). Mitotic arrest in budding yeast causes abnormal nuclear extension called 'flares' and is dependent on the phospholipid synthesis. During the mitotic arrest, phospholipid synthesis remains unperturbed, and they continue to accumulate. As a result, an extra membrane is sequestered in the NE to keep the intranuclear organization undisrupted during the mitotic delay (Witkin et al., 2012).

With emerging studies on NE remodeling during mitosis, it is becoming clear that true topologies of 'open' and close' may not exist (Dey & Baum, 2021). Despite the

dispersion of the nuclear membrane, remnants of the NE appear to interact with mitotic spindles in open mitosis (Larsson et al., 2018). Furthermore, recent studies found that in closed mitosis, the NE, which remains intact, can undergo local disassembly for the sake of chromosome organization and segregation during mitosis (Dey et al., 2020). Regardless of whether NE is subjected to either closed or open mitosis, in both cases, the nucleus undergoes dramatic structural changes and requires new membrane material.

A variety of lipid species decorate the NE. Several studies indicate the requirement of lipids (e.g., fatty acids) to maintain the structural integrity of the nucleus. Phospholipids are the major constituents and actively participate in regulating the size and shape of the nucleus. Symeon Siniossoglou and his colleagues found that altered phospholipid synthesis in budding yeast can disrupt the shape of the nucleus. Pah1p (Ned1 in fission yeast; lipin in the mammalian cell) is a phosphatase that dephosphorylates phosphatidic acid (PA) to diacylglycerol (DAG) and controls lipid metabolism, especially in the nucleus (Santos-Rosa et al., 2005) (Figure 9). Spo7p and Nem1p are the two ER-associated phosphatases in budding yeast that dephosphorylates Pah1p, thereby activating it (Santos-Rosa et al., 2005). Cells lacking Spo7p or Nem1p, or Pah1p, lead to excess phospholipids in budding yeast, causing ER expansion, and letting nucleus to form ‘flare’ protrusions (Campbell et al., 2006; Santos-Rosa et al., 2005).

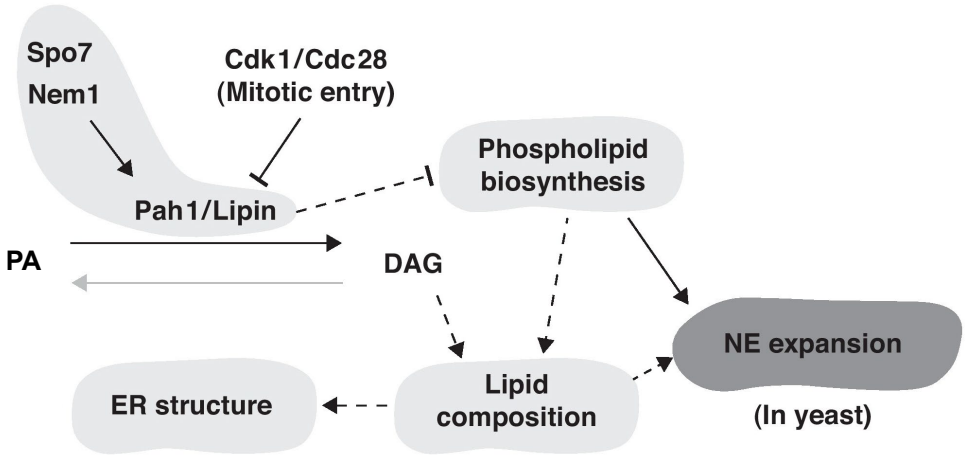

Figure 9 Potential mechanistic links between Pah1p (lipin) functions ad NE dynamics

Solid lines indicate direct functions; dotted lines suggest indirect contributions. PA: phosphatidic acid; DAG: diacylglycerol. The figure is adapted from the publication ‘ Remodeling the nuclear membrane during closed mitosis’ and printed with permission (D. Zhang & Oliferenko, 2013).

Along with yeasts, *C. elegans* also show alteration in nuclear shape due to the inactivation of lipid synthesis by inhibiting a lipin homolog in the worms (Golden et al., 2009). However, the phosphorylation of Pah1p is carried out by Cdk1p (Cdc28p), hinting at a cell cycle-dependent regulation of lipid metabolism (Bahmanyar & Schlieker, 2020). In yeast, an acyltransferase, Lro1p, is targeted to a subdomain of INM in a cell cycle-dependent manner to modulate the phospholipid remodeling pathway in the nucleus (Barbosa et al., 2019).

Fatty acids are the building blocks of every lipid. *De novo* fatty acid synthesis is equally essential for the maintenance of nuclear shape and size. In budding yeast, acetyl CoA carboxylase catalyzes the first reaction of *de novo* fatty acid synthesis. Defects in Acc1p can lead to aberrant nuclear envelope structure, and cells cannot exit mitosis. Inactivation of Acc1p increases the distance between ONM and INM, and nuclear pores cannot be inserted correctly due to lack of proper ONM and INM fusion (Schneiter et al., 1996; Al-Feel et al., 2003). Fission yeast mutants of acetyl CoA carboxylase lack functional spindles and produce unequal-sized daughter nuclei (Saitoh et al., 1996). Genetic or chemical perturbation can cause the nucleus to adopt an abnormal 'cut' phenotype in fission yeast (Zach et al., 2018). Other critical enzymes of the fatty acid synthesis pathway, Fas1p, and Fas2p, are also crucial in nuclear division. Evidence of involvement of Fas1p, Fas2p, and Acc1p can be found in the 'no-flare' nucleus screen from Orna Cohen-Fix's lab (Walters et al., 2014). Recently, they showed the direct involvement of fatty acids in nuclear membrane expansion (Walters et al., 2019). Moreover, Paul Nurse and colleagues have demonstrated that cells deficient in Fas1p do

not exhibit nuclear division (Takemoto et al., 2016). All these studies point towards the requirement of fatty acids and lipids in maintaining the shape and size of the mitotic nucleus.

Scientists have always considered lipids and fatty acid synthesis to be required for structural purposes or as nutrients. When inhibited by the administration of cerulenin (or cutin1) which inhibits fatty acid synthesis, nuclear division can completely shut down. However, in this dissertation (Chapter 3), we will encounter that lipids are not a mere requirement. Lipid synthesis can actively promote cell cycle events.

Membrane trafficking and PITPs

The endoplasmic reticulum (ER) is the main site for lipid synthesis, although some lipids are also synthesized in the mitochondria (Scharwey et al., 2013). Other membranous organelles cannot synthesize *de novo* lipids and thus rely on intracellular lipid trafficking (van Meer et al., 2008) either via vesicles or contact sites (with the ER; mitochondria (Tatsuta et al., 2014), and chloroplasts (Hölzl & Dörmann, 2019)). Once they reach their destination organelles, lipids serve as a structural component where they can undergo further modifications or be transported to a new destination. Lipids, owing to their hydrophobic nature, cannot be transported by free diffusion and require unique mechanisms (Blom et al., 2011).

Lipid transfer proteins enable coordination between lipid metabolism with the proteins of the membrane trafficking through the trans-Golgi network (TGN) and endosomal membranes (Bankaitis et al., 1990; Fang et al., 1996; Bard & Malhotra, 2006;

Graham & Burd, 2011). The TGN comprises maturing compartments that act as the regulatory center where lipid signaling is integrated with cargo sorting and membrane trafficking (Grabon et al., 2019).

Phosphatidylinositol transfer proteins (PITPs) are often referred to as the 'lipid carriers' that trigger phosphoinositide signaling that transfers the phosphatidylinositol (PtdIns) from the ER to other membranes (Grabon et al., 2019). Sec14p is one of the major and best understood PITPs. It serves as the founding member of these membrane trafficking proteins. Sec14p helps exchange phosphatidylinositol and phosphatidylcholine in a homotypic or heterotypic exchange (Bankaitis et al., 2010). Thus, Sec14p coordinates biosynthetic pathway of phosphatidylcholine with PtdIns mediated phosphoinositide signaling (Figure 10). It is a peripheral membrane protein of the Golgi apparatus (Cleves et al., 1991) and is found in all eukaryotes. Sec14-like proteins are highly diverse, with almost 500 members in all eukaryotes (Phillips et al., 2006), and Sec14p is the prototype. The various genetic and biochemical experiments suggest that it plays a significant role in the PtdCho and PtdIns homeostasis in the yeast cell.

SEC14 is a gene initially identified in the collection of yeast secretory (*sec*) mutants (Novick et al., 1980). The molecular characterization of *SEC14* later revealed that it is necessary for the viability of yeast cells, and the protein product facilitates membrane trafficking from the TGN in yeast (Cleves et al., 1991). Yeast cells deficient in Sec14p cannot form post-Golgi secretory vesicles from the TGN and the endomembrane system (Bankaitis et al., 1990; Novick et al., 1980). Sec14p contains a

binding pocket for the phospholipids. It comprises around 280 amino acids folded into two lobes forming a hydrophobic cavity (Schaaf et al., 2008; Ren et al., 2014; Sha et al., 1998). The cavity is of fixed size and can facilitate binding either PtdIns or phosphatidylcholine (PtdCho), one at a time (Grabon et al., 2019). A helical gate guards the hydrophobic cavity of the Sec14p, which flips back and forth to cause either "open" or "closed" conformations. During the lipid exchange reaction, the lipid-free state assumes an open conformation that Sec14p transiently places on the membrane surface. The hydrophobic cavity provides a similar chemical environment as that of the membrane surface, and thus, lipid exchange becomes feasible in an ATP-independent reaction (Grabon et al., 2019; Mousley et al., 2007). It is the membrane surface perturbation that might be responsible for triggering phospholipid transfer. The lipid-bound state of Sec14p assumes the "closed" conformation.

The most remarkable feature of the Sec14p molecule is the mechanism used to differentiate physically the PtdIns and PtdCho headgroups binding. While the PtdIns headgroup coordinates with the hydrogen bonding of the protein surface, the PtdCho headgroup is buried deeply within the interior of the lipid-binding cavity (Schaaf et al., 2008; Bankaitis et al., 2010). In recent studies, Sec14p has been described as a regulated nanoreactor that presents PtdIns to PtdIns kinases (e.g., Pik1p or Stt4p) and stimulates the synthesis of Phosphatidylinositol-4-phosphates (PI4Ps). The presentation happens during the heterotypic exchange reaction between PtdIns and the departing PtdCho (Figure 10). PtdIns is maintained in a transitional state between the membrane surface

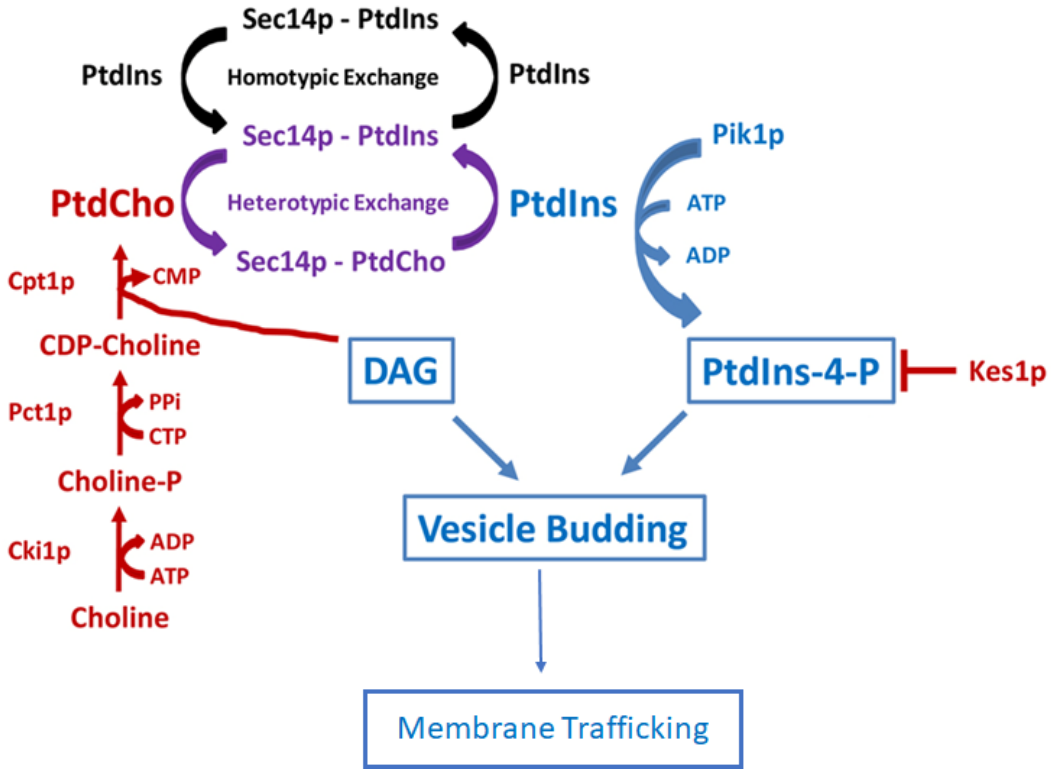

Figure 10 Schematic representation of Sec14p mediated membrane trafficking

Sec14 and coordination of lipid metabolism with membrane trafficking. A DAG-requiring vesicle formation pathway is sensitive to flux through the cytidine-diphosphate (CDP)-choline pathway activity because PtdCho production via this mechanism occurs at the expense of DAG. Sec14 surveys flux by binding (sensing) the newly synthesized PtdCho (i.e. the accessible PtdCho pool). Sec14p initiates heterotypic exchange reactions and stimulates PtdIns-4-phosphate production by the Pik1p PtdIns 4-OH kinase. In a single vesicle budding pathway model, PIP substitutes for DAG in promoting vesicle budding. Alternatively, in a model where there are two pathways for vesicle budding, the two modes are distinguished by their threshold requirements for DAG and PtdIns-4-phosphate. Sec14p inactivation compromises both vesicle budding pathways. The activity of multiple pathways for vesicle formation in the yeast TGN/endosomal system is well-established [40]. Negative regulators of Sec14p-dependent vesicle budding pathways are highlighted in red -- including the proteins identified by loss-of-function 'bypass Sec14p' mutations (choline kinase, Cki1p; the choline-phosphate cytidylyltransferase, Pct1p; choline phosphotransferase, Cpt1p, the PtdIns-4-phosphatase Sac1p, the oxysterol binding protein Kes1p). Positive regulators of Sec14p-dependent vesicle budding pathways are highlighted in blue. The interface between these two opposing is regulated by Sec14p-mediated heterotypic phospholipid exchange (purple). The image is reprinted with permission from the publication 'The Sec14 superfamily and mechanisms for crosstalk between lipid metabolism and lipid signaling'.

and the binding pocket. The transitional state PtdIns constitutes the PI4K substrate pool (Grabon et al., 2019; Schaaf et al., 2008; Bankaitis et al., 2012). While Pik1p shuttles between the cytosolic and nuclear pool and performs an essential function in both compartments (Garcia-Bustos et al., 1994), Stt4p mainly executes its function at the plasma membrane of budding yeast. However, the activity of the mammalian homolog of the enzyme can be found in the nucleus. Mss4p is another kinase that catalyzes the phosphorylation of PtdIns-4-P to PtdIns-4,5-P.

Several studies have demonstrated that Sec14p coordinates lipid metabolism with the TGN mediated membrane trafficking. This is evident from the isolation of the mutants with loss of function mutation in the non-essential genes, called the “bypass Sec14p mutant”. The mutants can revive yeast cells and restore the secretary competence in yeast cells deficient of the normal functioning Sec14p. Genetic ablation of the enzymes for PtdCho synthesis via the CDP-choline pathway can restore viability in yeast cells devoid of Sec14p (Cleves et al., 1991). The necessity of the PtdCho biosynthesis in the secretory function of Sec14 is obvious given PtdCho binds to Sec14p during the trafficking process. The genetic data further suggests that Sec14p is required to detoxify the effects of PtdCho on the TGN (Cleves et al., 1991) and loss of Sec14p enhances the level of PtdCho in the yeast TGN membranes (McGee et al., 1994).

An integral membrane protein, Sac1p, regulates the homeostasis of PtdIns at the Golgi and ER (Cleves et al., 1989; Kearns et al., 1997; Whitters et al., 1993). Inactivation of Sac1p in yeast cells can bypass the phenotypic consequences of the lack of functional Sec14p. Sac1p is a phosphatase and genetic ablation of Sac1p in yeast cells

leads to elevated PtdIns-3-P, PtdIns-3,5-P2, and PtdIns-4-P (Rivas et al., 1999; Guo et al., 1999) and derangements of neutral lipid metabolism (Rivas et al., 1999). It is proposed that higher levels of PtdIns-4-P mislocalizes other phosphoinositide binding proteins (Kes1p) and contributes to 'bypass Sec14p' (Mousley et al., 2007).

Functional ablation of a sterol binding protein can circumvent the Sec14p requirement of the yeast cell (Fang et al., 1996). Kes1p (also known as Osh4p) is one of the seven highly conserved oxysterol binding proteins (OSBP) in the yeast cell. It is the only OSBP that can 'bypass Sec14p' phenotypes (Fang et al., 1996; Beh et al., 2001). Kes1p is a peripheral protein residing in the yeast Golgi and regulates Pik1p. Genetic data confirms Kes1p to be a negative regulator of the Sec14p. While Sec14p is pro-trafficking, Kes1p sequesters the available PtdIns-4-P either by inhibiting Pik1p or activating a phosphatase or combination of both (Mousley et al., 2007).

How phosphoinositides regulate the morphology and division kinetics of the nucleus remains elusive. Seven different phosphoinositides are so far discovered in mammalian cells, of which only 5 of them exist in yeast cells (Grabon et al., 2019). It is proposed that cytoplasmic phosphoinositides translocate to the nucleus during the telophase just before the nuclear envelope starts reassembling in the mammalian cells (Castano et al., 2019). Several reports suggest that PITPs carry out the translocation (de Vries et al., 1995; 1996; Rubbini et al., 1997). The enzymes necessary for phosphoinositide metabolism already reside in the nucleus, indicating that cytoplasmic PtdIns imported to the nucleus can undergo the necessary modifications to generate the requisite phosphoinositides. Furthermore, the PI-4-OH kinases and the phosphatase

activity, and hence, the nuclear phosphoinositide levels, are dynamic and regulated during the cell cycle (Castano et al., 2019). Abundant evidence supports that phosphoinositides interact with nuclear protein and result in changes in protein conformation, localization, and activity. Hence, phosphoinositides modulate various nuclear events such as chromatin remodeling and modification, transcription, mRNA processing, RNA export, DNA damage response, and cell cycle regulations (Cocco et al., 1987; 1989; York et al., 1999; Li et al., 2013; Hamann & Blind, 2018; Chen et al., 2020; Castano et al., 2019). Both the kinases Pik1p and Stt4p produce the PtdIns-4-P that serves as the precursor to the nuclear pool of other phosphoinositides, e.g., PtdIns-4,5-P2.

Goal of this thesis

Cells maintain a tight balance between growth and division to ensure that they do not become progressively larger or smaller with each generation. A critical requirement to achieve this balance is the regulated synthesis of proteins and lipids during every cell cycle. Bulk protein synthesis is necessary to maintain the cell's mass, and lipids are required for membrane biogenesis and vital signaling components. However, how lipid homeostasis is held during the cell cycle is poorly understood. This thesis aims to elucidate how the synthesis and trafficking of lipids integrate with the cell cycle events.

In Chapter 2, I report that Kes1p, which inhibits the Sec14p mediated membrane trafficking, performs cell cycle control activities. The deficiency of Sec14p perturbs the cell cycle of yeast cells. A temperature-sensitive variant (*sec14-1*) is utilized to investigate the role of the protein product in the cell cycle. Even at their permissive

temperature, mutant cells are bigger, grow slowly, and exhibit a G2/M delay. However, the lack of Kes1p can bypass the cell cycle phenotypes of *sec14-1*. Among all the oxysterol binding proteins, Kes1p is unique. It is the only one that can suppress the cell cycle phenotypes. Moreover, under nutrient-poor conditions, Kes1p also functions as an inhibitor of G1/S transitions. To our knowledge, this is the first time a cell cycle role for these proteins is described, which is unrelated to lipid transfer. These data indicate that membrane trafficking is interlinked with the cell cycle transitions.

Chapter 3 primarily focuses on the translational control of lipogenic enzymes and ties it to a landmark event of the cell cycle. Specifically, this chapter investigates the upstream open reading frame (uORF) mediated control of the enzymes involved in *de novo* fatty acid synthesis. The enzymes have uORFs residing in their 5' leader sequence. Mutant lacking the uORFs synthesizes more lipids and becomes insensitive to a fatty acid synthesis inhibitor (cerulenin). Translation of the fatty acid synthesis enzymes is derepressed in the absence of the uORFs. Further studies reveal enhanced lipogenesis accelerates nuclear elongation and division. Derepressing translation of lipogenic enzymes suppresses the cell cycle phenotypes of Sec14p, including bigger cell size and delayed nuclear division. Furthermore, the aberrant nuclear morphology of mutants devoid of PtdIns4-OH kinase (Pik1p, Stt4p) is restored due to increased lipogenesis.

Taken together, my results suggest that translational control of lipid homeostasis during cell division links cell growth to nuclear envelope remodeling in mitosis, a key landmark of eukaryotic cell division.

CHAPTER III

A LIPID TRANSFER PROTEIN SIGNALING AXIS EXERTS DUAL CONTROL OF CELL CYCLE AND MEMBRANE TRAFFICKING SYSTEMS[*]

Disclaimer for Chapter II

Chapter II is a reprint of the publication, for which I am a third author. This study was performed in collaboration with the Bankaitis Lab in the Department of Biochemistry and Biophysics at Texas A&M University. Jin Huang and Carl J Mousley performed major experiments in the Bankaitis Lab. I performed the cell cycle experiments presented in figure 13B, 13C, 14, and 15C along with the figure A-1 of the publication. The summary section of this Chapter is the abstract of the publication. The rest is presented as in the publication.

[*] This chapter is reprinted with permission from 'A lipid transfer protein signaling axis exerts dual control of cell cycle and membrane trafficking systems' by Jin Huang[+], Carl J Mousley[+], Louis Dacquay, **Nairita Maitra**, Guillaume Drin, Chong He, Neale D. Ridgway, Ashutosh Tripathi, Michael Kennedy, Brian Kennedy, Wenshe Liu, Kristin Baetz, Michael Polymenis, & Vytas A Bankaitis (2018). *Developmental Cell*, *44*(3), 378-391.e5. (+ represents equal contribution)

Summary

Kes1/Osh4 is a member of the conserved, but functionally enigmatic, oxysterol binding protein-related protein (ORP) superfamily that inhibits phosphatidylinositol transfer protein (Sec14)-dependent membrane trafficking through the *trans*-Golgi (TGN)/endosomal network. We now report that Kes1, and select other ORPs, execute cell-cycle control activities as functionally non-redundant inhibitors of the G_1/S transition when cells confront nutrient-poor environments and promote replicative aging. Kes1-dependent cell-cycle regulation requires the Great-wall/MASTL kinase ortholog Rim15 and is opposed by Sec14 activity in a mechanism independent of Kes1/Sec14 bulk membrane-trafficking functions. Moreover, the data identify Kes1 as a non-histone target for NuA4 through which this lysine acetyltransferase co-modulates membrane-trafficking and cell-cycle activities. We propose the Sec14/Kes1 lipid-exchange protein pair constitutes part of the mechanism for integrating TGN/endosomal lipid signaling with cell-cycle progression and hypothesize that ORPs define a family of stage-specific cell-cycle control factors that execute tumor-suppressor-like functions.

Introduction

The *trans*-Golgi (TGN) network/endosomal system consists of highly dynamic organelles that sit at the confluence of antero-grade and endocytic membrane flow (Glick & Nakano, 2009). Thus, the TGN/endosomal system serves as an important membrane-sorting station, and as a major node for intracellular signaling. TGN/endosomal signaling programs involve multiple branches of lipid metabolism, with a robust and essential interface between lipid metabolism and membrane trafficking through these compartments (Bard & Malhotra, 2006;Graham & Burd, 2011).

Lipid exchange proteins play crucial roles in coordinating lipid metabolism with phosphoinositide signaling and membrane trafficking in TGN/endosomes (Bankaitis et al., 1990; 2010; Graham & Burd, 2011). This circuit is controlled by opposing actions of two lipid-exchange proteins: the PtdIns/PtdCho transfer protein Sec14 and Kes1/Osh4 (Fang et al., 1996; Mousley et al., 2012). Sec14 couples PtdCho biosynthesis with PtdIns-4-P production (Cleves et al., 1991; Schaaf et al., 2008). In turn, PtdIns-4-P signaling drives TGN/endosomal trafficking (Graham & Burd, 2011). Kes1 is one of seven yeast oxysterol binding-related proteins (ORPs) (Fang et al., 1996; Beh et al., 2001), and it antagonizes Sec14 activity by sequestering PtdIns-4-P from its pro-trafficking effectors (Li et al., 2002; de Saint-Jean et al., 2011). Recent studies indicate that a Kes1 sterol/PtdIns-4-P exchange cycle controls amplitude of this trafficking "brake" by tuning the ability of Kes1 to sequester PtdIns-4-P (Mousley et al., 2012).

Although conserved across the *Eukaryota*, ORPs remain functionally enigmatic, with conflicting data as to whether ORPs are intermembrane lipid transfer proteins or not (Schulz & Prinz, 2007; Georgiev et al., 2011; Stefan et al., 2011; Mousley et al., 2012). This confusion reflects the lack of information regarding the biological activities of these proteins. Kes1 is the exception. It is not only unique among yeast ORP proteins in its role as antagonist to Sec14-dependent PtdIns-4-P signaling in the TGN/endosomal system, but Kes1 is also an antagonist of nitrogen stress responses and mammalian target of rapamycin complex 1(TORC1) signaling (Mousley et al., 2012). Those results forecast complex physiological functions for Kes1 and identify homeostatic regulation of Kes1 activity as a key point of control at the interface of membrane-trafficking, nutrient signaling, and cell-cycle progression. Issues of how cells coordinate membrane growth and trafficking with nutrient signaling and entry into a new mitotic cycle define fundamental, but poorly understood, questions in contemporary cell biology (McCusker & Kellogg, 2012).

In this study, we characterize Kes1 activity as a negative regulator of progression through the G_1 stage of the cell cycle when cells confront nutrient-prohibitive environments. We further demonstrate that the antagonistic actions of Kes1 and Sec14 in TGN/endosomal membrane trafficking extend to cell-cycle contexts. Strikingly, these cell-cycle involvements are independent of the roles of these proteins in regulating bulk membrane trafficking. Thus, Kes1 and Sec14 execute dual functions in membrane-trafficking and cell-cycle control and are well positioned to coordinate cell-cycle progression with membrane flux through the TGN/endosomal system. We also show that

Kes1 activity is subject to regulation by the NuA4 lysine acetyltransferase (KAT). Together, the data reveal an interface between TGN/endosomal lipid signaling and cell-cycle control, identify the NuA4 KAT complex as a regulator of that interface, and suggest ORPs as stage-specific inhibitors of cell-cycle progression in eukaryotes.

Results

Kes1-Induced Cell-Cycle Arrest Exhibits Signatures of Quiescence

The first *in vivo* clues regarding ORP function came from demonstrations that Kes1 is an antagonist of Sec14 and PtdIns-4-P signaling in the context of membrane trafficking through the TGN-endosomal system. That functional readout is complex, however, as it is Kes1 LOF that restores growth and membrane trafficking to cells deficient in normally essential Sec14 activities (Fang et al., 1996; Li et al., 2002). A simpler context was suggested by (Mousley et al., 2012), who demonstrated that excessive Kes1 activity evokes an amino acid remedial growth arrest by attenuating TORC1 signaling. Upon elevation of Kes1 activity, most cells arrest in G_1, as determined by their terminal phenotype of large unbudded cells with 1N genome content (Figure 11). Furthermore, G_1 cells with excessive Kes1 activity are unable to initiate a new round of cell division in nutrient-replete media, even though these cells continue to increase their size at a rate similar to that of matched controls, demonstrating that inability to initiate cell division was not due to a general growth deficiency (Figure A-1). These collective data forecast a role for Kes1 in the G_1 phase when cells evaluate nutrient cues before committing to

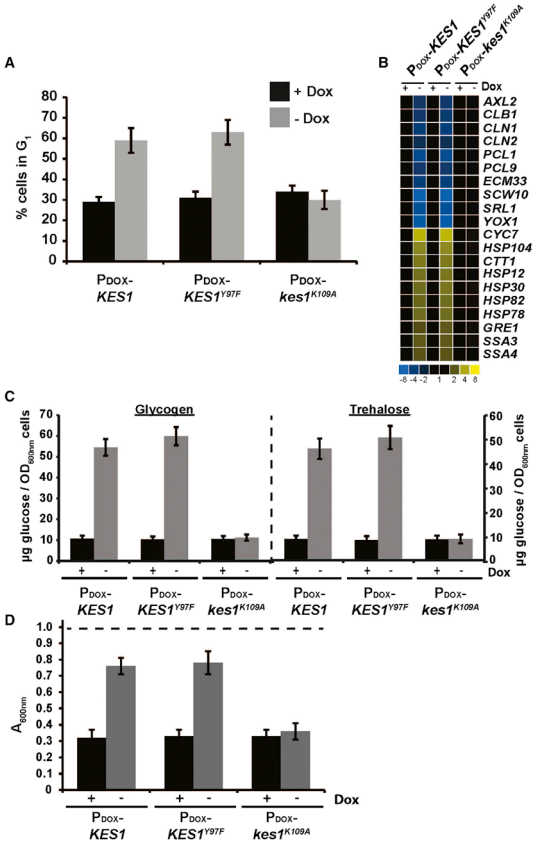

Figure 11 The quiescence response is activated upon Kes1-induced cell-cycle arrest

WT cells harboring the indicated plasmids were cultured in synthetic defined medium lacking uracil ± Dox as indicated. All experiments represent the averages of three independent biological replicates, and error bars indicate standard deviations. (A) Asynchronous cultures were fixed and stained with propidium iodide and the cell-cycle distribution was determined based on genome content by fluorescence-activated cell sorting analysis. Plotted is the percentage of cells in G_1. (B) Total RNA fractions were isolated and Msn2/4 and Gis1 target gene expression was surveyed by qRT-PCR and normalized to *ACT1* gene expression. (C) Glycogen and trehalose were extracted and hydrolyzed enzymatically to glucose with amylase and trehalase, respectively. Glucose was quantified and normalized per OD_{600} of cells. (D) Cells were washed and resuspended in water to an initial density of OD_{600} of ~0.9 (starting OD_{600} indicated as dashed line at top) prior to treatment with zymolyase 20T (150 µg/mL) for 30 min. Cell lysis was assessed by scoring the reduction in the OD_{600} of the suspended cell cultures.

another round of cell division. The MBF/SBF regulon defines a set of genes whose expression is required to negotiate the G_1/S transition or START (Spellman et al., 1998; Zaman et al., 2008). Transcription of multiple genes regulated by MBF and SBF was reduced ≥3-fold relative to control in otherwise wild-type (WT) yeast cells programmed for elevated (and doxycycline-repressible) expression of Kes1 or Kes1^{Y97F} (a dominant-active Kes1 defective in sterol-binding but competent for PtdIns-4-P binding; (Im et al., 2005; Mousley et al., 2012). The affected genes included those encoding G_1 cyclins (*CLN1*, *CLN2*, *PCL1*, *PCL2*, *PCL9*), a gene encoding a a gene encoding a homeobox transcription factor that promotes early cell-cycle box gene transcription (*YOX1*), and *AXL2* whose product specifies spatial organization of bud emergence from the mother cell during G_1 (Figure 11B). That reduced *AXL2* expression was of physiological significance was validated by the abnormal bipolar budding phenotype exhibited by Kes1-overexpressing haploid cells (Figure A-1A). Bipolar budding is a signature property of diploid yeast with normal Axl2 levels. Reduced transcription of MBF/SBF-controlled genes were not observed in cells expressing the nonfunctional Kes1^{K109A} defective in PtdIns-4-P binding (Li et al., 2002; de Saint-Jean et al., 2011), nor were these observed in cells where *KES1* or *kes1*^{Y97F} transcription was repressed by Dox (Figure 11B).

Reciprocally, Msn2/4- and Gis1-dependent transcriptional responses were activated in yeast with elevated Kes1 activity. Both Kes1- and Kes1^{Y97F}-arrested cells displayed ≥3-fold elevations in Msn2/4 and Gis1 target gene expression relative to control (*HSP12, HSP78, HSP82,* and *HSP104*, and *SSA3*, *GRE1,* and *CTT1*; (Figure

11B). Those derangements were not observed in cells expressing Kes1^{K109A}, nor in cells where ectopic *KES1* or *KES1*^{Y97F} expression was repressed by Dox. Activation of the Msn2/4 and Gis1 regulon is a hallmark of cells transitioning into quiescence in response to nutritional stress (Beck & Hall, 1999; Pedruzzi et al., 2000).

Kes1/Kes1^{Y97F}-arrested cells displayed metabolic signatures of quiescent cells as well. The storage carbohydrate glycogen and the stress protectant trehalose accumulate in yeast transitioning into quiescence (Lillie & Pringle, 1980). Both metabolites precociously accumulated in Kes1- and Kes1^{Y97F}-arrested cells incubated under nutrient-replete conditions, but not in cells expressing Kes1^{K109A} (Figure 11C). Phosphorylated long-chain sphingoid base (LCBP) accumulation is repressed by the Pho85 cyclin, and elevated LCBP represents another metabolic signature of quiescent cells (Lester et al., 2013). Intracellular LCBP levels of both the dihydro- and phyto-classes were dramatically increased in Kes1- and Kes1^{Y97F}-arrested yeast relative to control (Figure A-2B). Moreover, quiescent yeast exhibit reinforced cell walls. This property was scored by resistance to zymolyase digestion (Krause & Gray, 2002). Either Kes1- or Kes1^{Y97F}-overexpressing induced zymolyase resistance to cells cultured in nutrient-rich media (Figure 11D). Elevated Kes1^{K109A} expression had no such effect.

Kes1 antagonizes PKA Signaling

Entry into quiescence requires the balanced downregulation of both TORC1 (NH_4^+-dependent) and protein kinase A ([PKA]; carbohydrate-dependent) pathways for proliferative signaling (Wei et al., 2008). Two readouts confirmed PKA signaling was downregulated in Kes1/Kes1^{Y97F}-arrested yeast. First, PKA-catalyzed phosphorylation

of the model substrate choline kinase (Cki1; (Ramachandran et al., 2011) was reduced in Kes1/Kes1^{Y97F}-arrested cells, but not in cells expressing Kes1^{K109A} (Figure 12A). Second, processing bodies (P-bodies) are sites for storage, degradation and quality control of translationally repressed mRNAs. These structures, marked by Dcp2 and Xrn1, accumulate in cells as cytoplasmic puncta when PKA signaling is depressed (Ramachandran et al., 2011). Elevated Kes1/Kes1^{Y97F} expression (but not of Kes1^{K109A}) induced robust formation and stable maintenance of cytoplasmic Dcp2- and Xrn1-positive P-body puncta (Figure 12B).

Kes1-Chaperoned Entry into Quiescence Is Rim15 Dependent

The Rim15 kinase regulates exit from the cell cycle into quiescence (Cameroni et al., 2004; Swinnen et al., 2006). Ras/PKA, TORC1, and Pho85 cyclin-dependent kinase phosphate-sensing pathways promote cell proliferation, and inhibit entry into quiescence, by attenuating Rim15 activity in response to nutrient availability. If Kes1 operates upstream of Rim15 in the quiescence pathway, Rim15 activity will be required for entry of Kes1/Kes1^{Y97F}-overexpressing cells into quiescence. Indeed, *rim15Δ* cells were resistant to Kes1/Kes1^{Y97F}-overexpression (Figure 12C). Rim15-deficient cells also failed to present the quiescence signatures typically associated with Kes1/Kes1^{Y97F}-mediated growth arrest. That is, neither glycogen nor trehalose accumulated in *rim15Δ* mutants induced for Kes1/Kes1^{Y97F} expression upon withdrawal of Dox from the medium (Figure 12D), and *rim15Δ* mutant cell walls failed to acquire zymolyase resistance (Figure 12E). Steady-state Kes1 and Kes1^{Y97F} levels were appropriately elevated in *rim15Δ* cells after Dox withdrawal.

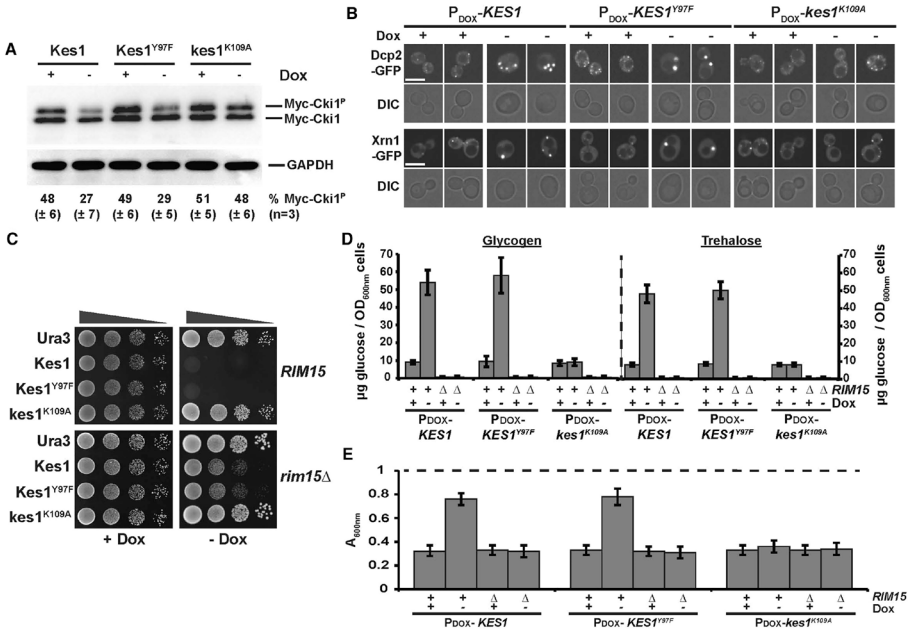

Figure 12 Kes1-dependent cell-cycle arrest exhibits reduced PKA signaling and is Rim15p dependent

(A) Left panel: WT yeast co-transformed with YCp(*PCUP1::myc-CKI1*), and either YCp(*PDOX::KES1*), YCp(*PDOX:: KES1*^{Y97F}), or YCp(*PDOX::kes1*^{K109A}) were cultured in selective media containing 10 µg/mL Dox. Subsequently, *KES, KES1*^{Y97F}, or *kes1*^{K109A} expression was induced for 12 hr (–Dox), or not (+Dox; 10 µg/mL), and cells were challenged with CuSO4 (100 µM for 1 hr) to induce myc-Cki1p expression. Lysates were prepared, normalized for total protein (10 µg loaded), and phosphorylated and non-phosphorylated myc-Cki1species and GAPDH were visualized by immunoblotting with anti-myc and anti-GAPDH antibodies, respectively. Phosphorylated and non-phosphorylated myc-Cki1species (myc-Cki1^{P} and myc-Cki1, respectively) and GAPDH are identified on the left. Fractional proportion of phosphorylated myc-Cki1 as determined by densitometric analysis using image lab software (Bio-Rad) is shown at the bottom. Experiments represent the average of three independent biological replicates. (B) Yeast cells expressing either Dcp2-GFP or Xrn1-GFP were transformed with the indicated plasmids and cultured in uracil-free medium ± Dox (10 µg/mL), as indicated, at 30°C. GFP profiles are shown with corresponding DIC images. Scale bar, 5 µm (C) WT (BY4742) and isogenic *rim15Δ* cells carrying the indicated plasmids were spotted in 10-fold dilution series on uracil-free media ± Dox (10 µg/mL) and incubated at 30°C. Images were taken after 72 hr of incubation. (D) Glycogen and trehalose were enzymatically hydrolyzed to glucose and quantified, as described in the legend to Figure 2.1C, in WT or *rim15Δ* cells harboring YCp(*PDOX::KES1*), YCp(*PDOX:: KES1*^{Y97F}), or YCp(*PDOX::kes1*^{K109A}), and cultured in synthetic defined medium lacking uracil ± Dox (10 µg/mL; black and gray bars, respectively). (E) WT and *rim15Δ* yeast (as indicated), harboring YCp(*PDOX::KES1*), YCp(*PDOX:: KES1*^{Y97F}), or YCp(*PDOX::kes1*^{K109A}) plasmids, were cultured in synthetic defined medium lacking uracil ± Dox (10 µg/mL) as indicated, washed, and resuspended in water to an initial density of OD600 of ~1.0 (starting OD600 depicted as dashed line at top) prior to treatment with zymolyase 20T (150 µg/mL). Cell

lysis was assessed by scoring the reduction in the OD600 of the suspended cell cultures after 30 min of incubation. Data represent the average of three independent biological replicates.

Cells lacking Kes1p are less responsive to nutrient deprivation signals

Kes1p loss-of-function (LOF) mutants did not appropriately exit the cell cycle when confronted by nutrient limitation. Whereas *KES1* cells ceased to proliferate upon reaching a density of ca. 1.5×10^8 cells/mL (Figure 13A , 12–48 hr time points), parallel *kes1Δ* cell cultures consistently reached cell densities of ca. 3×10^8 cells/mL (Figure 13A, 12–48 hr time points). Cells lacking Kes1p ultimately arrested, and the DNA content of *kes1Δ* cell populations in stationary phase exhibited G_1 signatures indistinguishable from those of their isogenic *KES1*$^+$ counterparts (Figure 13B). However, *kes1Δ*-arrested cells were only ~75% of the size of arrested WT cells (Figure 13C). Thus, Kes1-deficient mutants were licensed to initiate one supernumerary round of cell division under nutrient-prohibitive conditions of such severity that cell expansion could no longer be supported.

The supernumerary cell division phenotype of *kes1Δ* cells suggested that Kes1p is part of the quiescence response, which is engaged when yeasts are challenged with nutrient deprivation. In support, survey of multiple metabolic signatures of quiescence demonstrated that *kes1Δ* cells were defective in mounting quiescence responses. Relative to WT cells, Kes1-deficient mutants showed ca. 2-fold reductions in the magnitude of glycogen and trehalose accumulation when starved (Figure 13D). Moreover, nutrient-stressed *kes1Δ* cell walls failed to acquire zymolyase resistance (Figure 13E).

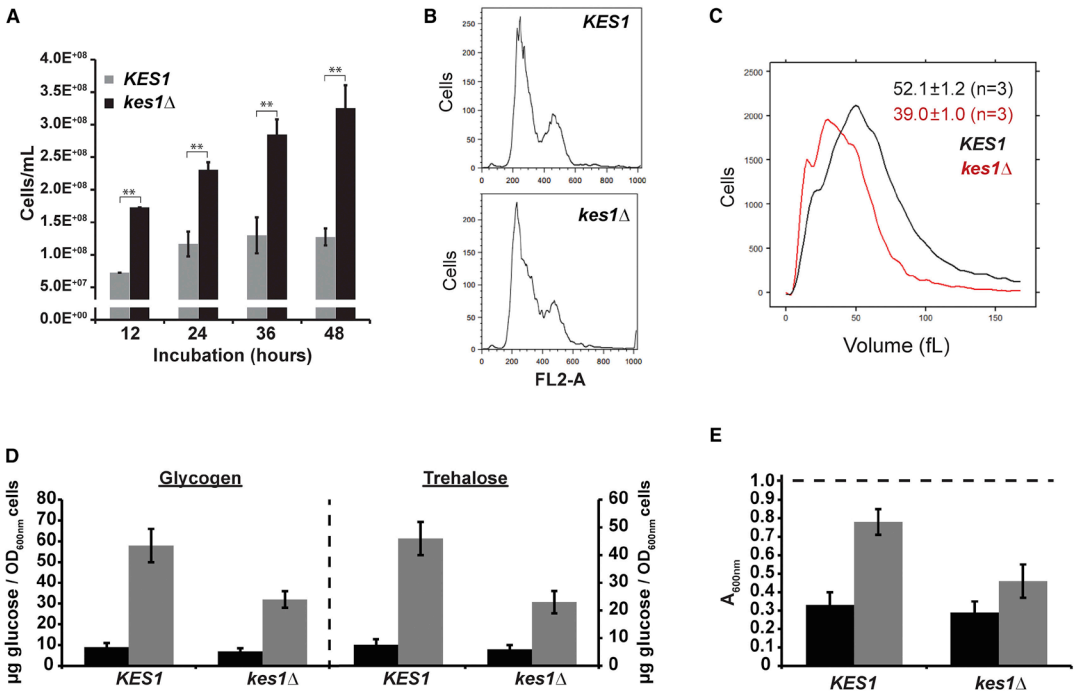

Chronological lifespan assays also showed *kes1Δ* cells displayed accelerated loss of viability when subjected to chronic nutrient limitation.

Figure 13 Cells lacking Kes1p respond aberrantly to nutrient-Restrictive environments

Unless otherwise indicated, all experiments represent the averages of three independent biological replicates, and error bars indicate SDs. (A) Cell densities of the indicated yeast strains (y axis) were quantified scored by light microscope hemacytometer counting at the indicated times as cells ceased to divide (x axis). Averages and standard deviations obtained from at least four independent experiments are shown. $^{**}p < 0.01$, Student's t test. (B) DNA content histograms of the indicated yeast strains collected at the 24 hr time point shown in (A) were generated by flow cytometry analyses. The number of cells analyzed in each case (y axis) is plotted as a function of fluorescence per cell (FL2-A; x axis). (C) Cell size histograms of the indicated yeast strains collected at the 24 hr time point shown in (A) represent the distributions produced by channelyzer cell volume measurements (>30,000 individual cells measured per biological replicate). Cell number is plotted as a function of cell volume (in fL). (D) Glycogen and trehalose were extracted from logarithmic (black bars) and stationary phase (gray bars) WT and *kes1Δ* cells grown in nutrient-rich media (YPD), hydrolyzed enzymatically to glucose, and glucose was quantified and normalized per OD600 cells. (E) WT and *kes1Δ* yeast were cultured in YPD to logarithmic (black bars) and stationary phase (gray bars), washed and resuspended in water to a density of OD600 of ~0.9 (indicated as dashed line at top) prior to treatment with zymolyase 20T (150 µg/mL). Cell lysis was assessed by the reduction in the OD600 of suspended cell cultures after 30 min of incubation.

Sec14p and Kes1p function in cell-cycle control in cycling cells

Kes1p antagonizes Sec14p and PtdIns-4-P signaling in the context of membrane trafficking through the TGN-endosomal system. Hence, we investigated whether introducing a *sec14*^{ts} allele into *kes1Δ* cells restored their ability to arrest properly in the face of nutrient exhaustion. Indeed, the license to undergo the supernumerary round of cell division in nutrient-prohibitive environments was partially suppressed in *sec14-1*^{ts} *kes1Δ* cells. Notably, this phenotypic suppression was evident for cells cultured at a permissive temperature (30°C), where the *sec14-1*^{ts} gene product retains sufficient activity to support WT kinetics of bulk membrane trafficking through the secretory and TGN/endosomal pathways.

We examined whether the antagonistic relationship between Sec14p and Kes1p was manifested in cycling cells in nutrient-replete medium. During exponential growth in rich media (YPD), *sec14-1*^{ts} cells exhibited doubling times that were ca. 10% longer than those of isogenic *SEC14* cells (108.7 ± 2.2 versus 93.4 ± 1.3 min, $p < 0.05$, Student's t test). This phenotype was reversed by Kes1p LOF, as *sec14-1*^{ts} *kes1Δ* cells exhibited WT population doubling times (92.6 ± 6.4 min). The population doubling time and DNA content of asynchronous and exponentially dividing *kes1Δ* cells did not differ from the corresponding parameters of isogenic *KES1* cells (Figure 14A).

However, *kes1Δ* and *sec14-1*^{ts} cells had altered size homeostasis. Compared with WT, *kes1Δ* cells were slightly smaller, while *sec14-1*^{ts} cells were larger (Figure 14B, left). These differences in the population mean cell size were not due to differences in birth size of these strains (Figure 14B, right), and the large cell size of *sec14-1*^{ts} cells

was corrected in *sec14-1*^{ts} *kes1Δ* cells (Figure 14B, left). "Bypass Sec14" mutations that inactivate PtdCho synthesis via the CDP-choline pathway (*pct1Δ*; Cleves et al., 1991) failed to reduce the size of *sec14-1*^{ts} cells (Figure 14B).

Since the decision to initiate a new round of cell division in response to nutrient signaling is exercised in G_1, we examined cell-cycle progression of highly synchronous early-G_1 daughter cells obtained by centrifugal elutriation. This approach holds the advantage that cell-cycle synchrony is achieved without applying arrest and release regimens that uncouple cell growth from cell division (e.g., shift of *cdc*^{ts} mutants to restrictive temperatures or pheromone arrest). The elutriated early-G_1 cells were allowed to progress in the cell cycle, and evaluated in a time course by scoring the incidence of budded cells, and the volume of cells, with a channelyzer. Since initiation of DNA replication in yeast is coupled to the formation of a bud (Johnston et al., 1977) the critical size is defined as the size at which 50% of the cells in a synchronous population have initiated a new round of cell division. *KES1*$^{+}$ and *kes1Δ* cells increased in size at the same rate (Figure 9C, left), and exhibited the same critical size (Figure 14C, right). However the critical size of *sec14-1*^{ts} cells was larger than that of isogenic WT cells (47.9 ± 2.1 versus 43.9 ± 1.8 fL, p = 0.003, Student's t test; Figure 14C, right). Because *sec14-1*^{ts} mutants increased in size at WT rates at 30°C (Figure 14C, left), but did not commit to divide until cells reached a larger critical size, their G_1 phase was extended. This protracted G_1 phase, in conjunction with the increase in G_2/M DNA content observed for *sec14-1*^{ts} cells (consistent with a second delay in mitosis; data not shown), accounted for the slower doubling time of *sec14*^{ts} cells at 30°C.

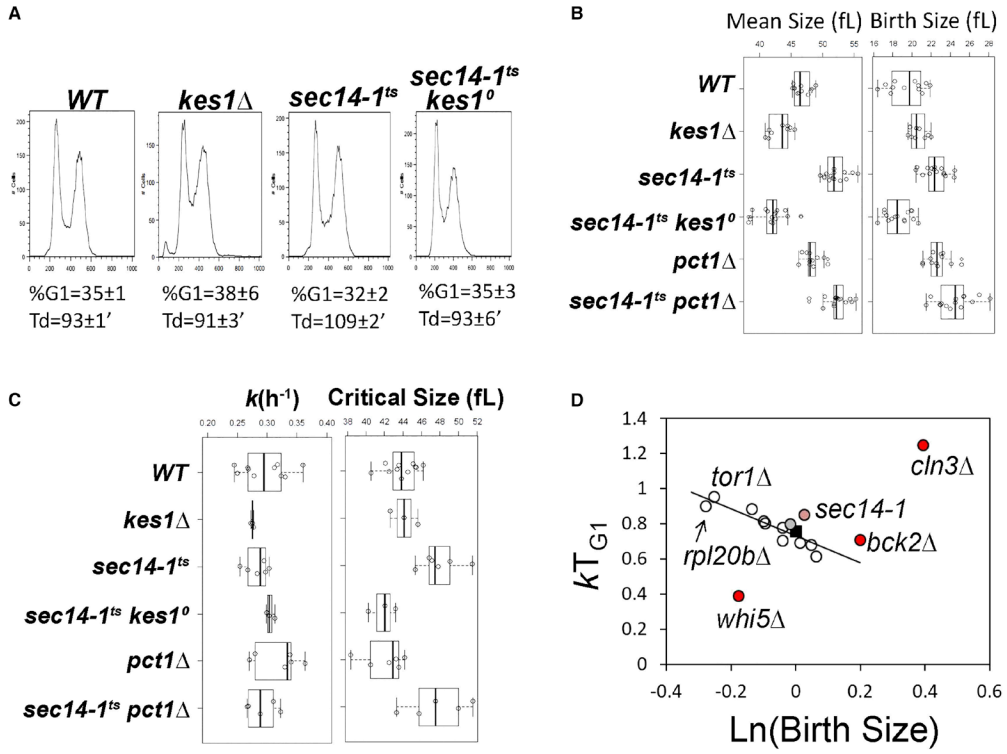

Figure 14 Mutual antagonism of Kes1p and Sec14p in cell-cycle control

(A) DNA content histograms were determined by flow cytometry. Fluorescence per cell (FL2-A) is plotted on the x axis, while the number of cells analyzed for each condition is plotted on the y axis. The average of the fractional representation of cells with G1 content in the population (% G1), and standard deviations (n = 6), are shown, along with the corresponding generation times (Td) in each case. Genotypes are identified at top. (B) Boxplots reporting the mean and birth cell size (y axis, in fL) of asynchronously proliferating populations of yeast with the indicated genotypes. Each symbol (open circle) corresponds to an independent biological replicate where 30,000–150,000 individual cells were measured for each replicate. (C) Boxplots depicting the specific rate of cell size increase, k (in hr^{-1}, left panel), and critical size (in fL, right panel) of synchronous cells of the indicated strains are shown. (D) The relative growth in size during the G1 phase (*k*TG1, y axis) for the indicated mutants are plotted as a function of the natural logarithm of normalized birth size values (WT = 1). The line depicts the linear fit (obtained with the regression function of Microsoft Excel) of data from all mutants. Established cell-cycle regulator mutants are shown as controls (in red; *whi5*, defective in the repressor of passage through G1; *cln3*, defective in a G1 cyclin; *bck2*, a transcriptional activator of G1 cyclins. Values for WT (black square), the *sec14-1*^{ts} mutant (light red), and *sec14-1*^{ts} *kes1Δ* cells (gray) are highlighted.

A proper coupling between cell growth and division was re-established in *sec14-1*^{ts} cells by Kes1 LOF, even though *kes1Δ* mutants by themselves had normal critical size and rate of size increase under nutrient-replete conditions. The corrective effects upon Kes1 LOF were specific because loss of Pct1 (i.e., an independent bypass Sec14 condition) failed to restore a proper critical size to *sec14-1*^{ts} cells (Figure 14C, right).

sec14^{ts} *Mutant Exhibits an Unusual Cell Size Control Phenotype*

The critical size data obtained from synchronously cycling cell cultures suggested *sec14-1*^{ts} cells, despite their normal rates of cell size increase, did not correctly register that they had grown sufficiently to commit to another round of cell division. This defect was visualized by plotting the logarithm of birth size against relative rate of cell size increase in the G_1 phase of the cell cycle (Figure 14D). Such plots relate the coherence of cell size control mechanisms, and the relevant values for *sec14-1*^{ts} mutants were compared with analogous values for a series of mutants analyzed previously (Soma et al., 2014). The increased cell growth requirements of *sec14-1*^{ts} yeast for the commitment of these cells to a new round of cell division were clear in such representations of the data.

The *sec14-1*^{ts} critical size phenotype was unusual in that mutants in growth control processes (e.g., the *rpl20b* ribosomal protein gene deletion) attain degrees of overall cell growth from birth to START that are indistinguishable from WT cells (Figure 14D). By contrast, the *sec14-1*^{ts} phenotype was qualitatively similar to the delay observed in cells lacking the G_1 cyclin Cln3, and was of at least the same magnitude as that observed upon loss of the Bck2 cell-cycle regulator which acts in parallel with Cln3 (Di Como et al., 1995). This delay was corrected by Kes1 LOF (Figure 14D).

Cell size and cell division phenotypes are associated with defects in other ORP proteins

In addition to Kes1p, yeast express three Kes1-like "short" ORPs (Osh5p, Osh6p, and Osh7p) and three "long" versions (Osh1p, Osh2p, and Osh3p). The functional differences between Kes1p and other members of the yeast ORP family were evident in: (1) phenotypic bypass Sec14p contexts (Figures 15A and Figure A-3A), and (2) CPY pulse-chase trafficking assays assessing bypass Sec14 phenotypes (Figures 15B and Figure A-3B). To determine whether cell-cycle dysregulation associated with Kes1p LOF was a unique property, we examined cells carrying deficiencies in individual members of the Osh protein family. Again, Kes1p LOF was unique in its ability to restore proper size homeostasis to exponentially growing *sec14-1*^{ts} cells at 30°C, and in reducing mean cell size of exponentially growing cells (Figure 15C).

In other contexts, however, loss of Osh protein function did evoke phenotypes similar to those associated with *kes1Δ*. For example, Osh1p, Osh3p, Osh6p, or Osh7p LOF restored WT doubling times to *sec14-1*^{ts} mutants (Figure A-3C). Moreover, as was the case for *kes1Δ* mutants, nutrient-deprived cells lacking any single Osh protein (other than Osh5) inappropriately passed through G_1 into another round of cell division (Figure A-3D). Analyses of *osh1Δ* and *osh6Δ* cell size profiles during starvation demonstrated that those cells phenocopied *kes1Δ* cells in their reduced cell size upon arrest. Thus, activities of other Osh proteins in cell proliferation resemble, but are not perfectly redundant with, those of Kes1p.

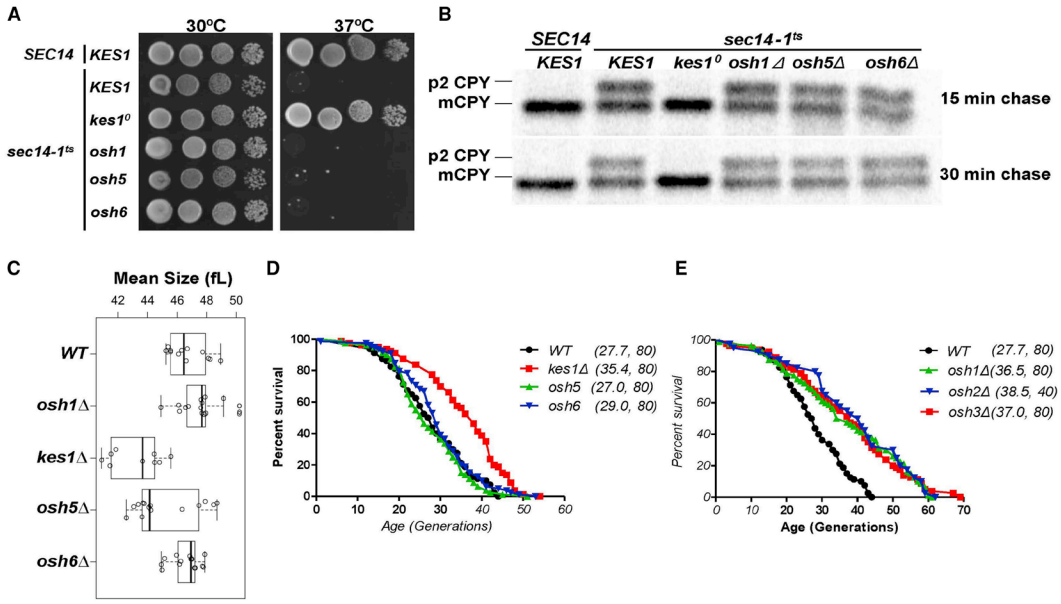

Figure 15 Functional specification of yeast ORPs

(A) *SEC14* or *sec14-1*^{ts} yeast (as indicated to the left of vertical line) with either a WT complement of yeast ORPs, or the indicated ORP deletion mutations (indicated to the right of the vertical line), were dilution spotted onto YPD agar and incubated at the indicated temperatures for 48 hr. Growth of *sec14-1*^{ts} derivative strains at 37°C identifies "bypass Sec14" phenotypes. (B) Yeast strains of the indicated genotype (at top) were cultured to mid-logarithmic growth phase at 30°C, shifted to 37°C for 2 hr, and pulse-radiolabeled with [^{35}S]amino acids for 30 min. After chase with excess unlabeled methionine and cysteine for the indicated times (at right), CPY species were immunoprecipitated from clarified lysates, resolved by SDS-PAGE, and visualized by autoradiography. p2 CPY and mCPY forms are identified at the left. (C) Boxplot reporting the mean cell size (in fL) of asynchronously proliferating populations of yeast with the indicated genotypes (at the left) in exponentially growing cultures. Each symbol (open circle) corresponds to an independent biological replicate consisting of 30,000–150,000 individual cells. (D and E) Survival curves for *MAT*α *kes1Δ* cells (BY4742 derivative) cells (red), compared with otherwise isogenic and experiment-matched *KES1*$^{+}$ cells (black), and cells carrying individual deletions in the indicated genes encoding the short Osh proteins (*osh5Δ* cells, green; *osh6Δ*, blue) (D), and survival curves for *MAT*α *KES1* cells (black; BY4742) compared with otherwise isogenic and experiment-matched cells (black) carrying deletions in the indicated long Osh protein-encoding genes (*osh1Δ* cells, green; *osh2Δ*, blue; *osh3Δ*, red) (E). Mean lifespans are shown in parentheses, along with the number of cells assayed.

Kes1p and long ORP defects extend replicative lifespan

As cells deficient in activities of Kes1 or the other Osh proteins (other than Osh5) showed G_1 control defects, we determined the effects of Kes1 LOF and of other Osh protein deficiencies on broader aspects of cell aging and longevity. Those parameters were interrogated in the context of replicative lifespan, i.e., the number of divisions mother cells undergo before reaching senescence. Kes1p LOF extended the mean and maximal replicative lifespan of cells continuously cultured in nutrient-replete media (Figure 15D). In those experiments, the WT strain exhibited a replicative lifespan of 27.7 generations, whereas the *kes1Δ* derivative exhibited an extended replicative lifespan (35.4 generations). LOF of any one of the three other "short" Kes1-like yeast ORPs had no such effect (Figure 15D). However, LOF of any one of the three "long" ORPs extended replicative lifespan (Figure 15E). Moreover, the small cell size of *kes1* mutants is consistent with those of other long-lived mutants with extended replicative lifespan (He et al., 2014). These findings suggest a trade-off between chronological and replicative lifespan assays for Kes1p activity. That is, Kes1p LOF mutants carry greater replicative potential, but are impaired in their ability to enter a growth-arrested state conducive to long chronological lifespan.

Acetylation of Kes1p residue K109 inactivates lipid Exchange in vitro

Kes1 involvement as a physiological brake on progression through START raises questions regarding how Kes1 activity is itself regulated. Two independent profiling studies of the yeast acetylome identify Kes1 as a protein modified at as many as nine lysine residues (Figure 16A; Henriksen et al., 2012; Madsen et al., 2015). To assess the

significance of each modification, Ala was substituted for each acetylated Kes1p Lys residue, and the activity of each protein was evaluated in a bypass Sec14p complementation assay, where Kes1p LOF permits growth of *sec14*^{ts} cells at 37°C. K_{109} was the only site for which an Ala substitution ablated Kes1 activity in cells (Figure 16A). This defect was not for trivial reasons as Kes1^{K109A} is a stable protein *in vivo* (X. Li et al., 2002). The K_{109} acetylation was of special interest because K_{109}: (1) sits within the invariant motif that defines the ORP superfamily (Figure 16A; (X. Li et al., 2002), and (2) forms a critical contact with the PtdIns-4-P molecule that occupies the Kes1 lipid-binding pocket (Figure 16B; de Saint-Jean et al., 2011). Thus, K_{109} acetylation potentially compromises the Kes1::PtdIns-4-P interaction.

To determine the effect of K_{109} acetylation on PtdIns-4-P binding, Kes1^{AcK109} was purified, and the site-specific acetylation was confirmed (Figure A-4). Kes1 proteins carrying the inactivating K_{109}A, the acetylation-mimetic K_{109}Q, and non-acetylatable K_{109}R substitutions were also purified. Activities of those proteins were then assessed in a liposome-based PtdIns-4-P extraction assay. Relative to Kes1p, the Kes1^{K109A}, Kes1^{K109Q}, Kes1^{K109R}, and Kes1^{AcK109} proteins all exhibited reduced abilities to extract PtdIns-4-P from liposomes *in vitro* (Figure 16C).

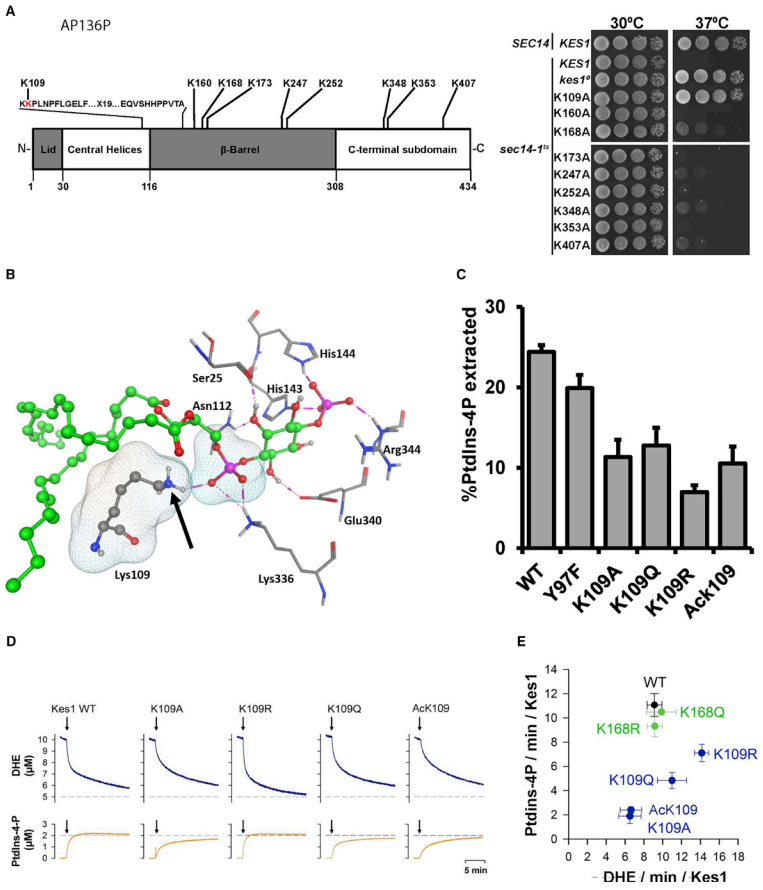

Figure 16 Functional analyses of Kes1p lysine acetylation

(A) Top panel: schematic representation of Kes1p is shown. The ORP signature motif is highlighted (X. Li et al., 2002), as are the lysine acetylation sites identified by acetylome profiling (Henriksen et al., 2012; Madsen et al., 2015). Bottom panel: *SEC14* or *sec14-1*^{ts} yeast expressing Kes1p, or the indicated K→A substitution mutants, were dilution spotted onto YPD agar and incubated at the indicated temperatures for 48 hr. The *SEC14 KES1* strain (positive control) and *sec14-1*^{ts} *KES1* (negative control at 37°C) are growth controls (two rows), the *sec14-1*^{ts}*, kes1*^{0} mutant defines the bypass Sec14 control (the *kes1*^{0} frameshift allele produces no Kes1 protein; third row). (B) K109A helps coordinate binding of the PtdIns-4-P head group. Kes1::PtdIns-4-P interactions are shown (PDB: 3SPW). Intermolecular H bonds between the PtdIns-4-P head group and the labeled Kes1p residues are shown by magenta dotted lines. PtdIns-4-P is rendered as green balls and sticks. Kes1p residues are shown in stick mode. Lys109 makes a critical H bond interaction with the phosphate oxygen of PtdIns-4-P (van der Waals molecular surfaces shown). The Lys amino group modified by acetylation is marked by the arrow. (C) PtdIns-4-P extraction activities for the indicated mutant/post-translationally modified Kes1 proteins were determined at 25°C in a 30 min endpoint format (see the STAR Methods). Mean ± standard deviations from three independent experiments are shown. (D) Real-time DHE and PtdIns-4-P transport kinetics measured with Kes1 or versions bearing the indicated substitution for, or acetylation of, Lys109. Top panel: DHE transport. Bottom panel: PtdIns-4-P transfer. (E) Plot of initial DHE transfer rate versus initial PtdIns-4-P transfer rate for WT Kes1 and indicated mutant/post-translationally modified Kes1 proteins. Mean ± standard deviations from at least three independent experiments are shown.

It is not PtdIns-4-P binding/extraction in isolation, rather a heterotypic ergosterol/PtdIns-4-P exchange cycle, that is central to the biochemical mechanism of Kes1 function *in vivo* (Mousley et al., 2012; Moser von Filseck et al., 2015). Thus, the consequences of K_{109} acetylation were also analyzed in dehydroergosterol (DHE)/PtdIns-4-P lipid transfer assays that measure inter-liposomal exchange of those lipids *in vitro* (de Saint-Jean et al., 2011). Indeed, Kes1p was proficient in transfer of both DHE (~9 molecules/Kes1/min) and PtdIns-4-P (~12 molecules/Kes1/min). $Kes1^{K109A}$ and $Kes1^{AcK109}$ were each reduced only ca. 30% for DHE transfer activity relative to Kes1 (Figures 16D and 16E). By contrast, both $Kes1^{K109A}$ and $Kes1^{AcK109}$ exhibited ca. 6-fold reductions in PtdIns-4-P transfer activity. $Kes1^{K109Q}$ was also reduced for PtdIns-4-P transfer (~60% reduction relative to Kes1), although the mutant protein exhibited greater DHE and PtdIns-4-P transfer activity than did $Kes1^{AcK109}$. $Kes1^{K109R}$ showed a ca. 70% increase in DHE transfer activity, but only modest reduction in PtdIns-4-P transfer activity relative to WT Kes1 (Figures 16D and 16E). Purified $Kes1^{K168Q}$ and $Kes1^{K168R}$ represented controls and were at least as active as Kes1 for DHE and PtdIns-4-P transfer *in vitro* (Figure 16E).

Identifying Candidate KATs that Regulate the Kes1/Sec14 Signaling Axis

The biochemical data indicated that K_{109} acetylation is a viable mechanism for downregulating Kes1 activity *in vivo*, and that KATs and lysine deacetylases are important regulators of the Kes1 DHE/PtdIns-4-P exchange cycle in cells. Two screens identified candidate KATs that regulate Kes1 activity. The first took advantage of the $Kes1^{Y97F}$ PtdIns-4-P clamp whose expression is detrimental to yeast (Mousley et al.,

2012). The strategy was to assess the relative toxicity of Kes1^{Y97F} expression to mutants with deficiencies in each of the yeast KATs. Kes1^{Y97F} expression was controlled by a Dox-inducible promoter, and defects in KATs that acetylate K_{109} (i.e., compromise dampening of Kes1p activity) were expected to exacerbate yeast growth sensitivities to Kes1^{Y97F} expression. Whereas all KAT mutants exhibited growth profiles similar to the corresponding controls cultured under non-inducing conditions, the *eaf1Δ*, *rtt109Δ*, and *gcn5Δ* mutants were sensitized to Kes1^{Y97F} expression relative to WT controls (Figure A-5A).

The second screen assessed which KAT deficiencies further sensitized *sec14-1*^{ts} mutants to elevated temperatures. Because enhanced Kes1 activity is especially detrimental to growth of *sec14-1*^{ts} mutants (Fang et al., 1996; Li et al., 2002) such a phenotype was expected to be associated with LOF in KAT activities that downregulate Kes1 via K_{109} acetylation. Again, *eaf1Δ* and *rtt109Δ* alleles enhanced the temperature sensitivity of *sec14-1*^{ts} mutants (Figure A-5B). Whereas *gcn5Δ* showed no synthetic effects in this context, *elp3Δ* mutants prohibited growth of *sec14-1*^{ts} cells at 33.5°C. Thus, only *eaf1Δ* and *rtt109Δ* satisfied both of the genetic criteria for KATs that target Kes1 *in vivo,* with *eaf1Δ* consistently showing the most pronounced effects.

Eaf1 is a scaffolding component of the 13-subunit NuA4 KAT complex (Auger et al., 2008). Deficiencies in other subunits of the NuA4 complex also evoked *eaf1Δ*-like phenotypes. The *eaf7Δ* and *esa1*^{ts} (*esa1-L254P*; Clarke et al., 1999) mutations satisfied the dual criteria of rendering WT cells less tolerant of Kes1^{Y97F} toxicity, and enhancing temperature sensitivity for growth of *sec14-1*^{ts} cells (Figure A-5C). Moreover, those

growth deficits associated with NuA4 deficiencies were alleviated in *kes1*^{0} and *kes1*^{K109A} genetic backgrounds (Figure A-5D). Bypass Sec14 mechanisms associated with inactivation of the CDP-choline pathway for PtdCho biosynthesis failed to rescue growth of *sec14-1*^{ts} *eaf1Δ* double mutants at restrictive temperatures (Figure A-5E). These phenotypic data were reinforced by assays monitoring recycling of the Snc1 t-SNARE through the endosomal system to the plasma membrane (Figure A-5A), and CPY trafficking through the secretory pathway to the vacuole (Figure A-5B). These results identified Kes1p as a key non-histone target of the NuA4 KAT.

Kes1^{K109R} *Is Defective In Vivo*

If Kes1p regulation is a case of the NuA4 KAT complex tuning Kes1p activity via K_{109} acetylation, then the acetylation mimic Kes1^{K168Q} should not be functional *in vivo*. Moreover, expression of a non-acetylatable Kes1p that retains PtdIns-4-P and sterol-binding activities (i.e., Kes1^{K109R}) should phenocopy the G_1-arrest phenotypes that come with enhanced Kes1 or Kes1^{Y97F} expression. The first prediction was fulfilled while the second was not. Whereas Kes1 re-expression reversed the bypass Sec14p phenotype of *kes1* null mutants, Kes1^{K109A}, Kes1^{K109Q}, or Kes1^{K109R} re-expression was not able to do so (Figure A-7A), even though these K_{109} mutant proteins were stable *in vivo*. Similar conclusions were forthcoming from pulse-chase experiments where CPY-trafficking kinetics were examined (Figure A-7B). Kes1^{K109A}, Kes1^{K109Q}, or Kes1^{K109R} expression did not reverse the bypass Sec14 status of *kes1* null cells. Moreover, in contrast to Kes1p or Kes1^{Y97F}, elevated Kes1^{K109R} did not inhibit growth of WT or *sec14-1*^{ts} strains. Thus,

despite the fact that Kes1^{K109R} was nearly as active as the WT protein in a coupled DHE/PtdIns-4-P transfer assay *in vitro*, Kes1^{K109R} was nonfunctional *in vivo*.

Discussion

Understanding how ORPs are integrated into the eukaryotic lipid signaling program requires a description of their individual biological activities. Herein, we identify a role for Kes1p, and other ORPs, in regulating cell-cycle progression and replicative lifespan in yeast. Those findings outline four conclusions: (1) Kes1p functions as a key brake on progression through G_1 and initiation of a new round of cell division upon nutrient limitation, (2) the antagonistic actions of Kes1p and Sec14p in regulating PtdIns-4-P signaling extend from membrane trafficking to cell-cycle contexts where the Sec14/Kes1 lipid signaling axis plays an important role in coordinating cell growth with initiation of cell division in nutrient-replete environments, (3) Kes1p is a key non-histone target for acetylation by the NuA4 lysine acetyltransferase, and (4) other members of the yeast ORP family also exhibit activities consistent with stage-specific inhibitors of cell-cycle progression and regulators of replicative lifespan. These data report that Kes1p and Sec14p execute dual membrane-trafficking and cell-cycle functions, and nominate this pair of lipid-exchange proteins as components of a regulatory axis that coordinates TGN/endosomal lipid signaling with cell-cycle progression. Moreover, these results offer fresh perspectives for interpreting ORP function in cell-cycle control, and suggest that ORPs execute unappreciated “tumor-suppressor”-like activities in mammalian cells.

Kes1 promotes exit from the cell cycle into quiescence

Kes1p action as an inhibitor of progression through G_1 is manifested by excessive Kes1p activity overriding the nutrient-responsive pro-proliferative signals that drive progression through G_1 into another round of cell division and, reciprocally, Kes1 LOF resulting in the licensing of nutrient-deprived cells to initiate and complete one extra cell division. Interestingly, accurate recapitulations of this *kes1Δ* phenotype, and of the premature entry into quiescence associated with excessive Kes1p activity, are apparent in complex developmental settings where exit from the cell cycle must be precisely timed. *Drosophila* embryonic cells lacking the Cdk inhibitor Dacapo undergo one extra cell division before the mid-blastula transition, whereas premature Dacapo expression induces G_1 arrest (de Nooij et al., 1996; Lane et al., 1996). Moreover, we also note the phenotypes of yeast expressing excessive Cln2 G_1 cyclin activity resemble *kes1Δ* cells in their ability to pass through G_1 in the face of severe nutrient deprivation (Hadwiger et al., 1989).

Sec14p and Kes1p function at START in cycling cells

The Sec14/Kes1 signaling axis also operates in cycling cells at the commitment step before initiation of DNA replication. The larger critical size of *sec14-1*^{ts} cells indicates that these cells were unable to properly interpret that they had reached a sufficient size to commit to a new round of cell division. This defective coupling is qualitatively similar to that observed in cells deficient in the G_1 cyclin Cln3p and was corrected by Kes1p LOF. Hence, the Sec14/Kes1 axis not only regulates when cells stop dividing upon nutrient exhaustion, but also when cells initiate a new round of cell division in nutrient-rich

conditions. Importantly, those interactions were evident in growing cells and without bulk membrane-trafficking deficits. Kes1p specificity in this level of control deserves emphasis. Other mechanisms for bypass Sec14 that correct the trafficking deficits associated with Sec14p LOF failed to correct the inability of *sec14-1*^{ts} mutants to properly register critical size. These results point to more specialized roles for Sec14/Kes1-regulated PtdIns-4-P-dependent signaling in cell-cycle control (Figure 17). This specific pool relevant to cell-cycle control is either: (1) functionally distinct from other Sec14/Kes1-regulated PtdIns-4-P pool(s) dedicated to bulk membrane-trafficking functions, or (2) involves the same pool but cell-cycle control exhibits a higher threshold requirement for PtdIns-4-P signaling.

Kes1 is a key non-histone substrate for the NuA4p lysine acetyltransferase

The role of Kes1 as inhibitor of progression through the START checkpoint argues for tight regulation of its activity. One such mechanism involves lipid binding/exchange as Kes1p is a brake on TGN/endosomal PtdIns-4-P signaling. The strength of that brake is regulated by a heterotypic sterol and PtdIns-4-P binding/exchange cycle that is itself responsive to the availability of these lipids on TGN/endosomal membranes (Mousley et al., 2012). Our data indicate a second mechanism that involves K_{109} acetylation (Figure 12). This modification is an inactivating one as determined by both *in vivo* and *in vitro* assays. Those defects are reconciled by the unmodified K_{109} side chain engaging a PtdIns-4-P molecule in the Kes1 lipid-binding pocket (de Saint-Jean et al., 2011).

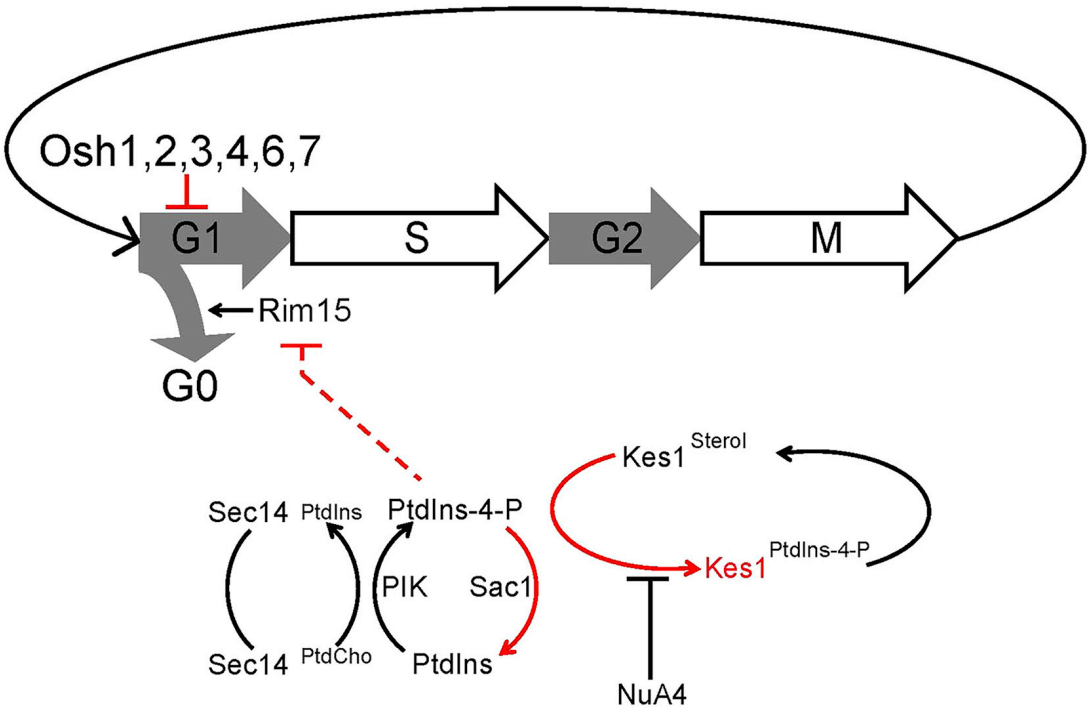

Figure 17 A Sec14/Kes1 PtdIns-4-P signaling axis in cell-cycle control

Heterotypic PtdCho/PtdIns exchange defines the machine by which Sec14 stimulates PtdIns 4-OH kinase-mediated production of a PtdIns-4-P pool that regulates progression through the G1 phases of the cell cycle. This signaling is antagonized by activity of the Sac1 PtdIns-4-P phosphatase and Kes1 binding and sequestering PtdIns-4-P from its effectors. The Kes1 brake is itself tuned by a heterotypic sterol/PtdIns-4-P exchange cycle and the activity of NuA4 KAT in acetylating K109. The Sec14/Kes1 checkpoint requires activity of the Rim15 kinase, and we propose this PtdIns-4-P pool is produced in a TGN/endosomal compartment. Functionally distinct, roles for other Osh proteins (other than Osh5) in regulating G1 progression are also indicated. Pathway brakes are highlighted in red.

Our data indicating that impaired activity of the NuA4 KAT complex enhanced Kes1p activity in cells, and that an unmodified K_{109} was required for those effects, argue that Kes1 is an important non-histone target for this enzyme complex. In that regard, synthetic genetic array studies identified strong interactions of NuA4p deficiencies with cell-cycle and membrane-trafficking mutants (Lin et al., 2008; Mitchell et al., 2008). Those interaction networks: (1) resemble those of Sec14 and Kes1 (Mousley et al., 2008), (2) establish that NuA4 potentiates PKA signaling (Filteau et al., 2015), and (3) show NuA4 depresses both expression of the Msn2/4 regulon and trehalase (Lindstrom et al., 2006; Mitchell et al., 2008). Such pleiotropic NuA4p interactions are interpreted to reflect broad alterations in the transcriptome as a result of deranged histone acetylation landmarks. We posit that these synthetic phenotypes also report NuA4-dependent modulation of Kes1p activity, which contributes to the role of NuA4 as global genetic "buffer" that governs cell fitness (Lin et al., 2008; Mitchell et al., 2008).

Mechanistic implications for Kes1p lipid-exchange activity

Regardless of whether one favors intermembrane lipid transfer models for Kes1p function (de Saint-Jean et al., 2011), or a lipid-exchange-dependent sensing mechanism that does not involve intermembrane lipid transfer (Mousley et al., 2012), there is general agreement that the Kes1 lipid-exchange cycle is intimately linked to its biological activity. Modulation of Kes1 activity by K_{109} acetylation has implications for how the Kes1 lipid exchange cycle relates to protein function in the cell.

The data also present a paradox that indicates we do not yet fully understand the details of Kes1 activity in cells. While $Kes1^{AcK109}$ was defective in the coupled

sterol/PtdIns-4-P countercurrent assay *in vitro*, the non-acetylated Kes1^{K109R} showed robust activity, with only modest reduction in PtdIns-4-P transfer. Yet, Kes1^{K109R} was nonfunctional *in vivo*. Those data suggest: (1) that Kes1^{K109R} represents a striking case where lipid transfer protein function has been uncoupled from lipid exchange, (2) that even modest defects in the PtdIns-4-P component of the heterotypic DHE/PtdIns-4-P exchange cycle are sufficient to render Kes1^{K109R} biologically inactive, or (3) that $K_{109}R$ interferes with, as yet, unidentified protein:protein or protein:lipid interactions critical for Kes1 biological activity. Either way, those results do not easily fit with models invoking intermembrane Kes1 lipid transfer mechanisms driven solely by differential sterol/PtdIns-4-P gradients.

ORPs and cell-cycle control

The long ORP Osh1 and short ORP Osh6 both exhibited features suggesting that these too operate as nutrient-regulated brakes on G_1 progression. Such Osh activities, while resembling those of Kes1, were not precise redundancies, as the corresponding phenotypes were apparent in the face of Kes1 activity. Rather, we interpret the data to report specific roles for these ORPs (Figure 12). Osh1 localization to the nuclear/vacuolar junction (and localization of its mammalian ortholog ORP1L to nuclear/lysosomal junctions) is interesting given the role of lysosomal compartments in nutrient signaling (Kvam & Goldfarb, 2004; Johansson et al., 2007). Osh6 is a PtdIns-4-P- and phosphatidylserine-binding protein (Maeda et al., 2013). We speculate that Osh6 couples its differential lipid-binding activities to other inputs into cell-cycle control.

While the LOF of the short ORPs, Osh5p or Osh6p, had no effect on replicative lifespan, Kes1 LOF (short ORP) or LOF of any of the three long ORPs (Osh1p, Osh2p, and Osh3p) extended both mean and maximal replicative lifespan. Mechanisms underlying the long replicative and short chronological lifespan of strains lacking Kes1 remain to be determined. Candidate pathways include TOR signaling and activation of the Gcn4 transcription factor (Mousley et al., 2012), altered trafficking processes related to PtdIns-4-P signaling (X. Li et al., 2002), and altered cell-cycle dynamics. Evidence to suggest that membrane trafficking integrates cell size homeostasis and cell-cycle progression (Anastasia et al., 2012), and building evidence for the involvement of cyclin-dependent kinase Cdk1 in this process (McCusker & Kellogg, 2012), suggest other possibilities.

Finally, the data hold implications for ORP involvement in mammalian cell-cycle control from the perspective of balancing cell proliferation with differentiation. High expression of Kes1-like short ORPs in mammalian tissues rich in post-mitotic cells is at least consistent with such a view (Johansson et al., 2003). We suggest that ORPs offer flexible mechanisms for coordinating endosomal membrane-trafficking flux and PtdIns-4-P signaling with cell-cycle progression, senescence, and transition of actively dividing cells into programs of differentiation and post-mitotic life.

Methods and materials

Expression vectors

Yeast and bacterial expression plasmids are listed in Key Resources. The P_{tet}-*KES1* and sterol-binding deficient mutant P_{tet}-*kes1*^{Y97F} vector was generated as

follows. *KES1* or *kes1*^{Y97F} and the tetracycline/doxycycline-responsive promoter were amplified by PCR (Q5® High-Fidelity DNA Polymerase kit, NEB #E0555S), using primers that includes homologous ends to each other and to the pRS415 vector (for P_{tet}-*KES1*) or pRS413 vector (for P_{tet}-*kes1*^{Y97F}). The linearized DNA sequences were cloned together by homologous recombination using SLICE (Zhang et al., 2008). Cloned vectors were isolated and confirmed by PCR. Tetracycline/doxycycline-inducible expression of *KES1*or *kes1*^{Y97F} was confirmed by immunoblot.

RT-PCR

Total RNA (1µg) templated reverse transcription to generate cDNA (20µl final volume). Expression of *AXL2, CLB1, CLN1, CLN2, PCL1, PCL9, ECM33, SCW10, SRL1, YOX1, CYC7, HSP104, CTT1, GPG1, GAD1, HSP12, HSP30, HSP82, HSP78, GRE1, SSA3* and *SSA4* relative to *ACT1* was determined using 0.5µl cDNA fraction as template and gene specific oligonucleotides as primers and the SensiFast Sybr Lo-Rox Kit (Bioline). Reactions were performed using a VIIA 7 Real-Time PCR System (Applied Biosystems).

Glycogen and trehalose measurements

Glycogen and trehalose were measured as described by (Parrou & François, 1997). Ten OD_{600nm} of cells were incubated in 250µl of 0.25M Na_2CO_3 at 95°C for 4 hr. After this the solution was adjusted to pH 5.2 with 150µl 1M acetic acid and 600 µl of 0.2M sodium acetate. For glycogen, samples were incubated overnight with 2 U/ml of amyloglucosidase isolated from *Aspergillus niger* (Sigma Aldrich) at 57°C with constant agitation. For trehalose, samples were incubated overnight with 0.05 U/ml of trehalose

(Sigma Aldrich) at 37°C. The glucose liberated from either glycogen or trehalose was determined by incubating 50µl of sample with 500µl of glucose oxidase reagent (Sigma) for 30 min at 37°C. The reaction was terminated with 500µl of 12M H_2SO_4 and the absorbance measured at 420 nm.

Zymolyase resistance measurements

Cell harboring YCp(P_{DOX}*::KES1*), YCp(P_{DOX}*:: KES1*^{Y97F}) or YCp(P_{DOX}*::kes1*^{K109A}) were cultured to OD_{600} < 0.05 in synthetic defined medium lacking uracil containing Dox. Cells were isolated, washed and cultured in synthetic defined medium lacking uracil ± Dox for 18 hrs to OD_{600} < 1.0. Zymolyase resistance assays were performed according to (Newman et al., 2005). Cells were grown in synthetic defined medium lacking uracil in the presence or absence of Dox at 30°C for the indicated times. Cells were isolated and resuspended in water at 1 OD_{600nm}/ml and incubated with zymolyase 20T (150µg/ml) (ICN Biomedicals) at 30°C for 5, 10, 20 and 30 minutes. Cell lysis was monitored by measurement the $OD_{600\ nm}$.

Cell cycle methods

Elutriation experiments and cell size measurements were performed as described by (Hoose et al., 2012). For elutriation experiments, cells were grown in YPD (1% $^{w}/_{v}$ yeast extract, 2% $^{w}/_{v}$ peptone, 2% $^{w}/_{v}$ dextrose) to a cell density of 1-5 X 10^7 cells/ml and loaded onto an elutriator chamber at a pump speed of 37 ml/min spinning at 3200 rpm (Beckman J-6M/E centrifuge). During all the centrifugation steps, the temperature in the centrifuge was 25°C. The elutriated small daughter cells were collected at 2400 rpm centrifuge speed and 42 ml/min pump speed, in tubes kept on ice.

The elutriated cells were recovered by centrifugation and re-suspended in fresh pre-warmed YPD medium, at a cell density of ca. 1 X 10^7 cells/ml. The elutriated cultures were then placed in a 30°C incubator and every 20 min we recorded their budding index and measured their cell size with a Beckman Z2 channelyzer. The geometric mean of the cell size of the population was recorded using the Accucomp software package of the instrument. Each cell size measurement represents the average of two technical duplicates taken at two different cell dilutions. The smoothened cell size histograms shown are the splines of the corresponding raw data, generated with the R software package "lattice".

Replicative lifespan assays were performed on YPD agar at 30°C by serial separations of daughter cells from mother cells using a manual micromanipulator equipped with a fiber-optic needle (Steffen et al., 2009).

Flow Cytometry

Yeast (5 OD_{600} units) were pelleted and fixed overnight in 70% (v/v) ethanol. Cells were washed with 1 ml of citrate buffer (50 mM sodium citrate, pH 7), briefly sonicated, resuspended in 1 ml of citrate buffer containing 0.25 mg/ml RNase A, and incubated overnight at 37°C. Cells were again washed in 50 mM sodium citrate, pH 7.0, resuspended in 1 ml of 50 mM sodium citrate, pH 7.0 containing 16 mg/ml of propidium iodide, and incubated at room temperature for 30 min. After a last wash in citrate buffer, cells were analyzed on a Beckman MoFlo flow cytometer.

Detection of Lysine Acetylation by Mass Spectrometry

Lysine-acetylated Kes1 were produced using the amber suppression method of (Hsu et al., 2016) where *E. coli* were cultured in Terrific broth supplemented with 0.2% arabinose, 5mM nicotinamide and 5mM Nε-Acetyl-L-lysine, and protein production was induced with IPTG at 16°C. In total, 4µg of purified protein (Kes1 or Kes1^{AcK109}) were digested with trypsin overnight. Resulting samples were analyzed by LC-MS/MS and acetylation sites were identified using a Mascot search engine (L. Mitchell et al., 2008).

PtdIns-4-P Extraction Assays

Extraction of [^{14}P]-PtdIns-4-P was measured as described (Goto et al., 2016). Liposomes (400 nm) composed of phosphatidylcholine (PtdCho), lactosyl-phosphatidylethanolamine (PtdEtn) and [^{14}P]-PtdIns-4-phosphate (86:10:4 molmol) were prepared by extrusion in liposome buffer (25 mM HEPES [pH 7.4], 150 mM, NaCl and 1 mM EDTA) and pre-cleared by centrifugation at 15,000xg for 5 min at 4°C. Extraction was measured by combining the appropriate Kes1p protein (100 pmol) with liposomes (400 pmol of PtdIns-4-phosphate) and 3 µg BSA in liposome buffer. After incubation at 25°C for 30 min, assays were placed on ice, *R. communis* agglutinin was added (10 µg) for 10 min and liposomes were sedimented by centrifugation at 15,000xg at 4°C for 5 min. [^{14}P]-PtdIns-4-phosphate was measured in supernatant fractions and PtdIns-4-P extraction was corrected for non-specific extraction (mock).

Lipids and Liposome Preparation for DHE and PtdIns-4-P Transfer Assays

1,2-dioleoyl-*sn*-glycero-3-phosphocholine (DOPC), brain L-α-phosphatidylinositol-4-phosphate (PtdIns-4-P), 1,2-dioleoyl-*sn*-glycero-3-phosphoethanolamine-N-(5-dimethylamino-1-naphthalenesulfonyl) (DNS-PE), and 1,2-dipalmitoyl-*sn*-glycero-3-phosphoethanolamine-N-lissamine rhodamine B sulfonyl (Rhod-PE) were from Avanti Polar Lipids. Dehydroergosterol (DHE) was from Sigma Aldrich. The concentration of the DHE stock solution in methanol was determined by UV-spectroscopy using an extinction coefficient of 13,000 $M^{-1}.cm^{-1}$.

Lipids, stored in stock solutions in $CHCl_3$ or methanol, were mixed at the desired molar ratios. Solvent was removed in a rotary evaporator under vacuum. For lipid films containing PtdIns-4-P, the mix was pre-warmed to 33°C for 5 minutes prior to drying. The films were hydrated in 50mM Hepes, pH 7.2, 120mM K-acetate (HK buffer) to obtain a suspension of multilamellar liposomes. After five thawing-freezing cycles with liquid nitrogen, the suspensions were extruded through polycarbonate filters of 0.2µm pore size using a mini-extruder (Avanti Polar Lipids). Liposomes were stored at 4°C in the dark when containing light-sensitive lipids (DHE, DNS-PE, Rhod-PE), and used within 2 days.

DHE and PtdIns-4-P Transfer Assays

DHE and PtdIns-4-P transport assays followed the protocols described (de Saint-Jean et al., 2011; Moser von Filseck et al., 2015) using purified recombinant His_6-tagged Kes1 proteins (X. Li et al., 2002). Experiments were carried out in a Shimadzu RF 5301-PC fluorimeter equipped with a cylindrical quartz cuvette. For measuring DHE transfer, a

suspension (570µl) of L_B liposomes (200µM lipids, final concentration) made of DOPC and containing 4% (mol/mol) PtdIns-4-P was incubated at 30°C under constant stirring in HKM (HK + 1mM $MgCl_2$) buffer. After 1 min, 30µl of L_A liposomes (200µM lipid final concentration) composed of 2.5% of DNS-PE and 5% DHE was added. After 3 min, Kes1 or the appropriate derivative was injected to a final concentration of 375nM. Lipid transport was measured by recording the DNS-PE signal at 525nm (bandwidth 10 nm) upon DHE excitation at 310nm (bandwidth 1.5nm). As the concentration of accessible DHE was equal to 10µM, the amount of DHE (in µM) transported from L_A to L_B membrane was equal to $10 * ((F-F_0)/(F_{max}-F_0))$ where F_{max} is the signal before Kes1 injection; F_0 is the signal measured upon total DHE extraction by 10mM methyl-β-cyclodextrin (Sigma). Liposomes and proteins were injected from stock solutions with Hamilton syringes through a guide in the cover of the fluorimeter.

To measure PtdIns-4-P transport, a suspension (570µL) of L_B liposome (200µM total lipid) composed of 2% Rhod-PE and 4% PtdIns-4-P was incubated with 250nM NBD-PH_{FAPP} at 30°C in HKM buffer under constant stirring. The concentration of accessible PtdIns-4-P (in the outer leaflet) is 4µM. After 1 min, 30µL of L_A liposome containing 10% DHE (200µM lipids, final concentration) were injected. After additional 3 min, Kes1 or mutant (375nM final concentration) was injected. PtdIns-4-P transport was followed by measuring the NBD signal at 530 nm (bandwidth 10nm) upon excitation at 460nm (bandwidth 1.5nm). The signal, which mirrors the redistribution of NBD-PH_{FAPP} between L_A and L_B liposomes, was normalized to determinate the amount of PtdIns-4-P transported by Kes1. For this, the NBD signal (F_{eq}) in a situation where

PtdIns-4-P is fully equilibrated between liposomes. NBD-PH_{FAPP} was mixed with L_A and L_B liposome (200μM total lipid each) that each contains initially 2% PtdIns-4-P. The fraction of PtdIns-4-P on the surface of L_B liposome, PtdIns-4-P_B/ PtdIns-4-$P_{T,}$ is equal to the fraction of PH_{FAPP} on L_B liposome and correspond to $F_{Norm} = 0.5*(F-F_0/F_{eq}-F_0)$ with F_0 corresponding to the NBD signal prior to the addition of Kes1 protein. The amount of PtdIns-4-P (in μM) transferred from L_B to L_A liposomes corresponds to $4*F_{Norm}$.

Fluorescence Microscopy

For GFP imaging, cells were grown in synthetic defined medium lacking uracil in the presence or absence of Dox at 30°C. Cells were then fixed in 3.75% formaldehyde and immobilized on concanavalin A coated slides and examined at 25°C. The imaging system employed a CFI plan apochromat lambda 100x oil immersion objective lens NA 1.45 mounted on a Nikon Ti-U microscope base (Nikon, Melville, NY) interfaced to a Photometrics CoolSNAP HQ2 high sensitivity monochrome CCD camera (Roper Scientific, Ottobrunn, Germany) or an Andor Neo sCMOS CCD camera (Andor Technology, Belfast, UK). A Lumen 200 Illumination System (Prior Scientific Inc., Rockland, MA.) was used in conjunction with a B-2E/C (465–495nm/515–555nm;EX/EM) or G-2E/C (528–553nm/590–650nm;EX/EM) filter set (Nikon, Melville, NY). Images were captured using the Nikon NIS Elements software package (Nikon, Melville, NY, version 4.10) and exported as .TIF files. Image analyses were performed using ImageJ (version 1.47t, National Institute of Health) and figures were constructed using Adobe Illustrator and Adobe Photoshop CS6 (version 15.0.0).

Metabolic Radiolabeling and CPY Immunoprecipitation

Yeast strains were grown in minimal media lacking methionine and cysteine to mid logarithmic phase (OD_{600nm} = 0.5) and radiolabeled with [^{35}S]-amino acids (Translabel; New England Nuclear; 100 μCi/ml). Chase was initiated by introduction of unlabeled methionine and cysteine (2 mM each, final concentration), and terminated by addition of trichloroacetic acid (5% w/v -- final concentration). CPY was pulled down from clarified cell-free lysates with rabbit polyclonal anti-CPY serum and radiolabeled CPY were resolved by SDS-PAGE and visualized by autoradiography (V. A. Bankaitis et al., 1986).

Quantification and Statistical Analysis

Data were quantified and analyzed as described in detail in the figure legends, figures, Results, and Method Details in STAR Methods. Statistical methods used included Student's t-test and one-way ANOVA, values are given as mean ± standard deviation and confidence intervals are identified. Exact definitions of n are identified throughout.

.

CHAPTER IV

TRANSLATIONAL CONTROL OF LIPOGENESIS LINKS PROTEIN SYNTHESIS AND PHOSPHOINOSITIDE SIGNALING WITH NUCLEAR DIVISION*

Summary

Continuously dividing cells coordinate their growth and division. How fast cells grow in mass determines how fast they will multiply. Yet, there are few, if any, examples of a metabolic pathway that actively drives a cell cycle event instead of just being required for it. Here, we show that translational upregulation of lipogenic enzymes in yeast increased the abundance of lipids and accelerated nuclear elongation and division. De-repressing translation of acetyl CoA carboxylase and fatty acid synthase also suppressed cell cycle-related phenotypes, including delayed nuclear division, associated with Sec14p phosphatidylinositol transfer protein deficiencies, and the irregular nuclear morphologies of mutants defective in phosphatidylinositol 4-OH kinase activities. Our results show that increased lipogenesis drives a critical cell cycle landmark and report a phosphoinositide signaling axis in control of nuclear division. The broad conservation of these lipid metabolic and signaling pathways raises the possibility these activities similarly govern nuclear division in mammals.

---

* This chapter is reprinted with permission from 'Translational control of lipogenesis links proteins synthesis and phosphoinositide signaling with nuclear division' by **Nairita Maitra**, Staci Hammer, Clara Kjerfve, Vytas A Bankaitis, & Michael Polymenis (2021). *Biorxiv*

Introduction

The sequential and essential action of acetyl-CoA carboxylase (Acc1p in yeast) and fatty acid synthase (FAS) make fatty acids in all organisms. Acc1p carboxylates acetyl-coenzyme A (CoA) to make malonyl-CoA (Al-Feel et al., 1992), which is subsequently consumed by FAS as the building block for fatty acid synthesis. Yeast FAS is made of two different polypeptides, α- (Fas2p) and β-subunits (Fas1p), in a 2.6 MDa $\alpha_6\beta_6$ dodecamer (Lomakin et al., 2007; Leibundgut et al., 2008; Jenni et al., 2007). The correct Fas1p and Fas2p stoichiometry is achieved by a mechanism where Fas1p controls *FAS2* mRNA levels (Wenz et al., 2001). Moreover, Fas1p initiates FAS assembly via a co-translational interaction with nascent Fas2p (Shiber et al., 2018; Fischer et al., 2020). The multiple catalytic activities of FAS iteratively add two carbons at a time from a malonyl-CoA donor to an acetyl-CoA acceptor. The reaction terminates after seven or eight cycles, generating 16-or 18-carbon fatty acids, respectively (Lomakin et al., 2007; Jenni et al., 2007).

There is intense contemporary interest in lipogenesis during cell division given the implications for cell proliferation (Storck et al., 2018). Higher levels of lipogenic enzymes are a near-universal marker of tumors (Kuhajda et al., 1994; Baenke et al., 2013; Beloribi-Djefaflia et al., 2016), and FAS is one of the few metabolic enzymes targeted in cancer clinical trials (NCT02595372, NCT02980029). Three lines of evidence suggest that *de novo* lipid synthesis impinges on events late in the cell cycle. First, the translational efficiency of acetyl-CoA carboxylase and fatty acid synthase mRNA transcripts peaks in mitosis (Blank et al., 2017; 2017). Second, the abundance of

lipids similarly peaks late in the cell cycle (Blank et al., 2020). The midbodies in human cells, where cleavage occurs at the end of the cell cycle, have a distinct lipid composition (Atilla-Gokcumen et al., 2014). Third, *de novo* lipid synthesis is essential for mitosis in humans (Scaglia et al., 2014) and yeast (Al-Feel et al., 2003; Schneiter et al., 1996).

Nuclear membrane dynamics are pronounced during mitosis. For example, there is a dramatic proliferation in new nuclear membranes during mitosis. This proliferation occurs irrespective of whether the mitosis is open (i.e., the nuclear envelope disassembles in mitosis as in animal cells) or whether it is closed (i.e., nuclear envelope integrity is maintained throughout mitosis as in fungi). In fission and budding yeast, loss-of-function mutations in lipid synthesis perturb the size and shape of the nuclear envelope (Witkin et al., 2012; Walters et al., 2014; 2012; Santos-Rosa et al., 2005Santos-Rosa et al., 2005; Kume et al., 2017; Zach & Převorovský, 2018; Siniossoglou, 2013). The evidence that lipid synthesis is required for cell division notwithstanding, it remains unclear whether lipid biogenesis promotes specific cell cycle events and, if so, what those events might be.

Sec14p is the founding member of a major family of phosphatidylinositol (PtdIns) transfer proteins (PITPs). Sec14p and other PITPs stimulate the activities of PtdIns 4-OH kinases by rendering PtdIns a superior substrate for these enzymes – thereby potentiating PtdIns(4)P-dependent signaling (Wang et al., 2019). Sec14p executes an essential cellular activity in promoting membrane trafficking from yeast Golgi/endosomal compartments, but this cellular requirement is obviated when lipid metabolism is appropriately altered. For example, inactivation of CDP-choline salvage

pathway for PtdCho synthesis relieves cells of the essential Sec14p requirement (Cleves et al., 1991). In addition to membrane trafficking, Sec14p also controls cell cycle progression (Huang et al., 2018). Reductions in Sec14p activity of insufficient magnitude to compromise cell viability nonetheless result in aberrantly larger cells that progress through the cell cycle more slowly with notable delays in progression through the G2/M phases (Huang et al., 2018). How Sec14p impinges on cell cycle progression and how it is functionally integrated with lipid synthesis in the cell cycle remains poorly understood.

Herein, we demonstrate that coordinate de-repression of *ACC1* and *FAS1* translation results in elevated lipogenesis that promotes nuclear division in yeast. Furthermore, we report that loss-of-function mutations in the conserved Sec14p delay nuclear division, and that de-repressing translational control of *ACC1* and *FAS1* not only corrects the delayed nuclear division associated with reduced Sec14 activity, but suppresses other mitotic phenotypes associated with Sec14p insufficiencies. Likewise, we document that loss of phosphatidylinositol 4-OH kinase activity deranges nuclear morphology, and that these phenotypes too are rescued by enhanced translation of *ACC1* and *FAS1* mRNAs. Taken together, these results identify translational control as a critical input for tuning lipid metabolism to progression through the cell cycle. The data also indicate that lipid synthesis is not only required for mitosis, but that it actively promotes nuclear division -- a key landmark of the eukaryotic cell cycle.

Results

Translational control elements in lipogenic enzymes

The translational efficiency of acetyl-CoA carboxylase and fatty acid synthase is upregulated late in the cell cycle and, in that regard, removing a uORF from the 5'-leader of the *ACC1* transcript de-represses the translation of *ACC1* (Blank et al., 2017) . The 5'-leader of *FAS1* is 551 nt-long (Xu et al., 2009), and has two uORFs (Figure 18A). Ribosome profiling experiments report that both *FAS1* uORFs are likely translated in *S. cerevisiae* (Ingolia et al., 2009). The longer and more distal uORF initiates from a non-AUG start codon. A uORF at the same position, albeit of varying length and sequence, is present in most *Saccharomyces* genomes, except in *S. mikatae*, where the AAG start codon is mutated to AAA (Figure B-1, top). The proximal uORF is short, encoding a six amino acid peptide, and it is well-conserved in the *Saccharomyces* genus (Figure B-1, bottom). There was a Tyr→Phe change in *S. kudriavzevii*, and a Phe→Leu change in *S. bayanus* (Figure B-1, bottom).

To test the role of translational control in fatty acid synthesis, a mutant yeast strain was generated where *cis* elements that could repress translation of *ACC1* and *FAS1* transcripts were inactivated. Simultaneous de-repression of both *ACC1* and *FAS1* translation was expected to increase metabolic flux through *de novo* lipogenesis pathways. Because the *FAS1* uORFs are likely translated in *S. cerevisiae*, and are well conserved in other species, their start codons were mutated. The *FAS1* uORF mutations were subsequently recombined into a yeast strain carrying the *ACC1* ORF mutation we

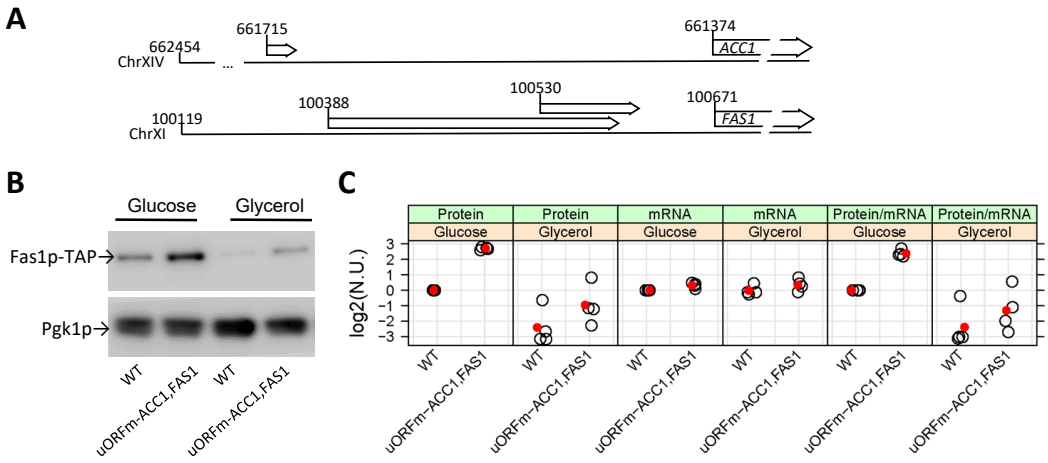

Figure 18 uORFs in *ACC1* and *FAS1*

A, The chromosomal coordinates of the 5'-leader sequences of the *ACC1* and *FAS1* transcripts. The 5'-ends are from (Xu et al., 2009). B, Steady-state Fas1p protein, and *FAS1* mRNA levels were measured in rich undefined media, differing in the carbon source (2% glucose or 3% glycerol) from the indicated strains carrying C-terminal TAP-tagged alleles of *FAS1* at their endogenous chromosomal locations. Protein levels were measured from immunoblots, a representative of which is shown. Transcript levels of *FAS1* and *UBC6* were quantified by Droplet Digital PCR, as described in Materials and Methods. The values in the strip charts depict the relative abundance of *FAS1* mRNA and protein in *uORFm-ACC1,FAS1* cells quantified from independent experiments. To obtain the normalized units (n.u.) on the y-axis, we first normalized for loading against the corresponding *UBC6* and Pgk1p values from the same samples. We then expressed these values as ratios against the corresponding values of wild-type *FAS1-TAP* cells, in which the uORFs are in place, from experiments run and analyzed in parallel.

had described previously (Blank et al., 2017). The strain carrying these three uORF mutations (*uORFm-ACC1,FAS1*) was also engineered so that the main *FAS1* ORF was TAP-tagged for purposes of protein surveillance (see Materials and Methods). As expected, asynchronous cultures of the triple uORF mutant produced elevated steady-state levels of Fas1p (Figure 18B). The ratio of the steady-state levels of the Fas1p protein over the *FAS1* mRNA was 3 to 4-fold higher in the uORF mutant cells compared to wild type cells (Figure 18C). These data were consistent with a translational de-repression mechanism for increased Fas1p expression.

To monitor Fas1p levels throughout the cell cycle, small early G1 wild-type and *uORFm-ACC1,FAS1* cells were isolated by centrifugal elutriation and Fas1p-TAP levels were examined as these cells progressed synchronously through the cell cycle (Figure B-2). Fas1p-TAP levels still oscillated in *uORFm-ACC1,FAS1* cells, albeit with dampened amplitude (Figure B-2). Acc1p levels were similarly periodic, with dampened amplitude, in the cell cycle when *ACC1* translation was de-repressed in cells lacking the *ACC1* uORF (Blank et al., 2017).

De-repressing translation of ACC1 and FAS1 alters lipid abundances

Two approaches were used to determine whether elevated levels of Acc1p and Fas1p in *uORFm-ACC1,FAS1* cells led to increased activity of these enzymes *in vivo*. The first was a bioassay where the sensitivity of wild-type and triple mutant cells to cerulenin was compared. Cerulenin is a validated inhibitor of fatty acid synthase that acts by binding and inhibiting the β-ketoacyl-acyl carrier protein (ACP) synthase domain of fatty acid synthase (Omura, 1976; Price et al., 2001). Whereas proliferation of wild type cells was

significantly reduced and then completely blocked at 1.5 and 2.5 μg/ml cerulenin, respectively, the *uORFm-ACC1,FAS1* cells were resistant to 2.5 μg/ml cerulenin (Figure B-2). The increased resistance of *uORFm-ACC1,FAS1* cells to cerulenin argues that translational de-repression of *ACC1* and *FAS1* leads to elevated activity of these lipogenic enzymes *in vivo*.

The second approach involved quantification of primary metabolites and complex lipids by GC-TOF MS, and CSH-QTOF MS/MS, respectively (See Materials and Methods). In these experiments, we examined cultures where glucose or glycerol served as sole carbon sources (Figure 19). Among the >300 metabolites that were confidently identified in cultures with glucose as sole carbon source, the alterations in metabolite abundance were almost entirely accounted for by alterations in the abundance of lipid molecular species. Increased levels of various molecular species of triglycerides (TG), phosphatidylinositol (PtdIns; PI), phosphatidylcholine (PtdCho; PC), phosphatidylethanolamine (PtdEtn; PE), and phosphatidylserine (PtdSer; PS) were recorded. A few species exhibited a lower abundance in *uORFm-ACC1,FAS1* cells and these represented the longer chain molecular species detected (PtdIns / PtdCho / PtdEtn 36:1; PtdCho 36:2; TG 50:1; TG 56:2). This pattern was reproduced in cultures where glycerol served as a carbon source although the roster of molecular species that were altered in abundance in glycerol conditions was expanded somewhat. We conclude that coordinate de-repression of *ACC1* and *FAS1* translation altered the lipidome predominantly by increasing the abundance of most lipid molecular species.

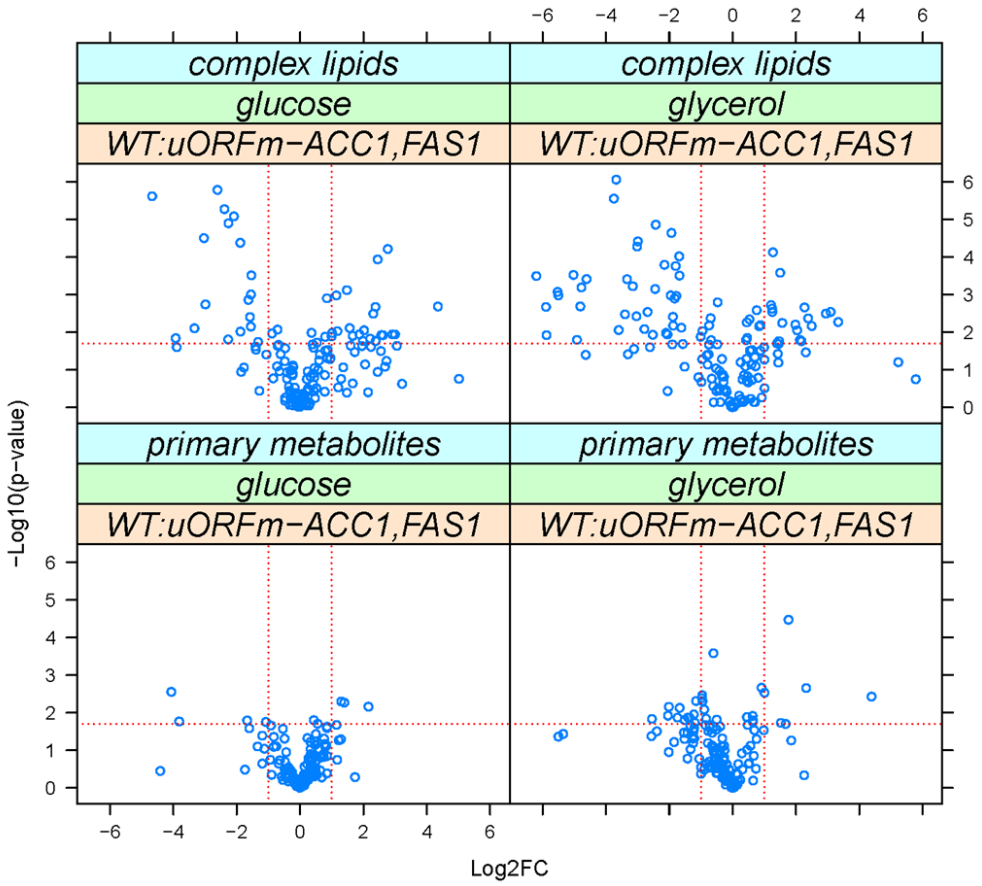

Figure 19 De-repressing the translational control of lipogenesis alters lipid abundances

Metabolites whose levels changed in WT vs. *uORFm-ACC1,FAS1* cells were identified from the magnitude of the difference (x-axis; Log2-fold change) and statistical significance (y-axis), indicated by the red lines. The analytical and statistical approaches are described in Materials and Methods.

Lipogenesis controls the timing of nuclear division

The *uORFm-ACC1,FAS1* cells represent a unique, gain-of-function context for interrogating the effects of increased lipogenesis on nuclear division. It is well-established that diminutions in lipid synthesis perturb the shape of the nuclear envelope in fungi (Witkin et al., 2012; Walters et al., 2012; Walters et al., 2014; Siniossoglou, 2013; Santos-Rosa et al., 2005; Zach & Převorovský, 2018; Kume et al., 2017). Those findings motivated examination of nuclear morphology in *uORFm-ACC1,FAS1* cells progressing synchronously through the cell cycle. As in our past studies (Blank et al., 2020; Blank et al., 2017; Huang et al., 2018), centrifugal elutriation was again employed to recover highly enriched populations of un-arrested early G1 cells where the coupling between cell growth and division is maintained (Aramayo & Polymenis, 2017; Creanor and Mitchison, 1979). The timing of nuclear division was then compared for synchronous wild-type and *uORFm-ACC1,FAS1* cultures.

To that end, the nuclear envelope was visualized by immunofluorescence using the Nsp1p component of the central core of the nuclear pore complex as a marker (see Materials and Methods and Figure B-3). For each cell scored at one point in the cell cycle, the longest axis across the nucleus was related to the diameter of the non-elongated, spherical nuclear space and expressed as a ratio (Figure B-3A). The cell size and percentage of budded cells from the same elutriated samples were also recorded. Since yeast bud emergence marks the initiation of cell division, this event serves as a convenient proxy for marking entry into the S phase. This landmark was therefore used to relate initiation of cell division to cell size.

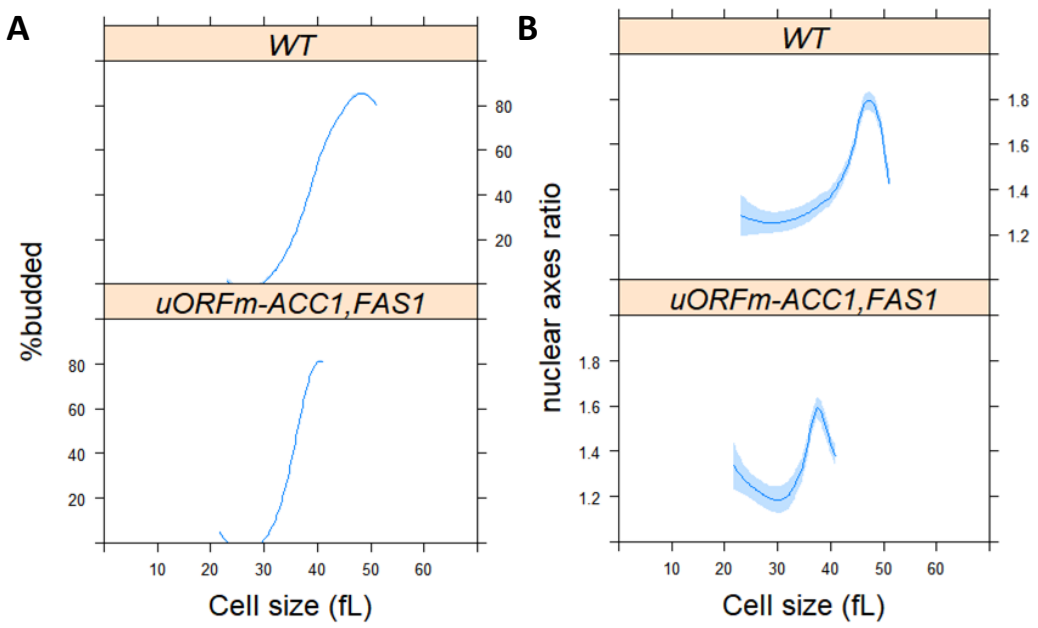

Figure 20 De-repressing translation of *ACC1* and *FAS1* promotes nuclear division

A, Synchronous cultures of the indicated strains and conditions were obtained by elutriation (see Materials and Methods), from which the percentage of budded cells (y-axis) is shown against the mean cell size (in fL; x-axis). B, From the same samples as in A, cells were processed for fluorescence microscopy to visualize the nucleus, as described in Materials and Methods (see also Figure 3 - figure supplement 1). Nuclear shape (y-axis) is shown against the mean cell size (in fL; x-axis), from >2,000 cells/strain. Loess curves and the std errors at a 0.95 level are shown.

A key parameter that derives from such an analysis is the critical size, and this metric is defined as the size at which half the cells are budded (Soma et al., 2014). The critical size of *uORFm-ACC1,FAS1* cells was slightly smaller than that of wild type cells (Figure 20A; 36.7±1 fL vs. 40.6±2 fL, based on four independent experiments). However, compared to wild type, *uORFm-ACC1,FAS1* mutants initiated nuclear elongation and completed nuclear division disproportionately sooner – i.e., at a cell size some 10 fL smaller relative to wild type cells (Figure 20B). However, the total cell cycle time was the same for both wild type and *uORFm-ACC1,FAS1* cells (93±2 m vs. 91±5 m, p=0.3, based on the Mann-Whitney test, from at least four independent experiments in each case). Thus, although *uORFm-ACC1,FAS1* cells complete nuclear division earlier than wild-type cells do, the mutant cells delay completion of cytokinesis and cell separation. These results reveal an active and sufficient role for lipid synthesis in promoting nuclear division.

De-repressing translation of ACC1 and FAS1 corrects mitotic phenotypes of sec14 mutants

Conditional *sec14* mutants proliferate at 25°C, but not at 37°C (Novick et al., 1980). Furthermore, inhibition of lipogenesis by cerulenin exacerbates the temperature sensitivity of *sec14-1* cells (Dacquay et al., 2017). Whereas the cerulenin effect is a rather non-specific phenotype (Lee et al., 2014), this observation raised the question of whether the increased lipogenesis in *uORFm-ACC1,FAS1* cells could suppress the temperature-sensitive proliferation of *sec14-1* cells. Indeed, coordinate *ACC1* and *FAS1* uORF inactivation partially rescued growth of *sec14-1* cells at the semi-permissive

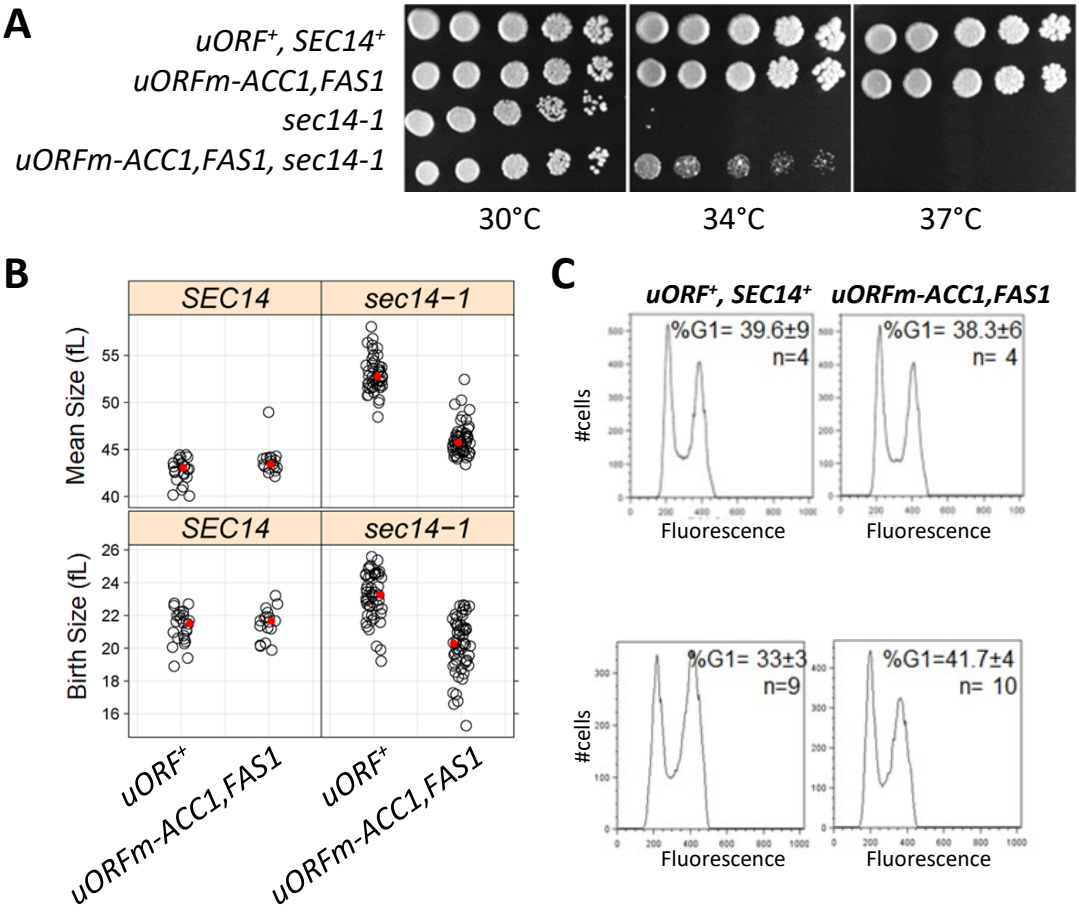

Figure 21 De-repressing the translational control of *ACC1* and *FAS1* suppresses the temperature sensitivity

(A), large size (B), and high G2/M DNA content (C) of *sec14-1* cells. A, Serial dilutions (5-fold) of cultures of the indicated strains were spotted on solid media and grown at the temperatures shown. B, Strip plots showing the mean (top panels) and birth (bottom panels) size (y-axis) for the indicated strains. The average in each case is in red. C, Flow cytometry histograms for the indicated strains, with cell number on the y-axis and fluorescence per cell on the x-axis.

temperature of 34°C (Figure 21A). This result suggests that increased lipogenesis reduced the threshold requirement of yeast cells for Sec14p.

Although the Sec14p requirement for membrane trafficking through the yeast TGN/endosomal system is well-established (Cleves et al., 1989; Bankaitis et al., 1989; Nile et al., 2014), this PITP also executes cell-cycle functions. Even at the permissive temperature of 30°C *sec14-1* cells exhibit larger birth and mean sizes and are delayed in passage through the G2/M stages of the cell cycle. This latter deficiency is manifested in asynchronous cultures as increased fractions of cells in G2/M (Huang et al., 2018). Also, *sec14-1* mutants must reach a larger critical size before initiating cell division (Huang et al., 2018). Strikingly, whereas *ACC1* and *FAS1* uORF mutations did not alter the size of wild type cells, these uORF mutations completely corrected the larger birth and mean size of *sec14-1* cells (Figure 21B, right panels; $p>0.05$, Kruskal-Wallis, and posthoc Nemenyi tests). Moreover, the combined uORF mutations fully corrected the G2/M delay characteristic of *sec14-1ts* cells (Figure 21C). (Figure 21B, left panels). These collective results cannot be accounted for by simple models where cell enlargement is accommodated by new plasma membrane synthesis before division.

Sec14p has not been previously implicated in nuclear division. But since our data suggest that *ACC1* and *FAS1* uORF mutations correct the various cell cycle-related phenotypes of *sec14-1* cells, we examined the timing of nuclear division in synchronized cultures produced by elutriation. As we had previously reported (Huang et al., 2018), the critical size of *sec14-1* cells is larger than that of wild type cells even at the permissive temperature of 30°C (Figure 22A, compare the top two panels). Furthermore, *sec14-1*

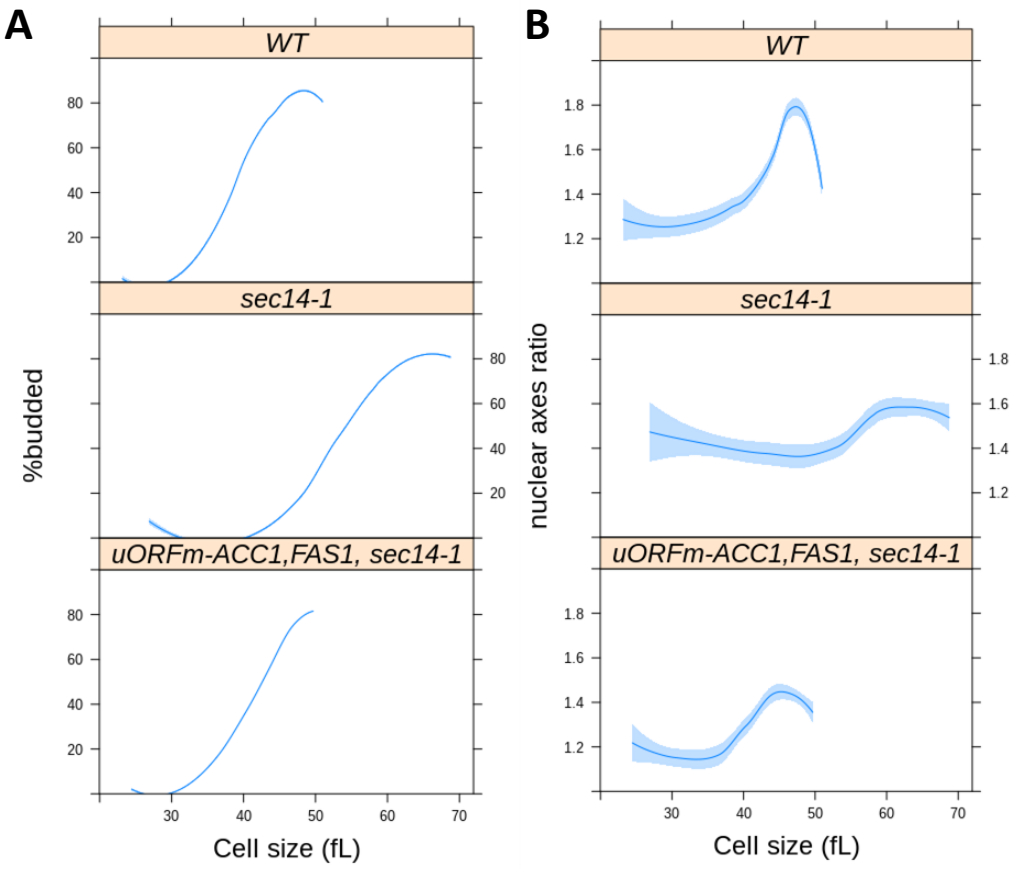

Figure 22 Loss-of-function *sec14-1* mutants delay nuclear division, but they are suppressed by the uORF mutations in *ACC1* and *FAS1*

From synchronous cultures of the indicated strains, the percentage of budded cells (A) and nuclear shape (B) as a function of cell size (x-axis) were measured and plotted as in Figure 3. For the wild type cells (WT), the values were the same as those in Figure 15.

cells both initiated and completed nuclear division at a significantly larger size relative to wild-type cells (Figure 22B). Strikingly, *ACC1* and *FAS1* uORF mutations corrected both the larger critical size and the delayed nuclear division of *sec14-1* cells (Figure 22A, 22B). However, the scheduling of nuclear division in *uORFm-ACC1,FAS1, sec14-1* mutants was similar to that of wild type cells and was not accelerated as observed in *uORFm-ACC1,FAS1* mutants (Figure 20B). These collective data not only strongly support the idea that increased lipogenesis provides for the mitotic functions of Sec14p, but also suggest that the accelerated nuclear division schedule associated with elevated lipogenesis still requires some Sec14p involvement.

Specificity of 'bypass Sec14p' mechanisms in correcting the delayed nuclear division of sec14-1 mutants

The *ACC1* and *FAS1* uORF mutations perturb lipid metabolism (Figure 19). But fatty acids are the precursors for all glycerolipids and sphingolipids. Hence, it is difficult to reduce to a manageable level the possibilities regarding which derangements in lipid metabolism are primarily responsible for disturbed nuclear morphogenesis. Since our data point to functional interactions between the increased lipogenesis in *uORFm-ACC1,FAS1* cells and Sec14p-dependent processes (Figures 21, 22), the known roles of Sec14p were exploited as a tool that reports on distinct arms of the lipid metabolome.

As a PtdIns/PtdCho transfer protein (Grabon et al., 2019; Bankaitis et al., 1990), Sec14p leverages its heterotypic lipid binding and exchange activities to potentiate the activities of PtdIns 4-OH kinases and thereby stimulate PtdIns-4-phosphate signaling (Schaaf et al., 2008; Bankaitis et al., 2010). It is by this mechanism that Sec14p and

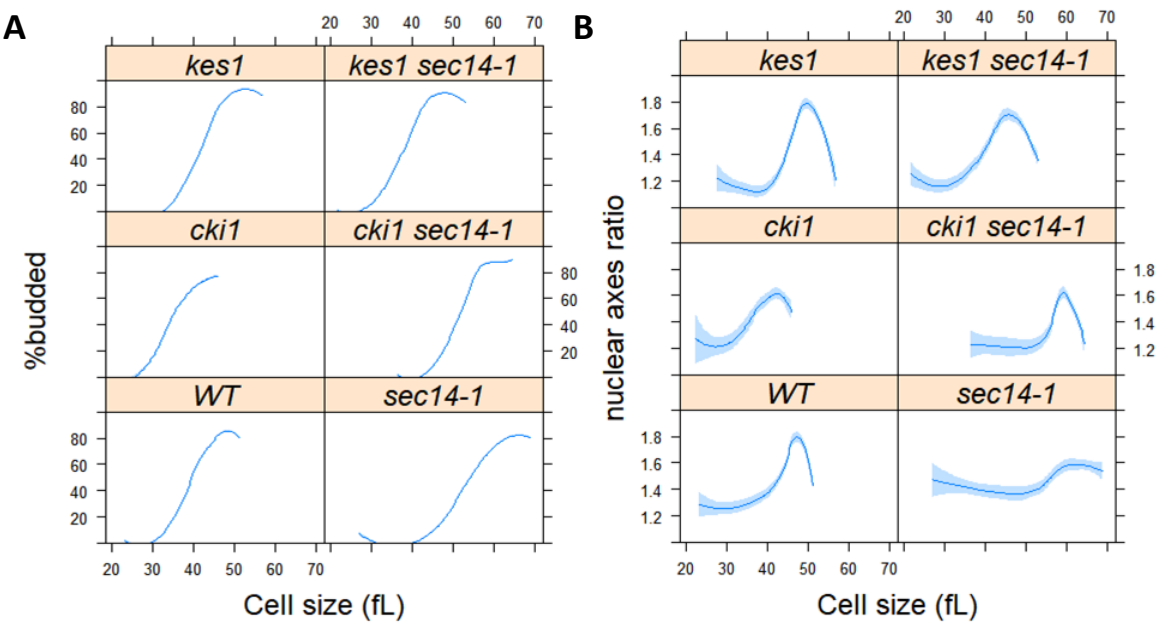

Figure 23 Loss of Kes1p, but not Cki1p, suppresses the delayed nuclear division of *sec14-1* mutants

From synchronous cultures of the indicated strains, the percentage of budded cells (A) and nuclear shape (B) as a function of cell size (x-axis) were measured and plotted as in Figure 5. For the wild type cells (WT) and *sec14-1* cells, the values were the same as those in Figure 17.

other PITPs function as sensors of lipid metabolism and integrate the activities of distinct arms of the lipid metabolome with localized outputs of PtdIns-4-phosphate signaling (Wang et al., 2019). In that regard, Sec14p executes essential cellular activities, but the normally essential Sec14p requirement for cell viability is bypassed by derangements in specific aspects of lipid metabolism. These include loss-of-function mutations in the PtdIns-4-phosphate phosphatase Sac1 (Cleves et al., 1989; Rivas et al., 1999), the CDP-choline pathway (but not the *de novo* pathway) for PtdCho biosynthesis (Cleves et al., 1991; Xie et al., 2001), and the ergosterol and PtdIns-4-phosphate exchange protein Kes1p (Fang et al., 1996; Li et al., 2002; Mousley et al., 2012).

With regard to bypass Sec14p mutations in the CDP-choline pathway, the lethality and secretory defects of *sec14-1* mutants at 37°C are suppressed by loss of the Cki1p choline kinase which catalyzes the first reaction of this PtdCho biosynthetic pathway (Cleves et al., 1991). However, even though genetic ablation of Cki1p activity yielded cells that exhibited a slightly smaller critical size (consistent with slightly accelerated initiation of cell division), this metabolic defect failed to suppress the delayed nuclear division of *sec14-1* mutants (Figure 23). Strikingly different results were obtained for Kes1p loss-of-function mutations which we previously demonstrated correct the large cell size and cell cycle delay of *sec14-1* cells ((Huang et al., 2018); see also Figure 23A). Kes1p inactivation fully corrected the delay in the nuclear division of *sec14-1* cells (Figure 23B). These results indicate a sharp differentiation between 'bypass Sec14p' mutants in their abilities to correct the derangements in nuclear division, normally associated with Sec14p dysfunction, even though these 'bypass

Sec14p' mutations share in common their abilities to restore cell viability and efficient membrane trafficking to cells ablated for Sec14p function. These data also indicate that defects in the CDP-choline pathway of PtdCho synthesis do not significantly impact nuclear division.

Enhanced ACC1 and FAS1 translation corrects the aberrant nuclear shape of PtdIns 4-OH kinase mutants

A major function of Sec14p in cells is to stimulate the activities of the Golgi/endosomal and plasma membrane PtdIns 4-OH kinases Pik1p and Stt4p, respectively (Schaaf et al., 2008; Bankaitis et al., 2010). We therefore interrogated the cell cycle and nuclear morphogenetic phenotypes of temperature-sensitive mutants defective in the activities of these two lipid kinases as each enzyme is individually essential for yeast cell viability and these two enzymes together account for nearly all of the PtdIns 4-OH kinase activity in cells (Audhya et al., 2000). Even at their permissive temperature (25°C), *pik1-101* and *stt4-4* cells grew slowly and exhibited aberrant cell morphologies. Indeed, we were unable to obtain synchronous cultures of these mutants by elutriation. In an alternative approach, asynchronous cultures of *pik1-101* and *stt4-4* cells were examined for cell cycle parameters including cell size and DNA content. At the permissive temperature of 25°C, both *pik1-101* and *stt4-4* cells were significantly larger than wild type cells (~50% and 25%, respectively; Figure B-5, top). Moreover, the DNA contents of both mutants were also irregular (Figure B-5, bottom). Although Pik1p inactivation results in a cytokinesis defect at 37°C (Garcia-Bustos et al., 1994), we did not obtain evidence of increased ploidy at 25°C. Rather, the DNA content profiles for both mutants consistently

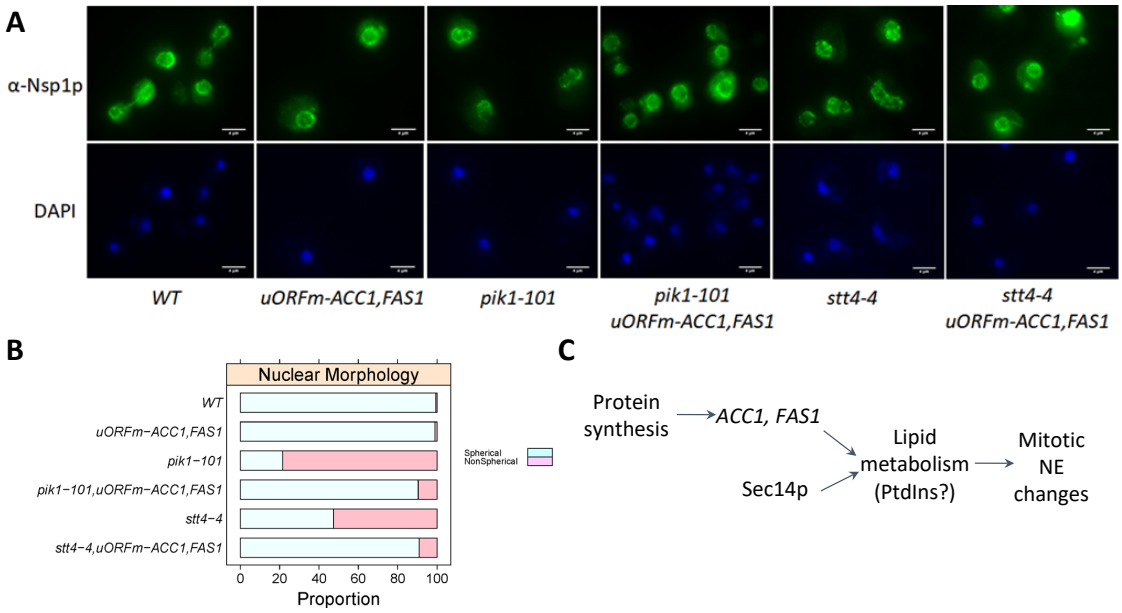

Figure 24 Upregulating translation of *ACC1* and *FAS1* corrects the aberrant nuclear shape of PI- 4-kinase mutants

A, Representative fluorescent microscopy images of cells from the indicated strains, stained with an α-Nsp1 antibody (top panels) or DAPI (bottom panels). B, Summary of the proportion of cells with spherical, or not, nuclei from the strains shown, calculated from three independent experiments. C, Schematic summary of our results.

reported a substantial delay in passage through S phase (Figure B-5, bottom).

The cell cycle phenotypes described above, when coupled with prior evidence that phospholipid and triacylglycerol synthesis impacts nuclear morphology (Barbosa et al., 2019; Siniossoglou, 2013; Webster et al., 2009), prompted us to examine the nuclear morphologies of *pik1-101* and *stt4-4* cells. These mutants exhibited morphologically deranged nuclei characterized by highly irregular shapes that were in stark contrast to the normal spherical shape (Figure 24). Remarkably, *uORFm-ACC1,FAS1* restored normal nuclear morphology to *pik1-101* mutants and, to a lesser extent, to *stt4-4* mutants (Figure 24). Although the effect did not reach statistical significance in the *stt4-4* context ($p=0.08$, based on the Kruskal Wallis and posthoc Nemenyi tests; see also Figure B-6), the *pik1-101* data indicated that increased lipogenesis levied a significant correction of the abnormal nuclear shape of PtdIns 4-OH kinase mutants. These results further support the notion that lipogenesis actively controls nuclear shape and division and identify a role for PtdIns-4-phosphate signaling in homeostatic control of nuclear morphology.

Discussion

Herein, we demonstrate that gain-of-function mutations affecting translational control of lipogenic enzymes accelerate nuclear division, a critical cell cycle process. These results provide the first example of a metabolic pathway that is not merely required for a cell cycle process but actively drives the process forward. These findings are discussed in the context of cell cycle-dependent translational control of lipogenesis as it relates to regulation of nuclear morphogenesis.

Translational control of lipogenic enzymes

The question of how mammalian acetyl-CoA carboxylase (ACC1, ACACA) and fatty acid synthase (FASN) are regulated is of intense interest because of the central role these enzymes play in the control of food intake, their contributions to obesity, and their association with cancer (Kuhajda et al., 1994; Baenke et al., 2013; Beloribi-Djefaflia et al., 2016). *ACC1* expression is increased in conjunction with FASN to upregulate lipid synthesis in human tumors. Multiple mechanisms have been associated with the levels and activity of these enzymes in mammals. The activities of these enzymes in mammals are subject to multiple layers of regulation, and the control of Acc1 activity by phosphorylation has garnered considerable attention (Kim, 1997). Acc1 is inactivated upon phosphorylation by AMPK and, as leptin activates AMPK, this regulation is a crucial aspect of the mechanism by which leptin suppresses appetite (Gao et al., 2007). Moreover, the AMPK-mediated inhibition of Acc1 is relieved just before cytokinesis, and this timing correlates with increased Acc1 enzymatic activity late in the HeLa cell cycle (Scaglia et al., 2014). However, the precise role of phosphorylation in the cell cycle regulation of Acc1p remains unclear. Large scale phosphoproteomic analyses identify several phosphorylation sites on yeast Acc1p. The major site is at residue S1157, which corresponds to S1216 in the human enzyme (Hunkeler et al., 2016). Although this site is conserved in the Acc1p enzymes of all eukaryotes, there are no reports that Acc1p^{S1216} phosphorylation is of any regulatory consequence for mammalian Acc1p. Moreover, there is no evidence that Acc1p phosphorylation is subject to cell cycle control in yeast.

Our data identify translation control as a mechanism for regulating lipogenesis as a function of the cell cycle. We had previously shown that translation of the mRNAs encoding Acc1p and Fas1,2p peaks late in the cell cycle ((Blank et al., 2017); see also Figure B-2). That this represents a broadly conserved layer of regulation is indicated by subsequent studies that showed translational control of human *ACC1* is required for the progression of quiescent T cells into a proliferative state (Ricciardi et al., 2018). These prior studies linking elevated Acc1p and Fas1p activity with increased cell proliferation established these enzymes are necessary for lipogenesis and cell division. In that regard, there are numerous other examples where metabolic and cell growth processes are required for various cell cycle events (Johnston et al., 1977).

The novelty of the current study rests on our demonstration that upregulating Acc1p and Fas1p (by abrogating translational inhibitory elements) is sufficient to drive a critical cell cycle process – i.e., nuclear division. Functional ablation of the inhibitory uORFs that lie upstream of each of the corresponding structural genes elevated the overall levels of these enzymes while preserving the cell cycle-dependent oscillations in their abundance, albeit with a dampened amplitude ((Blank et al., 2017); see also Figure B-2). This is an expected result because, for the uORF-mediated control to fully account for the mitotic peak of translation of *ACC1* and *FAS1*, the cellular ribosome content must also fluctuate as cells progress through the cell cycle. Evidence from our lab and others argues against such cell cycle fluctuations in ribosome content (Blank et al., 2020; Elliott et al., 1979; Shulman et al., 1973). Whole-cell metabolic profiling demonstrates lipid abundance (including all major classes; PtdIns, PtdCho, PtdEtn, and triglycerides) is the

most periodic metabolic parameter as a function of the cell cycle and that it peaks in mitosis (Blank et al., 2020). Furthermore, we now show that enhanced *ACC1* and *FAS1* translation was sufficient to increase most lipids' abundances (Figure 19).

Nuclear morphology and lipogenesis

Yeast and other fungi undergo closed mitosis, where the nuclear envelope remains intact throughout the entirety of the cell cycle. The nucleus maintains a spherical shape throughout interphase and then elongates during mitosis (Meseroll & Cohen-Fix, 2016).The fact that nuclear envelope expansion depends on cell cycle progression, and not on a general increase in cell size, argues for specialized metabolic inputs, including fatty acid and phospholipid synthesis (Walters et al., 2019). Indeed, nuclear membrane proliferation is required for progression through mitosis, regardless of whether it is closed or disassembled before reassembling during telophase as in mammalian cells. Inhibition of fatty acid synthase impairs nuclear elongation and chromosome segregation in fission yeast (Takemoto et al., 2016). A mitotic delay is occasionally accompanied by the appearance of nuclear membrane extensions, or flares, in budding yeast. These flares are interpreted as evidence for continued nuclear elongation on the face of some cell cycle arrest (Walters et al., 2012; Meseroll & Cohen-Fix, 2016). In support of this interpretation, *ACC1*, *FAS1*, or *FAS2* loss-of-function mutations impair flare formation and nuclear elongation (Walters et al., 2014). However, we emphasize that the acceleration of nuclear elongation and division that we observed in the face of the upregulated translation of lipogenic enzymes is without precedent. Those data are not

only fully consistent with the requirement lipogenesis in nuclear elongation and division, but these also establish that enhanced lipogenesis is sufficient to drive these processes.

Phosphoinositide signaling in control of nuclear division and morphology

While the role of the normally essential Sec14p in membrane trafficking is well documented (Bankaitis et al., 1989; Cleves et al., 1989; Fang et al., 1996), there is evidence that the essential cellular function(s) executed by Sec14p are not solely at the level of membrane trafficking control but also at the level of cell cycle control (Mousley et al., 2012). In that regard, Sec14p hypomorphisms manifest themselves in cell cycle phenotypes such as delay in the passage through G2/M and progression from G1 into S-phase (Huang et al., 2018). In that context, we report an unexpected confluence of translational control of lipogenesis with Sec14p-dependent phosphoinositide signaling in the cell cycle. We find that *sec14-1* mutants are not only delayed in the initiation and completion of nuclear division, but that gain-of-function mutations that functionally ablate the *ACC1* and *FAS1* uORFs (with the result that the two corresponding mRNAs are translationally derepressed) partially rescue *sec14-1* growth defects. Moreover, functional ablation of the uORFs fully rescued the delays in progression through G2/M and G1/S in Sec14p-deficient mutants. What is particularly striking in light of those data is that the accelerated timing of nuclear division in the uORF mutants was corrected in the *sec14-1* genetic background. These collective data not only indicate that increased lipogenesis suppresses the mitotic functions of Sec14p but also suggest that the accelerated nuclear division schedule associated with elevated lipogenesis requires Sec14p involvement.

The available evidence indicates that the Sec14p involvement was independent of its role in membrane trafficking on two counts. First, these phenotypes were manifested at permissive temperatures for *sec14-1* mutants where membrane trafficking pathways are operating normally by all measurable criteria. Second, the 'bypass Sec14' mutant that inactivates Cki1p (i.e., the choline kinase representing the first step in the CDP-choline pathway for PtdCho biosynthesis) corrects the membrane trafficking defects of *sec14* mutants but fails to correct the deranged scheduling of nuclear elongation and division in *sec14-1* mutants. Rather, as Sec14p stimulates PtdIns-4-P synthesis by both the Pik1p and Stt4p kinases *in vivo*, the data argue that Sec14p-mediated phosphoinositide signaling is involved in regulating nuclear elongation and division. Two lines of evidence support this interpretation of the data. First, inactivation of Kes1p, an antagonist of Sec14p- and Pik1p-dependent PtdIns-4-P signaling (Fang et al., 1996; Li et al., 2002), corrects both the membrane trafficking and the nuclear elongation/division defects associated with Sec14p deficiencies. In this manner, the *kes1* 'bypass Sec14p' mutants differ from *cki1* mutants that correct only the membrane trafficking deficits. Second, cells compromised for Pik1p activity presented misshapen nuclei whose morphological derangements were corrected by increased lipogenesis. These data are intriguing in light of previous demonstrations that Pik1p shuttles between cytosolic and nuclear pools and executes essential cellular functions in both compartments (Garcia-Bustos et al., 1994; Strahl et al., 2005).

Precisely how PtdIns-4-P signaling modulates nuclear division remains to be determined. One execution point could be at the translational control level as

inactivation of Pik1p or Stt4p triggers a block in protein synthesis through phosphorylation of translation initiation factor eIF2α (Cameroni et al., 2006). Another attractive and not mutually exclusive possibility is that PtdIns-4-P serves as a precursor to synthesizing a nuclear pool of PtdIns-4,5-bisphosphate (PtdIns-4,5-P2). There is abundant literature regarding nuclear PtdIns-4,5-P2 and its roles (direct and indirect) in regulating multiple nuclear events such as transcription, mRNA processing and polyadenylation, and mRNA export (Cocco et al., 1987; 1989; York et al., 1999; Li et al., 2013; Hamann & Blind, 2018; Chen et al., 2020). We attempted to assess the relationship between PtdIns-4,5-P2 synthesis and *ACC1* and *FAS1* translational control but were unsuccessful in generating the requisite strains for the analysis. So, the relationship between PtdIns-4-P and PtdIns-4,5-P2 signaling related to nuclear elongation and division remains to be resolved.

In summary, the results reported herein emphasize the physiological significance of generating specific lipid pools that drive a crucial cell cycle process – i.e., nuclear elongation and division. These lipids pools represent metabolic inputs that do not merely 'fuel' a cell cycle process but, rather, play heretofore unappreciated active and instructive signaling roles in driving landmark cell cycle events. The collective data integrate protein synthesis, lipogenesis and phosphoinositide signaling with the timing of nuclear elongation and division. In this manner, this study sets the stage for deciphering the specific identities and compartmental organization of the relevant lipid pools that control these signaling processes.

Materials and methods

Strains and media

All the strains used in this study are shown in the Key Resources Table (Table 1) , above. Unless noted otherwise, the cells were cultivated in the standard, rich, undefined medium YPD (1% $^{w}/_{v}$ yeast extract, 2% $^{w}/_{v}$ peptone, 2% $^{w}/_{v}$ dextrose), at 30°C. To modify the *FAS1*-5' leader, we first inserted a *URA3* gene (amplified from a prototrophic strain X1280) upstream, at position ChrXI99751 with the PCR-mediated methodology of (Longtine et al., 1998), using primers XI99701-URA-F1 and XI99800-URA-R1 (see Key Resources Table). The PCR product was transformed into a yeast strain carrying the TAP epitope at the 5' end of the *FAS1* main ORF (FAS1-TAP, see Key Resources Table). The resulting strain, NM21, was genotyped by PCR for the presence of the insertion at the expected location, using primers (XI99514-F1 and XI99895-R1) that flank the insertion. Genomic DNA of NM21 was then used as a template in a PCR reaction with the forward primer XI99514-F1 and reverse primers FAS1-141-REV, or FAS1-279-REV, to introduce point mutations at the start codon of the proximal uORF (T141A), or the distal uORF (G279A), respectively. The strains obtained were mutant for the proximal (NM19), or distal uORF (NM24). The introduced mutations were verified by PCR (with primers XI100101-F1 and XI100698-R1) followed by restriction digestion with enzymes PsiI (for the proximal uORF mutation) and RsaI (for the distal uORF mutation). The T141A mutation introduces a restriction

Table 1 Key resource table

Reagent type (species) or resource	Designation	Source or reference	Identifiers	Additional information
strain, strain background (*S. cerevisiae*)	BY4743	(Giaever et al., 2002)	RRID:SCR_003093	*MAT*a/α *his3Δ1/his3Δ1 leu2Δ0/leu2Δ0 LYS2/lys2Δ0 met15Δ0/MET15 ura3Δ0/ura3Δ0*
strain, strain background (*S. cerevisiae*)	BY4742	(Giaever et al., 2002)	RRID:SCR_003093	*MATα his3Δ1 leu2Δ0 lys2Δ0 ura3Δ0*
strain, strain background (*S. cerevisiae*)	BY4741	(Giaever et al., 2002)	RRID:SCR_003093	*MATa his3Δ1 leu2Δ0 met15Δ0 ura3Δ0*
strain, strain background (*S. cerevisiae*)	FAS1-TAP	Dharmacon	YSC1178-202232118	*MATa FAS1-TAP::HIS3MX6*, BY4741 otherwise
strain, strain background (*S. cerevisiae*)	X1280-5A	Yeast Genetic Stock Center		*MATα SUC2 mal mel gal2 CUP1*
strain, strain background (*S. cerevisiae*)	NM19	This study		*MATa ChrXI:99751::URA3 (T141A)*, FAS1-TAP otherwise
strain, strain background (*S. cerevisiae*)	NM21	This study		*MATa ChrXI:99751::URA3* FAS1-TAP otherwise
strain, strain background (*S. cerevisiae*)	NM24	This study		*MATa ChrXI:99751::URA3* (G279A), FAS1-TAP otherwise
strain, strain background (*S. cerevisiae*)	NM30	This study		*MATa ChrXI:99751::URA3 (T141A) (G279A)*, FAS1-TAP otherwise
strain, strain background (*S. cerevisiae*)	NM31	This study		*MATα ChrXI:99751::URA3 (T141A) (G279A)*, FAS1-TAP otherwise

Table 1 Continued

Reagent type (species) or resource	Designation	Source or reference	Identifiers	Additional information
strain, strain background (*S. cerevisiae*)	NM33	This study		*MATa ChrXIV:662143::kan MX6, ChrXI:99751::URA3*, FAS1-TAP otherwise
strain, strain background (*S. cerevisiae*)	NM34	This study		*MATα ChrXIV:662143::kan MX6, ChrXI:99751::URA3*, FAS1-TAP otherwise
strain, strain background (*S. cerevisiae*)	NM35	This study		*MATα ChrXIV:662143::kan MX6 (TG340AA), ChrXI:99751::URA3 (T141A) (G279A)*, FAS1-TAP otherwise
strain, strain background (*S. cerevisiae*)	NM36	This study		*MATa ChrXIV:662143::kan MX6 (TG340AA), ChrXI:99751::URA3 (T141A) (G279A)*, FAS1-TAP otherwise
strain, strain background (*S. cerevisiae*)	HB1	(Blank et al., 2017)		*MATa ChrXIV:662143::kan MX6 (TG340AA),* BY4741 otherwise
strain, strain background (*S. cerevisiae*)	HB13	(Blank et al., 2017)		*MATα ChrXIV:662143::kan MX6,* BY4742 otherwise
strain, strain background (*S. cerevisiae*)	CTY1-1A	(Bankaitis et al., 1989; Xie et al., 2001)		*MATa,ura3-52Δ,his3-200Δ,lys2-801Δ, sec14-1*
strain, strain background (*S. cerevisiae*)	NM39	This study		*MATα, ChrXIV:662143::kan MX6 ChrXI:99751::URA3*, *sec14-1,* FAS1-TAP otherwise

Table 1 Continued

Reagent type (species) or resource	Designation	Source or reference	Identifiers	Additional information
strain, strain background (*S. cerevisiae*)	NM42	This study		*MATα, ChrXIV:662143::kanMX6 (TG340AA), ChrXI:99751::URA3 (T141A) (G279A)*, *sec14-1,* FAS1-TAP otherwise
strain, strain background (*S. cerevisiae*)	VBY79	Bankaitis lab collection		*MATa, pik1-101^{ts} ura3-52Δ leu2Δ Gal^{+}*
strain, strain background (*S. cerevisiae*)	NM83	This study		*MATa, pik1-101^{ts},ChrXIV:662143::kanMX6 (TG340AA), ChrXI:99751::URA3 (T141A) (G279A), FAS1-TAP otherwise*
strain, strain background (*S. cerevisiae*)	VBY76	Bankaitis lab collection		*MATα, leu2Δ ura3Δ his3Δ trpΔ lysΔ suc2-Δg Δstt4Δ::HIS3 YCp(stt4-4, LEU2)*
strain, strain background (*S. cerevisiae*)	NM86	This study		*MATa, lysΔ, Δstt4Δ::HIS3 YCp(stt4-4, LEU2), ChrXIV:662143::kanMX6 (TG340AA), ChrXI:99751::URA3 (T141A) (G279A), LEU+, TRP+, MET+, FAS1-TAP otherwise*

Table 1 Continued

Reagent type (species) or resource	Designation	Source or reference	Identifiers	Additional information
Sequence-based reagent	XI99701-URA-F1	This study		GCTATTTGCCTTCG TATATACCTTTCTA TACCAAGTAATGA ATGTCTTGAGTTTT GATTCCGGTTTCTT TG
Sequence-based reagent	XI99800-URA-R1	This study		GGGCCCGTATGGC CGCGCGAAGGCTT AGTTAAGATGTTT CAGCAAACGGCTT GGTTCTGGCGAGG TATTG
Sequence-based reagent	XI99514-F1	This study		TGGATGGCGACCT CGTTAT
Sequence-based reagent	XI99895-R1	This study		CGGAGCAGACGCT GCTATAA
Sequence-based reagent	FAS1-(-279)-REV	This study		ATAACAAGTATGA AAAGGCCCAATGT ATTTTTTTATATTT TTCCCTTGGTTCTT TTTCCTTATCAATC AATACC
Sequence-based reagent	FAS1-(-141)-REV	This study		ATATATTTTTCAG AAATATTCAAAGA GTTTATAAGAATA TATTTGACCTTGA ATTGTATGGAAAA AAAGAATTAATAA ATTG
Sequence-based reagent	XI100101-F1	This study		CCTTTCCCAATCA CCGAAAA

Table 1 Continued

Reagent type (species) or resource	Designation	Source or reference	Identifiers	Additional information
Sequence-based reagent	XI100698-R1	This study		TCTTGTGGAGTAAGCGTCCAT
Sequence-based reagent	FAS1-FAM-probe	Sc04141945_s1, Cat# 4351372	Thermo Fisher Scientific, Taqman® Assays and Arrays	RNA surveillance
Sequence based reagent	UBC6-VIC-probe	Sc04118595_s1, Cat# 4448489	Thermo Fisher Scientific, Taqman® Assays and Arrays	RNA surveillance
other	Yeast extract	Sigma-Aldrich	Y1625	
other	Peptone	Sigma-Aldrich	P5905	
chemical compound, drug	Dextrose	Sigma-Aldrich	D9434	
chemical compound, drug	Cycloheximide	Calbiochem	239763-M	
chemical compound, drug	Zymolyase 20T	MP biomedicals	SKU 08320921	
chemical compound, drug	Cerulenin	EMD Millipore	219557-5MG	
chemical compound, drug	Sodium azide	Sigma-Aldrich	S2002	
chemical compound, drug	Tris(hydroxymethyl)aminomethane	Sigma-Aldrich	252859	

Table 1 Continued

Reagent type (species) or resource	Designation	Source or reference	Identifiers	Additional information
chemical compound, drug	Tris base	Roche	TRIS-RO	
chemical compound, drug	Sodium chloride	Sigma-Aldrich	S7653	
chemical compound, drug	Magnesium chloride hexahydrate	USP	1374248	
chemical compound, drug	DTT	Sigma-Aldrich	D0632	
chemical compound, drug	Triton™ X-100	Sigma-Aldrich	T8787	
other	Glass beads	Scientific Industries	SI-BG05	
chemical compound, drug	Phosphate buffered saline (PBS)	Sigma-Aldrich	P4417	
chemical compound, drug	DAPI (4',6-Diamidino-2-Phenylindole, Dihydrochloride)	Vectashield	H-1200-10	
antibody	Peroxidase Anti-Peroxidase (PAP) Soluble Complex	Sigma-Aldrich	P1291	(1:4000)

site for PsiI at the proximal uORF. On the other hand, the G279A mutation eliminated the RsaI restriction site at the distal uORF. Next, to obtain a double uORF *FAS1* mutant, the genomic DNA of NM24 was used as a template in a PCR reaction with forward primer XI99514-F1, and reverse primer FAS1-141-REV. The resulting product was transformed into FAS1-TAP cells, to generate strain NM31, which was verified by PCR, followed by restriction digestion PsiI. The introduced uORF mutations were also confirmed by sequencing the strains' genomic DNA using the primers XI100101-F1 and XI100698-R1.

To de-repress translation of both *ACC1* and *FAS1* in the same cells, we crossed strain NM31 with the *ACC1-uORF* mutant (carrying the TG340AA substitutions in the 5'-leader of *ACC1*; strain HB1, see Key Resources Table and (Blank, Perez, et al., 2017), followed by sporulation and tetrad dissection. The resulting strains (NM36, NM35) have point mutations at the start codons of the uORFs of both *ACC1* and *FAS1* (*uORFm-ACC1, FAS1*). To obtain wild type strains with markers matching those of *uORFm-ACC1, FAS1* cells, we crossed NM21 with HB13 (ChrXIV 662143::kanMX6, see (Blank et al., 2017b)), followed by sporulation and tetrad dissection, yielding strains NM33 and NM34. Unless indicated otherwise, strains NM33, and NM36, were used as the wild type, and *uORFm-ACC1, FAS1*, strains shown in Figures.

To introduce the *sec14-1* allele, strains NM34 and NM35 were crossed with CTY1-1A (Xie et al., 2001), sporulated, and the tetrads dissected to generate the marker-matched *sec14-1*(NM39), and the *sec14-1*, *uORFm-ACC1, FAS1* quadruple mutant

(NM42), respectively. Similarly, we generated all other mutants combinations shown in Figures 17,18.

Sample-size and replicates

For sample-size estimation, no explicit power analysis was used. All the replicates in every experiment shown were biological ones, from independent cultures. A minimum of three biological replicates was analyzed in each case, as indicated in each corresponding figure's legends. Where three replicates were the minimum number of samples analyzed, the robust bootstrap ANOVA was used to compare different populations via the t1waybt function, and the posthoc tests via the mcppb20 function, of the WRS2 R language package. For measurements where at least four independent replicates were analyzed, we used non-parametric statistical methods, as indicated in each case. No data or outliers were excluded from any analysis.

Immunoblot analysis

For protein surveillance, protein extracts were made as described previously (Amberg et al., 2006), and run on 4–12% Tris-Glycine SDS-PAGE gels. To detect TAP-tagged proteins with the PAP reagent, we used immunoblots from extracts of the indicated strains, as we described previously (Blank, Perez, et al., 2017; 2020). Loading was evaluated with an anti-Pgk1p antibody. Images were processed with the ImageJ software package. Briefly, the ‘Subtract background’ tool was applied, followed by the ‘Measure’ tool to obtain a mean intensity for each band. The area measured was kept constant for a sample series for each blot analyzed.

Transcript abundance using ddPCR

For RNA surveillance, RNA extracts were made as described previously (Blank, Perez, et al., 2017). Briefly, RNA was extracted using the hot acidic phenol method (Collart and Oliviero, 2001). Cell pellets were resuspended in 0.4 ml of TES buffer (10 mM Tris, pH 7.5; 10 mM EDTA, and 0.5% SDS) with 0.1 ml of glass beads. Then, 0.4 ml of acid phenol, pH 4.5, was added, and the samples were heated at 65°C for 0.5 h with occasional vortexing for 10 s each time. The samples were then centrifuged for 5 m at 13,000 *g*. The aqueous layer was transferred to a new tube containing 1 ml of cold 100% ethanol with 40 µl of 3 M sodium acetate and incubated overnight at 4°C. The next day, the samples were centrifuged at 13,000 *g* for 20 min at 4°C, washed with 80% ethanol, and centrifuged again for 5 min at 13,000 *g*. The pellets were resuspended in 25 µl water. The amount of total RNA in each sample was measured with a spectrometer. For the quantification of transcript abundance, 0.75 ng of total RNA was used for each sample.

The ddPCR reaction mixture was prepared by following the manufacturer's protocol, using the Taqman hydrolysis probes labeled with FAM (for *FAS1*) and VIC (for *UBC6*) reporter fluorophores. The mixture was kept on ice throughout the whole experiment. Once the reaction mixture was prepared, the samples were placed into a droplet generator (QX200™ AutoDG™ Droplet Digital™ PCR System), which uses specially developed reagent and microfluidics to partition each sample into 20,000 nl-sized droplets. Once the droplets were generated, the samples were transferred to a thermal cycler (C1000 Touch™ Thermal cycler) for PCR. Following the PCR, the plate

containing the droplets was placed in a droplet reader (Bio-Rad, QX200 Droplet reader). The autosampler of the droplet reader picks up droplets from each of the wells of the PCR plate, and fluorescence is measured for individual droplets.

The abundance of the transcripts was obtained using the QuantaSoft™ Software. Transcript levels of *FAS1* were normalized against the corresponding transcript levels of *UBC6*.

Centrifugal elutriation, cell size and DNA content measurements

All methods have been described previously (Hoose et al., 2012; Soma et al., 2014).

Metabolite profiling

The untargeted, primary metabolite and complex lipid analyses were done at the NIH-funded West Coast Metabolomics Center at the University of California at Davis, according to their established mass spectrometry protocols, as we described previously (Blank et al., 2020; Maitra et al., 2020). To identify significant differences in the comparisons among the different strains, we used the robust bootstrap ANOVA, as described above. The input values we used were first scaled-normalized for input intensities per sample. Detected species that could not be assigned to any compound were excluded from the analysis.

Fluorescence microscopy

Cells were fixed with 3.7% $^{v}/_{v}$ formaldehyde at room temperature for 30 m, washed three times with 0.1 M potassium phosphate buffer, followed by a wash and resuspension in 1.2 M sorbitol. Next, the fixed cells were digested with 0.06 mg/ml zymolyase 20T for 5 m at 37°C, and later washed and resuspended again in 1.2 M

sorbitol. 20 µl of the fixed and digested cells were added on a poly-lysinated slide and incubated at room temperature in a moist chamber for 20 m. The liquid was removed, and the slide was dehydrated by ice-cold methanol, and then acetone, for 3 m, and 10 s, respectively. The slide was air-dried and incubated in 0.1 % BSA/PBS for 30 m at room temperature. The BSA/PBS solution was removed, and the α-Nsp1 antibody was added at a dilution of 1:100 dilution and incubated overnight at 4°C. Nsp1p is a nucleoporin (Hurt, 1988) used in our experiments to decorate the nuclear envelope (Figure B-4). The next day, the slide was washed five times with 0.1% BSA/PBS, followed by the addition of secondary antibody (Alexa Fluor 488 AffiniPure Goat α-Mouse IgG, at a dilution of 1:100 and incubated at room temperature for 1 h. The slide was then washed with 0.1% BSA/PBS and mounted with the Vectashield mounting media containing DAPI to visualize the nuclear DNA.

Cells were viewed with a Nikon Eclipse TS100 microscope, with a 100X objective, and the images were captured with a CoolSnap Dyno 4.5 Nikon camera. The exposure time for the DAPI and GFP filters (Alexa Fluor 488) was 50 ms and 500 ms, respectively. All images were captured in NIS Elements Advanced Research (version 4.10) software. The fluorescent images acquired with the GFP and DAPI filters were processed in ImageJ. The ratio of two axes (long axis and the short axis) of the nuclear mass were measured using the 'line' tool followed by the 'measure' tool in the ImageJ software package. When the nucleus is near-spherical, the ratio is 1. However, as the nucleus starts to expand, the ratio increases, signifying the elongation of the nuclear envelope (Figure B-4).

CHAPTER V

CONCLUSIONS AND FUTURE OUTLOOK

In this dissertation, I demonstrate that lipid homeostasis plays a critical role in maintaining the proper morphology of the nucleus and the timing of the nuclear division. I provide an example of a metabolic pathway that is not just a requirement but can promote cell cycle events. Lipid metabolism has usually been considered a process happening in the background to meet the need for the structural components in the cell, including components required for cell division (Scaglia et al., 2014; Al-Feel et al., 2003; Atilla-Gokcumen et al., 2014; Takemoto et al., 2016). A role for lipid synthesis in actively promoting any cell cycle event was unheard of. Nevertheless, recent work indicates that essential lipid species are higher in abundance late in the cell cycle (Blank et al., 2020). Proteins synthesizing fatty acids peak during mitosis (Blank et al., 2017). Furthermore, lack of fatty acid synthesis arrests the cell in the later phases of the cell cycle (Scaglia et al., 2014). Thus, the evidence indicates that lipid synthesis impinges on late cell cycle events. However, it was unclear what these events might be. The main conclusion of my thesis is that *lipogenesis promotes nuclear division*.

For each concluding result, I provide a list of unresolved questions and have proposed experiments and their significance.

Translational control of lipogenic enzymes alters lipid abundance

Studies on the role of lipid synthesis during the cell cycle have traditionally relied on loss-of-function mutations in genes encoding critical enzymes of the process. This dissertation describes the first example of a gain-of-function mutant for lipogenesis and translational control as a new regulatory mechanism for lipid synthesis during mitosis.

Acetyl CoA carboxylase (*ACC1*) and Fatty acid synthase (*FAS1*) are critical enzymes of *de novo* fatty acid synthesis (Klug & Daum, 2014). Previously, our lab had identified a cis-element on the 5' leader sequence of *ACC1* that can adjust the protein levels as a function of different nutrients (Blank, Perez, et al., 2017). The 5' leader of *FAS1* has two uORFs, 141 and 279 nucleotides upstream of the main ORF (Ingolia et al., 2009; Blank et al., 2017). Ribosome footprints from all three of the uORFs residing in the 5' leader of *ACC1* (one) and *FAS1* (two) of budding yeast suggest that the uORFs are translated (Ingolia et al., 2009). We introduced point mutation at the start codons of the uORFs and found the steady-state level of Fas1p to be elevated 3 to 4-fold without any significant change in the mRNA level. Furthermore, simultaneous de-repression of the translation of *ACC1* and *FAS1* increased lipogenesis. Moreover, the yeast strain carrying the mutations at the three uORFs overcame the inhibitory effect of the cerulenin, the fatty acid synthesis inhibitor. Hence, we conclude that uORFs can regulate the steady-state level of the lipogenic enzymes and de-repressing translation of the enzymes resulted in enhanced lipogenesis.

Unresolved questions

- What is the molecular mechanism of the cell cycle-dependent translational control of *FAS1* and *ACC1?*
- Does translational control of the lipogenic enzymes impact histone acetylation?

Proposed experiments

What is the molecular mechanism of the cell cycle-dependent translational control of *FAS1* and *ACC1?*

While the uORFs in the 5' leader sequence of *ACC1* and *FAS1* can modulate the steady-state protein levels as a function of different nutrients (Blank et al., 2017; Maitra et al., 2021), they cannot abolish the cell cycle-dependent translation of the lipogenic enzymes. For the uORF-mediated control to fully account for the mitotic peak of translation of *ACC1* and *FAS1*, the cellular ribosome content must also vary as cells progress through the cell cycle. Evidence from our lab and others argues against such cell cycle fluctuations in ribosome content (Blank et al., 2020). Hence, the cumulative results indicate the existence of additional mechanisms of translational control.

One possible mechanism is that RNA binding proteins can engage the mRNAs encoding lipogenic enzymes in a cell cycle-dependent manner. There is evidence that shows Dhh1p (Jungfleisch et al., 2017) binds to *ACC1* and *FAS1* while Pat1p (S. F. Mitchell et al., 2013) and Bfr1p (Lapointe et al., 2015) bind to *FAS1* mRNA. To test the involvement of these RNA binding proteins, we can monitor the *ACC1* and *FAS1* mRNA and Acc1p and Fas1p protein levels in the cell cycle in cells lacking Dhh1p,

Pat1p, and Bfr1p. Recent proximity-labeling approaches, using Cas13-based APEX targeting, have shown promise in human cells and could be adapted for yeast, to identify all proteins that interact with *ACC1* and *FAS1* transcripts (Han et al., 2020).

Another plausible mechanism of translational efficiency can be the cell cycle-dependent sequestration of *ACC1* and *FAS1* mRNA. Several studies have shown a granular body within the cell that actively sequesters mRNA (Lavut & Raveh, 2012; C. Wang et al., 2018). Utilizing fluorophores, we can monitor these cytoplasmic granules. Moreover, we can observe the mRNA's localization by employing RNA-specific tags on these mRNAs (Park et al., 2010; Braselmann et al., 2019).

Does translational efficiency of *ACC1* and *FAS1* impact histone acetylation?

Acetyl CoA initiates the *de novo* fatty acid synthesis, catalyzed by Acc1p to malonyl CoA. On the other hand, it also serves as the substrate for lysine acetyltransferase (KAT), which catalyzes acetyl group transfer to the lysine residue of histones and other proteins (Feron, 2019). Histone acetylation is primarily associated with transcriptional activation. Collective data from several studies indicate that fatty acid synthesis in the cytoplasm competes for the nucleocytoplasmic pool of acetyl CoA. As a result, acetyl CoA serves as a central metabolite that connects metabolism with chromatin structure and transcription (Galdieri et al., 2014). Moreover, attenuated expression of *ACC1* increases acetylation of histones and alters transcriptional regulation (Galdieri & Vancura, 2012). Hence, Acc1p activity monitors the availability of acetyl CoA for histone acetyltransferase.

Now the question is, does higher lipogenesis decrease the level of acetyl CoA and reduce histone acetylation? We can address the question by targeting histone acetylation via immunoblotting using specific primary antibodies (e.g., anti-acetylated histone H3 and H4; (Rigby et al., 2012)). We can compare the acetylation between wild type cells and the uORF mutant cells. Studies show that acetyl CoA can affect gene expression, including cell cycle genes, such as *CLN3* (Shi & Tu, 2013). We can perform RNAseq and compare the gene expression profile between the uORF mutant cells and the wild type cells.

Enhanced lipogenesis promotes early nuclear division

Yeast nuclei are spherical during the earlier stages of the cell cycle and expand during mitosis. Unlike the mammalian nuclei, the yeast nuclei do not undergo disassembly during cell division. The nucleus expands to accommodate the dynamic movement of chromosomes during segregation. Our results emphasize that upregulated translation of lipogenic enzymes accelerates nuclear elongation and division. Hence, we argue that lipid synthesis is not a mere requirement; instead, lipogenesis can actively drive nuclear envelope remodeling during late cell cycle phases. Cells with a de-repressed synthesis of lipogenic enzymes make more lipids and promote nuclear elongation and division sooner than the wild type cells. Thus, my work shows that translational control of lipogenic enzymes couples lipogenesis with nuclear division.

Unresolved questions

- Does translational control of lipogenesis impact the endoplasmic reticulum during mitosis?

Proposed experiment

Does translational control of lipogenesis impact the endoplasmic reticulum during mitosis?

The nuclear envelope is continuous with the endoplasmic reticulum, and the outer membrane shares a similar lipidomic profile with the ER membrane. Hence, the ER should be our next candidate organelle to test in the cell cycle due to translational control mediated lipogenesis. How the ER divides and segregates to the daughter cell remains unresolved. We can address this issue by visualizing the ER in the uORF mutant both in asynchronous cultures and in the cells progressing synchronously in the cell cycle. We can use an ER specific protein marker, which can be targeted for immunofluorescence. However, since ER is continuous with the NE, it becomes difficult to visualize the ER just by immunofluorescence. We should rely on electron microscopy to obtain a well-resolved image of ER in the strains mentioned above.

Moreover, the ER, under stress, triggers the unfolded protein response (UPR). Hence, if the enhanced lipogenesis causes ER stress, we can determine its response by testing the UPR in the uORF mutant under different nutrients. We can induce UPR in the cells by using a drug such as tunicamycin. The ER responds to the accumulation of misfolded/unfolded proteins by signaling transcriptional activation, manifested in non-

conventional splicing of *HAC1* (Back et al., 2005). Therefore, we can query for *HAC1* via RNA blot to determine its splicing in the mutant cells under the effect of the drug.

Phosphoinositide signaling impinges on nuclear division

In collaboration with the Bankaitis lab, we identified an additional role of the PITPs in cell cycle transitions. Mutants lacking Sec14p have perturbed G1 and M phases in the cell cycle. The cells grow slowly. They are born bigger and undergo DNA replication at a bigger cell size (Huang et al., 2018). However, unlike other 'bypass Sec14p' mutants, we found that Kes1p is the only candidate to suppress the cell cycle phenotypes. Furthermore, under nutrient-limiting conditions, Kes1p serves as a brake to G1 cell progression and can help initiate a new round of cell division. The antagonistic action of Kes1p and Sec14p extends from membrane trafficking to cell cycle contexts behaving as a signaling axis in coordinating cell growth with the initiation of cell division in a nutrient-limiting environment (Huang et al., 2018). Hence, Kes1p and Sec14p perform dual membrane trafficking and cell cycle functions and act as a regulatory component that couples TGN/endosomal lipid signaling with cell cycle progression.

Further investigation leads to a unique convergence of translational control of fatty acid synthesis with Sec14p mediated phosphoinositide signaling. Previously, it was reported that the growth of cells lacking Sec14p function is worsened when fatty acid synthesis is inhibited (Dacquay et al., 2017). We tested our gain of function mutant in the Sec14p-deficient background. We found a partial rescue of the growth of cells without Sec14p functions. Moreover, additional cell cycle phenotypes were also

suppressed, including bigger cell size and a G2/M delay (Maitra et al., 2021). The studies suggest an unknown mechanism that feeds *de novo* fatty acids in the Sec14p mediated membrane trafficking pathway. Cells deficient in Sec14p may suffer from low amounts of fatty acids. We also found that the *sec14-1* mutant cells have a delayed nuclear division. Interestingly, the accelerated nuclear division of the uORF mutant was corrected in this mutant, and a timely nuclear division to the mutant cells was promoted. These data suggest that enhanced lipid synthesis can suppress the mitotic phenotypes of Sec14p and indicate that the accelerated nuclear division due to enhanced lipogenesis requires Sec14p functions.

Is there a specific class of phospholipids that contributes to cell cycle events such as nuclear division? Two major phospholipids are involved in the Sec14p mediated membrane trafficking, phosphatidylcholine and phosphatidylinositol (Grabon et al., 2019). Cki1p is a choline kinase that catalyzes the first step of the phosphatidylcholine synthesis pathway. It has been previously shown that *cki1* can bypass the Sec14p membrane trafficking phenotypes (Cleves et al., 1991). However, the lack of Cki1p is unable to suppress the cell cycle phenotypes of Sec14p. On the contrary, Kes1p suppresses all the cell cycle phenotypes and corrects the nuclear division timing. In this manner, the *kes1* 'bypass Sec14p' mutants differ from *cki1* mutants that correct only the membrane trafficking deficits.

Moreover, our study shows that yeast cells lacking Pik1p and Stt4p proteins have an abnormally shaped nucleus. Interestingly, de-repressing the translational control of lipogenic enzymes can restore the correct morphology of the nucleus in the *pik1* mutants

(suppression is not statistically significant in *stt4* mutant cells). We attempted to investigate the role of Mss4p in the translational control of the lipogenic enzymes. However, we were unable to generate the required strain. Nonetheless, the misshapen nucleus in the cells lacking Pik1p and Stt4p argues the requirement of phosphoinositide signaling in managing the nuclear morphology, hinting at the activity of TGN in transporting phosphoinositides to the nucleus. We are yet to determine this transport mechanism.

Unresolved question

- What are the lipid species that decorate the nuclear envelope, and what happens to nuclear morphology due to altered lipid homeostasis?
- Does localization of Pik1p change with cell cycle, and how does it affect the nuclear morphology?

Proposed Experiments

<u>What are the lipid species that decorate the nuclear envelope, and what happens to nuclear morphology due to altered lipid homeostasis?</u>

We can address the question in part by investigating the nuclear lipidome. Previously, we have queried the lipids of the whole cell and not the isolated nucleus. To determine which lipids mainly contribute to nuclear envelope remodeling, we can analyze nuclear lipids by mass spectrometry at different cell cycle stages. We could target the nuclear lipidome for the first time in the yeast cells during the cell cycle. Centrifugal elutriation will enable a collection of yeast cells at the G1 phase, and physiological coupling

between cell growth and division can be maintained. Nuclei can be purified at different stages and be subjected to lipid extraction and subsequent mass spectrometry analysis.

Moreover, the lipid sensing properties of Sec14p and other Phosphatidylinositol transfer proteins (PITPs) can serve as a tool to identify the branches of lipid metabolism contributing to mitosis. Sec14p causes exchange between PtdIns and PtdCho. Other Sec14p homologs participate in the transfer of different lipid species. For instance, Shf2p and Shf3p facilitate exchange between PtdIns/squalene and PtdIns/ergosterol, respectively (Tripathi et al., 2019). The PITP requirement for nuclear envelope remodeling can shed some light on the need for the nuclear division's specific lipid metabolism branch. We can use centrifugal elutriation to get synchronous culture in G1 and follow them through the cell cycle. We can monitor nuclear division by indirect immunofluorescence of a nuclear envelope protein (e.g., Nsp1p) in well-elutriated yeast cells lacking the function of the PITPs. Fluorescence monitoring of nuclear division under different PITP mutants and the mass spectrometry analysis of the nuclear lipidome together will facilitate the identification of specific lipids, lipid metabolism branches, and the carrier of the lipid.

Does localization of Pik1p change with cell cycle, and how does it affect the nuclear morphology?

Our result shows that the misshapen nuclei in the cells lacking the function Pik1p is significantly corrected by enhanced lipogenesis. However, we are unaware if the abnormal nuclear shape is due to the cytoplasmic or the nuclear function of the Pik1p. Two different plasmids are available from the Thorner Lab (Strahl et al., 2005). The

plasmids induce synthesis of the Pik1p, but either Pik1p stays in the nucleus (nuclear export deficient) or the cytoplasm. Our goal will be to transform these plasmids individually into the yeast strains with temperature-sensitive *pik1* mutants and determine which one of the plasmids can rescue the nuclear shape and cell cycle phenotypes, such as bigger cell size and S-phase delay.

Overall, the results reported in the dissertation and the proposed experiments illuminate the physiological significance of generating specific lipid pools that drive a crucial cell cycle process – i.e., nuclear elongation and division. These lipids pools represent metabolic inputs that do not merely 'fuel' a cell cycle process but, rather, play instructive signaling roles in driving landmark cell cycle events. The collective data integrate protein synthesis, lipogenesis, and phosphoinositide signaling with nuclear elongation and division timing.

REFERENCES

Accioly, M. T., Pacheco, P., Maya-Monteiro, C. M., Carrossini, N., Robbs, B. K., Oliveira, S. S., Kaufmann, C., Morgado-Diaz, J. A., Bozza, P. T., & Viola, J. P. B. (2008). Lipid bodies are reservoirs of cyclooxygenase-2 and sites of prostaglandin-E2 synthesis in colon cancer cells. *Cancer Research*, *68*(6), 1732–1740. https://doi.org/10.1158/0008-5472.CAN-07-1999

Alfaro-Aco, R., & Petry, S. (2015). Building the Microtubule Cytoskeleton Piece by Piece. *The Journal of Biological Chemistry*, *290*(28), 17154–17162. https://doi.org/10.1074/jbc.R115.638452

Al-Feel, W., Chirala, S. S., & Wakil, S. J. (1992). Cloning of the yeast FAS3 gene and primary structure of yeast acetyl-CoA carboxylase. *Proceedings of the National Academy of Sciences of the United States of America*, *89*(10), 4534–4538. https://doi.org/10.1073/pnas.89.10.4534

Al-Feel, Walid, DeMar, J. C., & Wakil, S. J. (2003). A Saccharomyces cerevisiae mutant strain defective in acetyl-CoA carboxylase arrests at the G2/M phase of the cell cycle. *Proceedings of the National Academy of Sciences of the United States of America*, *100*(6), 3095–3100. https://doi.org/10.1073/pnas.0538069100

Amodeo, A. A., & Skotheim, J. M. (2016). Cell-Size Control. *Cold Spring Harbor Perspectives in Biology*, *8*(4), a019083. https://doi.org/10.1101/cshperspect.a019083

Amon, A. (2002). Synchronization procedures. *Methods in Enzymology*, *351*, 457–467. https://doi.org/10.1016/s0076-6879(02)51864-4

Anastasia, S. D., Nguyen, D. L., Thai, V., Meloy, M., MacDonough, T., & Kellogg, D. R. (2012). A link between mitotic entry and membrane growth suggests a novel model for cell size control. *The Journal of Cell Biology*, *197*(1), 89–104. https://doi.org/10.1083/jcb.201108108

Aramayo, R., & Polymenis, M. (2017). Ribosome profiling the cell cycle: Lessons and challenges. *Current Genetics*, *63*(6), 959–964. https://doi.org/10.1007/s00294-017-0698-3

Arnone, J. T., Walters, A. D., & Cohen-Fix, O. (2013). The dynamic nature of the nuclear envelope: Lessons from closed mitosis. *Nucleus (Austin, Tex.)*, *4*(4), 261–266. https://doi.org/10.4161/nucl.25341

Arribere, J. A., & Gilbert, W. V. (2013). Roles for transcript leaders in translation and mRNA decay revealed by transcript leader sequencing. *Genome Research*, *23*(6), 977–987. https://doi.org/10.1101/gr.150342.112

Atilla-Gokcumen, G. E., Muro, E., Relat-Goberna, J., Sasse, S., Bedigian, A., Coughlin, M. L., Garcia-Manyes, S., & Eggert, U. S. (2014). Dividing cells regulate their lipid composition and localization. *Cell*, *156*(3), 428–439. https://doi.org/10.1016/j.cell.2013.12.015

Audhya, A., Foti, M., & Emr, S. D. (2000). Distinct roles for the yeast phosphatidylinositol 4-kinases, Stt4p and Pik1p, in secretion, cell growth, and

organelle membrane dynamics. *Molecular Biology of the Cell*, *11*(8), 2673–2689. https://doi.org/10.1091/mbc.11.8.2673

Auger, A., Galarneau, L., Altaf, M., Nourani, A., Doyon, Y., Utley, R. T., Cronier, D., Allard, S., & Côté, J. (2008). Eaf1 is the platform for NuA4 molecular assembly that evolutionarily links chromatin acetylation to ATP-dependent exchange of histone H2A variants. *Molecular and Cellular Biology*, *28*(7), 2257–2270. https://doi.org/10.1128/MCB.01755-07

Back, S. H., Schröder, M., Lee, K., Zhang, K., & Kaufman, R. J. (2005). ER stress signaling by regulated splicing: IRE1/HAC1/XBP1. *Methods (San Diego, Calif.)*, *35*(4), 395–416. https://doi.org/10.1016/j.ymeth.2005.03.001

Baenke, F., Peck, B., Miess, H., & Schulze, A. (2013). Hooked on fat: The role of lipid synthesis in cancer metabolism and tumour development. *Disease Models & Mechanisms*, *6*(6), 1353–1363. https://doi.org/10.1242/dmm.011338

Bahmanyar, S., & Schlieker, C. (2020). Lipid and protein dynamics that shape nuclear envelope identity. *Molecular Biology of the Cell*, *31*(13), 1315–1323. https://doi.org/10.1091/mbc.E18-10-0636

Banfalvi, G. (2008). Cell cycle synchronization of animal cells and nuclei by centrifugal elutriation. *Nature Protocols*, *3*(4), 663–673. https://doi.org/10.1038/nprot.2008.34

Bankaitis, V. A., Aitken, J. R., Cleves, A. E., & Dowhan, W. (1990). An essential role for a phospholipid transfer protein in yeast Golgi function. *Nature*, *347*(6293), 561–562. https://doi.org/10.1038/347561a0

Bankaitis, V. A., Johnson, L. M., & Emr, S. D. (1986). Isolation of yeast mutants defective in protein targeting to the vacuole. *Proceedings of the National Academy of Sciences of the United States of America*, *83*(23), 9075–9079. https://doi.org/10.1073/pnas.83.23.9075

Bankaitis, V. A., Malehorn, D. E., Emr, S. D., & Greene, R. (1989). The Saccharomyces cerevisiae SEC14 gene encodes a cytosolic factor that is required for transport of secretory proteins from the yeast Golgi complex. *The Journal of Cell Biology*, *108*(4), 1271–1281. https://doi.org/10.1083/jcb.108.4.1271

Bankaitis, Vytas A., Ile, K. E., Nile, A. H., Ren, J., Ghosh, R., & Schaaf, G. (2012). Thoughts on Sec14-like nanoreactors and phosphoinositide signaling. *Advances in Biological Regulation*, *52*(1), 115–121. https://doi.org/10.1016/j.jbior.2011.11.001

Bankaitis, Vytas A., Mousley, C. J., & Schaaf, G. (2010). The Sec14 superfamily and mechanisms for crosstalk between lipid metabolism and lipid signaling. *Trends in Biochemical Sciences*, *35*(3), 150–160. https://doi.org/10.1016/j.tibs.2009.10.008

Barbosa, A. D., Lim, K., Mari, M., Edgar, J. R., Gal, L., Sterk, P., Jenkins, B. J., Koulman, A., Savage, D. B., Schuldiner, M., Reggiori, F., Wigge, P. A., & Siniossoglou, S. (2019). Compartmentalized Synthesis of Triacylglycerol at the Inner Nuclear Membrane Regulates Nuclear Organization. *Developmental Cell*, *50*(6), 755-766.e6. https://doi.org/10.1016/j.devcel.2019.07.009

Barbosa, C., Peixeiro, I., & Romão, L. (2013). Gene expression regulation by upstream open reading frames and human disease. *PLoS Genetics*, *9*(8), e1003529. https://doi.org/10.1371/journal.pgen.1003529

Bard, F., & Malhotra, V. (2006). The formation of TGN-to-plasma-membrane transport carriers. *Annual Review of Cell and Developmental Biology*, *22*, 439–455. https://doi.org/10.1146/annurev.cellbio.21.012704.133126

Beach, D., Durkacz, B., & Nurse, P. (1982). Functionally homologous cell cycle control genes in budding and fission yeast. *Nature*, *300*(5894), 706–709. https://doi.org/10.1038/300706a0

Beck, T., & Hall, M. N. (1999). The TOR signalling pathway controls nuclear localization of nutrient-regulated transcription factors. *Nature*, *402*(6762), 689–692. https://doi.org/10.1038/45287

Beh, C. T., Cool, L., Phillips, J., & Rine, J. (2001). Overlapping functions of the yeast oxysterol-binding protein homologues. *Genetics*, *157*(3), 1117–1140.

Beloribi-Djefaflia, S., Vasseur, S., & Guillaumond, F. (2016). Lipid metabolic reprogramming in cancer cells. *Oncogenesis*, *5*, e189. https://doi.org/10.1038/oncsis.2015.49

Biggins, S., Hartwell, L., & Toczyski, D. (2020). Fifty years of cycling. *Molecular Biology of the Cell*, *31*(26), 2868–2870. https://doi.org/10.1091/mbc.E20-07-0495

Björklund, M. (2019). Cell size homeostasis: Metabolic control of growth and cell division. *Biochimica Et Biophysica Acta. Molecular Cell Research*, *1866*(3), 409–417. https://doi.org/10.1016/j.bbamcr.2018.10.002

Blank, H. M., Alonso, A., Winey, M., & Polymenis, M. (2020). Translational control of *MPS1* links protein synthesis with the initiation of cell division and spindle pole body duplication in yeast. *BioRxiv*, 2020.12.29.424704. https://doi.org/10.1101/2020.12.29.424704

Blank, H. M., Callahan, M., Pistikopoulos, I. P. E., Polymenis, A. O., & Polymenis, M. (2018). Scaling of G1 Duration with Population Doubling Time by a Cyclin in Saccharomyces cerevisiae. *Genetics*, *210*(3), 895–906. https://doi.org/10.1534/genetics.118.301507

Blank, H. M., Maitra, N., & Polymenis, M. (2017). Lipid biosynthesis: When the cell cycle meets protein synthesis? *Cell Cycle (Georgetown, Tex.)*, *16*(10), 905–906. https://doi.org/10.1080/15384101.2017.1312851

Blank, H. M., Papoulas, O., Maitra, N., Garge, R., Kennedy, B. K., Schilling, B., Marcotte, E. M., & Polymenis, M. (2020). Abundances of transcripts, proteins, and metabolites in the cell cycle of budding yeast reveal coordinate control of lipid metabolism. *Molecular Biology of the Cell*, *31*(10), 1069–1084. https://doi.org/10.1091/mbc.E19-12-0708

Blank, H. M., Perez, R., He, C., Maitra, N., Metz, R., Hill, J., Lin, Y., Johnson, C. D., Bankaitis, V. A., Kennedy, B. K., Aramayo, R., & Polymenis, M. (2017). Translational control of lipogenic enzymes in the cell cycle of synchronous,

growing yeast cells. *The EMBO Journal*, *36*(4), 487–502. https://doi.org/10.15252/embj.201695050

Blom, T., Somerharju, P., & Ikonen, E. (2011). Synthesis and biosynthetic trafficking of membrane lipids. *Cold Spring Harbor Perspectives in Biology*, *3*(8), a004713. https://doi.org/10.1101/cshperspect.a004713

Bloom, J., & Cross, F. R. (2007). Multiple levels of cyclin specificity in cell-cycle control. *Nature Reviews. Molecular Cell Biology*, *8*(2), 149–160. https://doi.org/10.1038/nrm2105

Braselmann, E., Stasevich, T. J., Lyon, K., Batey, R. T., & Palmer, A. E. (2019). Detection and quantification of single mRNA dynamics with the Riboglow fluorescent RNA tag. *BioRxiv*, 701649. https://doi.org/10.1101/701649

Calvo, S. E., Pagliarini, D. J., & Mootha, V. K. (2009). Upstream open reading frames cause widespread reduction of protein expression and are polymorphic among humans. *Proceedings of the National Academy of Sciences of the United States of America*, *106*(18), 7507–7512. https://doi.org/10.1073/pnas.0810916106

Cameroni, E., De Virgilio, C., & Deloche, O. (2006). Phosphatidylinositol 4-phosphate is required for translation initiation in Saccharomyces cerevisiae. *The Journal of Biological Chemistry*, *281*(50), 38139–38149. https://doi.org/10.1074/jbc.M601060200

Cameroni, E., Hulo, N., Roosen, J., Winderickx, J., & De Virgilio, C. (2004). The novel yeast PAS kinase Rim 15 orchestrates G0-associated antioxidant defense mechanisms. *Cell Cycle (Georgetown, Tex.)*, *3*(4), 462–468.

Campbell, J. L., Lorenz, A., Witkin, K. L., Hays, T., Loidl, J., & Cohen-Fix, O. (2006). Yeast nuclear envelope subdomains with distinct abilities to resist membrane expansion. *Molecular Biology of the Cell*, *17*(4), 1768–1778. https://doi.org/10.1091/mbc.e05-09-0839

Castagnetti, S., Oliferenko, S., & Nurse, P. (2010). Fission yeast cells undergo nuclear division in the absence of spindle microtubules. *PLoS Biology*, *8*(10), e1000512. https://doi.org/10.1371/journal.pbio.1000512

Castano, E., Yildirim, S., Fáberová, V., Krausová, A., Uličná, L., Paprčková, D., Sztacho, M., & Hozák, P. (2019). Nuclear Phosphoinositides-Versatile Regulators of Genome Functions. *Cells*, *8*(7). https://doi.org/10.3390/cells8070649

Chen, M., Wen, T., Horn, H. T., Chandrahas, V. K., Thapa, N., Choi, S., Cryns, V. L., & Anderson, R. A. (2020). The nuclear phosphoinositide response to stress. *Cell Cycle (Georgetown, Tex.)*, *19*(3), 268–289. https://doi.org/10.1080/15384101.2019.1711316

Cho, R. J., Campbell, M. J., Winzeler, E. A., Steinmetz, L., Conway, A., Wodicka, L., Wolfsberg, T. G., Gabrielian, A. E., Landsman, D., Lockhart, D. J., & Davis, R. W. (1998). A genome-wide transcriptional analysis of the mitotic cell cycle. *Molecular Cell*, *2*(1), 65–73. https://doi.org/10.1016/s1097-2765(00)80114-8

Clarke, A. S., Lowell, J. E., Jacobson, S. J., & Pillus, L. (1999). Esa1p is an essential histone acetyltransferase required for cell cycle progression. *Molecular and Cellular Biology*, *19*(4), 2515–2526. https://doi.org/10.1128/mcb.19.4.2515

Cleves, A. E., McGee, T. P., Whitters, E. A., Champion, K. M., Aitken, J. R., Dowhan, W., Goebl, M., & Bankaitis, V. A. (1991). Mutations in the CDP-choline pathway for phospholipid biosynthesis bypass the requirement for an essential phospholipid transfer protein. *Cell*, *64*(4), 789–800. https://doi.org/10.1016/0092-8674(91)90508-v

Cleves, A. E., Novick, P. J., & Bankaitis, V. A. (1989). Mutations in the SAC1 gene suppress defects in yeast Golgi and yeast actin function. *The Journal of Cell Biology*, *109*(6 Pt 1), 2939–2950. https://doi.org/10.1083/jcb.109.6.2939

Cocco, L., Gilmour, R. S., Ognibene, A., Letcher, A. J., Manzoli, F. A., & Irvine, R. F. (1987). Synthesis of polyphosphoinositides in nuclei of Friend cells. Evidence for polyphosphoinositide metabolism inside the nucleus which changes with cell differentiation. *The Biochemical Journal*, *248*(3), 765–770. https://doi.org/10.1042/bj2480765

Cocco, L., Martelli, A. M., Gilmour, R. S., Ognibene, A., Manzoli, F. A., & Irvine, R. F. (1989). Changes in nuclear inositol phospholipids induced in intact cells by insulin-like growth factor I. *Biochemical and Biophysical Research Communications*, *159*(2), 720–725. https://doi.org/10.1016/0006-291x(89)90054-5

Cooper, S. (2003). Rethinking synchronization of mammalian cells for cell cycle analysis. *Cellular and Molecular Life Sciences: CMLS*, *60*(6), 1099–1106. https://doi.org/10.1007/s00018-003-2253-2

Dacquay, L., Flint, A., Butcher, J., Salem, D., Kennedy, M., Kaern, M., Stintzi, A., & Baetz, K. (2017). NuA4 Lysine Acetyltransferase Complex Contributes to Phospholipid Homeostasis in Saccharomyces cerevisiae. *G3 (Bethesda, Md.)*, *7*(6), 1799–1809. https://doi.org/10.1534/g3.117.041053

Dahl, K. N., Ribeiro, A. J. S., & Lammerding, J. (2008). Nuclear shape, mechanics, and mechanotransduction. *Circulation Research*, *102*(11), 1307–1318. https://doi.org/10.1161/CIRCRESAHA.108.173989

de Nooij, J. C., Letendre, M. A., & Hariharan, I. K. (1996). A cyclin-dependent kinase inhibitor, Dacapo, is necessary for timely exit from the cell cycle during Drosophila embryogenesis. *Cell*, *87*(7), 1237–1247. https://doi.org/10.1016/s0092-8674(00)81819-x

de Saint-Jean, M., Delfosse, V., Douguet, D., Chicanne, G., Payrastre, B., Bourguet, W., Antonny, B., & Drin, G. (2011). Osh4p exchanges sterols for phosphatidylinositol 4-phosphate between lipid bilayers. *The Journal of Cell Biology*, *195*(6), 965–978. https://doi.org/10.1083/jcb.201104062

de Vries, K. J., Heinrichs, A. A., Cunningham, E., Brunink, F., Westerman, J., Somerharju, P. J., Cockcroft, S., Wirtz, K. W., & Snoek, G. T. (1995). An isoform of the phosphatidylinositol-transfer protein transfers sphingomyelin and is associated with the Golgi system. *The Biochemical Journal*, *310 (Pt 2)*, 643–649. https://doi.org/10.1042/bj3100643

de Vries, K. J., Westerman, J., Bastiaens, P. I., Jovin, T. M., Wirtz, K. W., & Snoek, G. T. (1996). Fluorescently labeled phosphatidylinositol transfer protein isoforms

(alpha and beta), microinjected into fetal bovine heart endothelial cells, are targeted to distinct intracellular sites. *Experimental Cell Research*, *227*(1), 33–39. https://doi.org/10.1006/excr.1996.0246

Dey, G., & Baum, B. (2021). Nuclear envelope remodelling during mitosis. *Current Opinion in Cell Biology*, *70*, 67–74. https://doi.org/10.1016/j.ceb.2020.12.004

Dey, G., Culley, S., Curran, S., Schmidt, U., Henriques, R., Kukulski, W., & Baum, B. (2020). Closed mitosis requires local disassembly of the nuclear envelope. *Nature*, *585*(7823), 119–123. https://doi.org/10.1038/s41586-020-2648-3

Di Como, C. J., Chang, H., & Arndt, K. T. (1995). Activation of CLN1 and CLN2 G1 cyclin gene expression by BCK2. *Molecular and Cellular Biology*, *15*(4), 1835–1846. https://doi.org/10.1128/mcb.15.4.1835

Di Talia, S., Skotheim, J. M., Bean, J. M., Siggia, E. D., & Cross, F. R. (2007). The effects of molecular noise and size control on variability in the budding yeast cell cycle. *Nature*, *448*(7156), 947–951. https://doi.org/10.1038/nature06072

Di Talia, S., Wang, H., Skotheim, J. M., Rosebrock, A. P., Futcher, B., & Cross, F. R. (2009). Daughter-specific transcription factors regulate cell size control in budding yeast. *PLoS Biology*, *7*(10), e1000221. https://doi.org/10.1371/journal.pbio.1000221

Ding, R., West, R. R., Morphew, D. M., Oakley, B. R., & McIntosh, J. R. (1997). The spindle pole body of Schizosaccharomyces pombe enters and leaves the nuclear envelope as the cell cycle proceeds. *Molecular Biology of the Cell*, *8*(8), 1461–1479. https://doi.org/10.1091/mbc.8.8.1461

Dorée, M., & Hunt, T. (2002). From Cdc2 to Cdk1: When did the cell cycle kinase join its cyclin partner? *Journal of Cell Science*, *115*(Pt 12), 2461–2464.

Dorsey, S., Tollis, S., Cheng, J., Black, L., Notley, S., Tyers, M., & Royer, C. A. (2018). G1/S Transcription Factor Copy Number Is a Growth-Dependent Determinant of Cell Cycle Commitment in Yeast. *Cell Systems*, *6*(5), 539-554.e11. https://doi.org/10.1016/j.cels.2018.04.012

Elliott, S. G., Warner, J. R., & McLaughlin, C. S. (1979). Synthesis of ribosomal proteins during the cell cycle of the yeast Saccharomyces cerevisiae. *Journal of Bacteriology*, *137*(2), 1048–1050. https://doi.org/10.1128/JB.137.2.1048-1050.1979

Epstein, C. J. (1967). Cell size, nuclear content, and the development of polyploidy in the Mammalian liver. *Proceedings of the National Academy of Sciences of the United States of America*, *57*(2), 327–334. https://doi.org/10.1073/pnas.57.2.327

Evans, T., Rosenthal, E. T., Youngblom, J., Distel, D., & Hunt, T. (1983). Cyclin: A protein specified by maternal mRNA in sea urchin eggs that is destroyed at each cleavage division. *Cell*, *33*(2), 389–396. https://doi.org/10.1016/0092-8674(83)90420-8

Facchetti, G., Chang, F., & Howard, M. (2017). Controlling cell size through sizer mechanisms. *Current Opinion in Systems Biology*, *5*, 86–92. https://doi.org/10.1016/j.coisb.2017.08.010

Fang, M., Kearns, B. G., Gedvilaite, A., Kagiwada, S., Kearns, M., Fung, M. K., & Bankaitis, V. A. (1996). Kes1p shares homology with human oxysterol binding

protein and participates in a novel regulatory pathway for yeast Golgi-derived transport vesicle biogenesis. *The EMBO Journal*, *15*(23), 6447–6459.

Fantes, P. A., Grant, W. D., Pritchard, R. H., Sudbery, P. E., & Wheals, A. E. (1975). The regulation of cell size and the control of mitosis. *Journal of Theoretical Biology*, *50*(1), 213–244. https://doi.org/10.1016/0022-5193(75)90034-x

Feron, O. (2019). The many metabolic sources of acetyl-CoA to support histone acetylation and influence cancer progression. *Annals of Translational Medicine*, *7*(Suppl 8), S277. https://doi.org/10.21037/atm.2019.11.140

Filteau, M., Diss, G., Torres-Quiroz, F., Dubé, A. K., Schraffl, A., Bachmann, V. A., Gagnon-Arsenault, I., Chrétien, A.-È., Steunou, A.-L., Dionne, U., Côté, J., Bisson, N., Stefan, E., & Landry, C. R. (2015). Systematic identification of signal integration by protein kinase A. *Proceedings of the National Academy of Sciences of the United States of America*, *112*(14), 4501–4506. https://doi.org/10.1073/pnas.1409938112

Fischer, M., Joppe, M., Mulinacci, B., Vollrath, R., Konstantinidis, K., Kötter, P., Ciccarelli, L., Vonck, J., Oesterhelt, D., & Grininger, M. (2020). Analysis of the co-translational assembly of the fungal fatty acid synthase (FAS). *Scientific Reports*, *10*(1), 895. https://doi.org/10.1038/s41598-020-57418-8

Fitch, I., Dahmann, C., Surana, U., Amon, A., Nasmyth, K., Goetsch, L., Byers, B., & Futcher, B. (1992). Characterization of four B-type cyclin genes of the budding yeast Saccharomyces cerevisiae. *Molecular Biology of the Cell*, *3*(7), 805–818. https://doi.org/10.1091/mbc.3.7.805

Folch-Mallol, J. L., Garay-Arroyo, A., Lledías, F., & Covarrubias Robles, A. A. (2004). [The stress response in the yeast Saccharomyces cerevisiae]. *Revista Latinoamericana De Microbiologia*, *46*(1–2), 24–46.

Foltman, M., Molist, I., & Sanchez-Diaz, A. (2016). Synchronization of the Budding Yeast Saccharomyces cerevisiae. *Methods in Molecular Biology (Clifton, N.J.)*, *1369*, 279–291. https://doi.org/10.1007/978-1-4939-3145-3_19

Forsburg, S. L., & Rhind, N. (2006). Basic methods for fission yeast. *Yeast (Chichester, England)*, *23*(3), 173–183. https://doi.org/10.1002/yea.1347

Furse, S., & Shearman, G. C. (2018). Do lipids shape the eukaryotic cell cycle? *Biochimica Et Biophysica Acta. Molecular and Cell Biology of Lipids*, *1863*(1), 9–19. https://doi.org/10.1016/j.bbalip.2017.09.010

Futcher, B. (1999). Cell cycle synchronization. *Methods in Cell Science: An Official Journal of the Society for In Vitro Biology*, *21*(2–3), 79–86. https://doi.org/10.1023/a:1009872403440

Galdieri, L., & Vancura, A. (2012). Acetyl-CoA carboxylase regulates global histone acetylation. *The Journal of Biological Chemistry*, *287*(28), 23865–23876. https://doi.org/10.1074/jbc.M112.380519

Galdieri, L., Zhang, T., Rogerson, D., Lleshi, R., & Vancura, A. (2014). Protein acetylation and acetyl coenzyme a metabolism in budding yeast. *Eukaryotic Cell*, *13*(12), 1472–1483. https://doi.org/10.1128/EC.00189-14

Gao, S., Kinzig, K. P., Aja, S., Scott, K. A., Keung, W., Kelly, S., Strynadka, K., Chohnan, S., Smith, W. W., Tamashiro, K. L. K., Ladenheim, E. E., Ronnett, G.

V., Tu, Y., Birnbaum, M. J., Lopaschuk, G. D., & Moran, T. H. (2007). Leptin activates hypothalamic acetyl-CoA carboxylase to inhibit food intake. *Proceedings of the National Academy of Sciences of the United States of America*, *104*(44), 17358–17363. https://doi.org/10.1073/pnas.0708385104

Garcia-Bustos, J. F., Marini, F., Stevenson, I., Frei, C., & Hall, M. N. (1994). PIK1, an essential phosphatidylinositol 4-kinase associated with the yeast nucleus. *The EMBO Journal*, *13*(10), 2352–2361.

Gebauer, F., & Hentze, M. W. (2004). Molecular mechanisms of translational control. *Nature Reviews. Molecular Cell Biology*, *5*(10), 827–835. https://doi.org/10.1038/nrm1488

Georgiev, A. G., Sullivan, D. P., Kersting, M. C., Dittman, J. S., Beh, C. T., & Menon, A. K. (2011). Osh proteins regulate membrane sterol organization but are not required for sterol movement between the ER and PM. *Traffic (Copenhagen, Denmark)*, *12*(10), 1341–1355. https://doi.org/10.1111/j.1600-0854.2011.01234.x

Giaever, G., Chu, A. M., Ni, L., Connelly, C., Riles, L., Véronneau, S., Dow, S., Lucau-Danila, A., Anderson, K., André, B., Arkin, A. P., Astromoff, A., El-Bakkoury, M., Bangham, R., Benito, R., Brachat, S., Campanaro, S., Curtiss, M., Davis, K., … Johnston, M. (2002). Functional profiling of the Saccharomyces cerevisiae genome. *Nature*, *418*(6896), 387–391. https://doi.org/10.1038/nature00935

Givan, A. L. (2001). Principles of flow cytometry: An overview. *Methods in Cell Biology*, *63*, 19–50. https://doi.org/10.1016/s0091-679x(01)63006-1

Glick, B. S., & Nakano, A. (2009). Membrane traffic within the Golgi apparatus. *Annual Review of Cell and Developmental Biology*, *25*, 113–132. https://doi.org/10.1146/annurev.cellbio.24.110707.175421

Golden, A., Liu, J., & Cohen-Fix, O. (2009). Inactivation of the C. elegans lipin homolog leads to ER disorganization and to defects in the breakdown and reassembly of the nuclear envelope. *Journal of Cell Science*, *122*(Pt 12), 1970–1978. https://doi.org/10.1242/jcs.044743

Goto, A., Charman, M., & Ridgway, N. D. (2016). Oxysterol-binding Protein Activation at Endoplasmic Reticulum-Golgi Contact Sites Reorganizes Phosphatidylinositol 4-Phosphate Pools. *The Journal of Biological Chemistry*, *291*(3), 1336–1347. https://doi.org/10.1074/jbc.M115.682997

Grabon, A., Bankaitis, V. A., & McDermott, M. I. (2019). The interface between phosphatidylinositol transfer protein function and phosphoinositide signaling in higher eukaryotes. *Journal of Lipid Research*, *60*(2), 242–268. https://doi.org/10.1194/jlr.R089730

Graham, T. R., & Burd, C. G. (2011). Coordination of Golgi functions by phosphatidylinositol 4-kinases. *Trends in Cell Biology*, *21*(2), 113–121. https://doi.org/10.1016/j.tcb.2010.10.002

Green, M. D., Sabatinos, S. A., & Forsburg, S. L. (2009). Microscopy techniques to examine DNA replication in fission yeast. *Methods in Molecular Biology (Clifton, N.J.)*, *521*, 463–482. https://doi.org/10.1007/978-1-60327-815-7_26

Guo, S., Stolz, L. E., Lemrow, S. M., & York, J. D. (1999). SAC1-like domains of yeast SAC1, INP52, and INP53 and of human synaptojanin encode polyphosphoinositide phosphatases. *The Journal of Biological Chemistry*, *274*(19), 12990–12995. https://doi.org/10.1074/jbc.274.19.12990

Güttinger, S., Laurell, E., & Kutay, U. (2009). Orchestrating nuclear envelope disassembly and reassembly during mitosis. *Nature Reviews. Molecular Cell Biology*, *10*(3), 178–191. https://doi.org/10.1038/nrm2641

Haase, S. B., & Lew, D. J. (1997). Flow cytometric analysis of DNA content in budding yeast. *Methods in Enzymology*, *283*, 322–332. https://doi.org/10.1016/s0076-6879(97)83026-1

Hadwiger, J. A., Wittenberg, C., Richardson, H. E., de Barros Lopes, M., & Reed, S. I. (1989). A family of cyclin homologs that control the G1 phase in yeast. *Proceedings of the National Academy of Sciences of the United States of America*, *86*(16), 6255–6259. https://doi.org/10.1073/pnas.86.16.6255

Hague, C. V., Postle, A. D., Attard, G. S., & Dymond, M. K. (2013). Cell cycle dependent changes in membrane stored curvature elastic energy: Evidence from lipidomic studies. *Faraday Discussions*, *161*, 481–497; discussion 563-589. https://doi.org/10.1039/c2fd20078c

Hamann, B. L., & Blind, R. D. (2018). Nuclear phosphoinositide regulation of chromatin. *Journal of Cellular Physiology*, *233*(1), 107–123. https://doi.org/10.1002/jcp.25886

Han, S., Zhao, B. S., Myers, S. A., Carr, S. A., He, C., & Ting, A. Y. (2020). RNA-protein interaction mapping via MS2- or Cas13-based APEX targeting. *Proceedings of the National Academy of Sciences of the United States of America*, *117*(36), 22068–22079. https://doi.org/10.1073/pnas.2006617117

Harper, J. V. (2005). Synchronization of cell populations in G1/S and G2/M phases of the cell cycle. *Methods in Molecular Biology (Clifton, N.J.)*, *296*, 157–166. https://doi.org/10.1385/1-59259-857-9:157

Hartwell, L. H. (1973). Synchronization of haploid yeast cell cycles, a prelude to conjugation. *Experimental Cell Research*, *76*(1), 111–117. https://doi.org/10.1016/0014-4827(73)90425-4

Hartwell, L. H., Culotti, J., Pringle, J. R., & Reid, B. J. (1974). Genetic control of the cell division cycle in yeast. *Science (New York, N.Y.)*, *183*(4120), 46–51. https://doi.org/10.1126/science.183.4120.46

Hartwell, L. H., Culotti, J., & Reid, B. (1970). Genetic control of the cell-division cycle in yeast. I. Detection of mutants. *Proceedings of the National Academy of Sciences of the United States of America*, *66*(2), 352–359. https://doi.org/10.1073/pnas.66.2.352

Hartwell, L. H., & Unger, M. W. (1977). Unequal division in Saccharomyces cerevisiae and its implications for the control of cell division. *The Journal of Cell Biology*, *75*(2 Pt 1), 422–435. https://doi.org/10.1083/jcb.75.2.422

He, C., Tsuchiyama, S. K., Nguyen, Q. T., Plyusnina, E. N., Terrill, S. R., Sahibzada, S., Patel, B., Faulkner, A. R., Shaposhnikov, M. V., Tian, R., Tsuchiya, M.,

Kaeberlein, M., Moskalev, A. A., Kennedy, B. K., & Polymenis, M. (2014). Enhanced longevity by ibuprofen, conserved in multiple species, occurs in yeast through inhibition of tryptophan import. *PLoS Genetics*, *10*(12), e1004860. https://doi.org/10.1371/journal.pgen.1004860

Hengst, L., & Reed, S. I. (1996). Translational control of p27Kip1 accumulation during the cell cycle. *Science (New York, N.Y.)*, *271*(5257), 1861–1864. https://doi.org/10.1126/science.271.5257.1861

Henriksen, P., Wagner, S. A., Weinert, B. T., Sharma, S., Bacinskaja, G., Rehman, M., Juffer, A. H., Walther, T. C., Lisby, M., & Choudhary, C. (2012). Proteome-wide analysis of lysine acetylation suggests its broad regulatory scope in Saccharomyces cerevisiae. *Molecular & Cellular Proteomics: MCP*, *11*(11), 1510–1522. https://doi.org/10.1074/mcp.M112.017251

Hetzer, M. W. (2010). The nuclear envelope. *Cold Spring Harbor Perspectives in Biology*, *2*(3), a000539. https://doi.org/10.1101/cshperspect.a000539

Hinnebusch, A. G. (2005). Translational regulation of GCN4 and the general amino acid control of yeast. *Annual Review of Microbiology*, *59*, 407–450. https://doi.org/10.1146/annurev.micro.59.031805.133833

Hinnebusch, A. G., Ivanov, I. P., & Sonenberg, N. (2016). Translational control by 5'-untranslated regions of eukaryotic mRNAs. *Science (New York, N.Y.)*, *352*(6292), 1413–1416. https://doi.org/10.1126/science.aad9868

Hoelz, A., Debler, E. W., & Blobel, G. (2011). The structure of the nuclear pore complex. *Annual Review of Biochemistry*, *80*, 613–643. https://doi.org/10.1146/annurev-biochem-060109-151030

Holcik, M., & Sonenberg, N. (2005). Translational control in stress and apoptosis. *Nature Reviews. Molecular Cell Biology*, *6*(4), 318–327. https://doi.org/10.1038/nrm1618

Hölzl, G., & Dörmann, P. (2019). Chloroplast Lipids and Their Biosynthesis. *Annual Review of Plant Biology*, *70*, 51–81. https://doi.org/10.1146/annurev-arplant-050718-100202

Hoose, S. A., Rawlings, J. A., Kelly, M. M., Leitch, M. C., Ababneh, Q. O., Robles, J. P., Taylor, D., Hoover, E. M., Hailu, B., McEnery, K. A., Downing, S. S., Kaushal, D., Chen, Y., Rife, A., Brahmbhatt, K. A., Smith, R., & Polymenis, M. (2012). A systematic analysis of cell cycle regulators in yeast reveals that most factors act independently of cell size to control initiation of division. *PLoS Genetics*, *8*(3), e1002590. https://doi.org/10.1371/journal.pgen.1002590

Hsu, W. W., Wu, B., & Liu, W. R. (2016). Sirtuins 1 and 2 Are Universal Histone Deacetylases. *ACS Chemical Biology*, *11*(3), 792–799. https://doi.org/10.1021/acschembio.5b00886

Huang, J., Mousley, C. J., Dacquay, L., Maitra, N., Drin, G., He, C., Ridgway, N. D., Tripathi, A., Kennedy, M., Kennedy, B. K., Liu, W., Baetz, K., Polymenis, M., & Bankaitis, V. A. (2018). A Lipid Transfer Protein Signaling Axis Exerts Dual

Control of Cell-Cycle and Membrane Trafficking Systems. *Developmental Cell*, *44*(3), 378-391.e5. https://doi.org/10.1016/j.devcel.2017.12.026

Hunkeler, M., Stuttfeld, E., Hagmann, A., Imseng, S., & Maier, T. (2016). The dynamic organization of fungal acetyl-CoA carboxylase. *Nature Communications*, *7*, 11196. https://doi.org/10.1038/ncomms11196

Hurt, E. C. (1988). A novel nucleoskeletal-like protein located at the nuclear periphery is required for the life cycle of Saccharomyces cerevisiae. *The EMBO Journal*, *7*(13), 4323–4334.

Hyland, P. L., Keegan, A. L., Curran, M. D., Middleton, D., McKenna, P. G., & Barnett, Y. A. (2000). Effect of a dCTP:dTTP pool imbalance on DNA replication fidelity in Friend murine erythroleukemia cells. *Environmental and Molecular Mutagenesis*, *36*(2), 87–96. https://doi.org/10.1002/1098-2280(2000)36:2<87::aid-em2>3.0.co;2-a

Im, Y. J., Raychaudhuri, S., Prinz, W. A., & Hurley, J. H. (2005). Structural mechanism for sterol sensing and transport by OSBP-related proteins. *Nature*, *437*(7055), 154–158. https://doi.org/10.1038/nature03923

Ingolia, N. T. (2014). Ribosome profiling: New views of translation, from single codons to genome scale. *Nature Reviews. Genetics*, *15*(3), 205–213. https://doi.org/10.1038/nrg3645

Ingolia, N. T., Brar, G. A., Rouskin, S., McGeachy, A. M., & Weissman, J. S. (2012). The ribosome profiling strategy for monitoring translation in vivo by deep

sequencing of ribosome-protected mRNA fragments. *Nature Protocols*, *7*(8), 1534–1550. https://doi.org/10.1038/nprot.2012.086

Ingolia, N. T., Ghaemmaghami, S., Newman, J. R. S., & Weissman, J. S. (2009). Genome-wide analysis in vivo of translation with nucleotide resolution using ribosome profiling. *Science (New York, N.Y.)*, *324*(5924), 218–223. https://doi.org/10.1126/science.1168978

Jaspersen, S. L., & Winey, M. (2004). The budding yeast spindle pole body: Structure, duplication, and function. *Annual Review of Cell and Developmental Biology*, *20*, 1–28. https://doi.org/10.1146/annurev.cellbio.20.022003.114106

Jenni, S., Leibundgut, M., Boehringer, D., Frick, C., Mikolásek, B., & Ban, N. (2007). Structure of fungal fatty acid synthase and implications for iterative substrate shuttling. *Science (New York, N.Y.)*, *316*(5822), 254–261. https://doi.org/10.1126/science.1138248

Jeon, S., & Kim, J. (2010). Upstream open reading frames regulate the cell cycle-dependent expression of the RNA helicase Rok1 in Saccharomyces cerevisiae. *FEBS Letters*, *584*(22), 4593–4598. https://doi.org/10.1016/j.febslet.2010.10.019

Johansson, M., Bocher, V., Lehto, M., Chinetti, G., Kuismanen, E., Ehnholm, C., Staels, B., & Olkkonen, V. M. (2003). The two variants of oxysterol binding protein-related protein-1 display different tissue expression patterns, have different intracellular localization, and are functionally distinct. *Molecular Biology of the Cell*, *14*(3), 903–915. https://doi.org/10.1091/mbc.e02-08-0459

Johansson, M., Rocha, N., Zwart, W., Jordens, I., Janssen, L., Kuijl, C., Olkkonen, V. M., & Neefjes, J. (2007). Activation of endosomal dynein motors by stepwise assembly of Rab7-RILP-p150Glued, ORP1L, and the receptor betalll spectrin. *The Journal of Cell Biology*, *176*(4), 459–471. https://doi.org/10.1083/jcb.200606077

Johnson, A., & Skotheim, J. M. (2013). Start and the restriction point. *Current Opinion in Cell Biology*, *25*(6), 717–723. https://doi.org/10.1016/j.ceb.2013.07.010

Johnson, R. T., & Rao, P. N. (1970). Mammalian cell fusion: Induction of premature chromosome condensation in interphase nuclei. *Nature*, *226*(5247), 717–722. https://doi.org/10.1038/226717a0

Johnston, G. C., Pringle, J. R., & Hartwell, L. H. (1977). Coordination of growth with cell division in the yeast Saccharomyces cerevisiae. *Experimental Cell Research*, *105*(1), 79–98. https://doi.org/10.1016/0014-4827(77)90154-9

Jorgensen, P., & Tyers, M. (2004). How cells coordinate growth and division. *Current Biology: CB*, *14*(23), R1014-1027. https://doi.org/10.1016/j.cub.2004.11.027

Juanes, M. A. (2017). Methods of Synchronization of Yeast Cells for the Analysis of Cell Cycle Progression. *Methods in Molecular Biology (Clifton, N.J.)*, *1505*, 19–34. https://doi.org/10.1007/978-1-4939-6502-1_2

Jungfleisch, J., Nedialkova, D. D., Dotu, I., Sloan, K. E., Martinez-Bosch, N., Brüning, L., Raineri, E., Navarro, P., Bohnsack, M. T., Leidel, S. A., & Díez, J. (2017). A novel translational control mechanism involving RNA structures within coding

sequences. *Genome Research*, *27*(1), 95–106. https://doi.org/10.1101/gr.209015.116

Kearns, B. G., McGee, T. P., Mayinger, P., Gedvilaite, A., Phillips, S. E., Kagiwada, S., & Bankaitis, V. A. (1997). Essential role for diacylglycerol in protein transport from the yeast Golgi complex. *Nature*, *387*(6628), 101–105. https://doi.org/10.1038/387101a0

Kilmartin, J. V. (2014). Lessons from yeast: The spindle pole body and the centrosome. *Philosophical Transactions of the Royal Society of London. Series B, Biological Sciences*, *369*(1650). https://doi.org/10.1098/rstb.2013.0456

Kim, K. H. (1997). Regulation of mammalian acetyl-coenzyme A carboxylase. *Annual Review of Nutrition*, *17*, 77–99. https://doi.org/10.1146/annurev.nutr.17.1.77

Klug, L., & Daum, G. (2014). Yeast lipid metabolism at a glance. *FEMS Yeast Research*, *14*(3), 369–388. https://doi.org/10.1111/1567-1364.12141

Krause, S. A., & Gray, J. V. (2002). The protein kinase C pathway is required for viability in quiescence in Saccharomyces cerevisiae. *Current Biology: CB*, *12*(7), 588–593. https://doi.org/10.1016/s0960-9822(02)00760-1

Kuhajda, F. P., Jenner, K., Wood, F. D., Hennigar, R. A., Jacobs, L. B., Dick, J. D., & Pasternack, G. R. (1994). Fatty acid synthesis: A potential selective target for antineoplastic therapy. *Proceedings of the National Academy of Sciences of the United States of America*, *91*(14), 6379–6383. https://doi.org/10.1073/pnas.91.14.6379

Kume, K., Cantwell, H., Neumann, F. R., Jones, A. W., Snijders, A. P., & Nurse, P. (2017). A systematic genomic screen implicates nucleocytoplasmic transport and membrane growth in nuclear size control. *PLoS Genetics*, *13*(5), e1006767. https://doi.org/10.1371/journal.pgen.1006767

Kvam, E., & Goldfarb, D. S. (2004). Nvj1p is the outer-nuclear-membrane receptor for oxysterol-binding protein homolog Osh1p in Saccharomyces cerevisiae. *Journal of Cell Science*, *117*(Pt 21), 4959–4968. https://doi.org/10.1242/jcs.01372

Labbé, J. C., Picard, A., Karsenti, E., & Dorée, M. (1988). An M-phase-specific protein kinase of Xenopus oocytes: Partial purification and possible mechanism of its periodic activation. *Developmental Biology*, *127*(1), 157–169. https://doi.org/10.1016/0012-1606(88)90197-2

Lane, M. E., Sauer, K., Wallace, K., Jan, Y. N., Lehner, C. F., & Vaessin, H. (1996). Dacapo, a cyclin-dependent kinase inhibitor, stops cell proliferation during Drosophila development. *Cell*, *87*(7), 1225–1235. https://doi.org/10.1016/s0092-8674(00)81818-8

Lange, H. C., & Heijnen, J. J. (2001). Statistical reconciliation of the elemental and molecular biomass composition of Saccharomyces cerevisiae. *Biotechnology and Bioengineering*, *75*(3), 334–344. https://doi.org/10.1002/bit.10054

Lapointe, C. P., Wilinski, D., Saunders, H. A. J., & Wickens, M. (2015). Protein-RNA networks revealed through covalent RNA marks. *Nature Methods*, *12*(12), 1163–1170. https://doi.org/10.1038/nmeth.3651

Larsson, V. J., Jafferali, M. H., Vijayaraghavan, B., Figueroa, R. A., & Hallberg, E. (2018). Mitotic spindle assembly and γ-tubulin localisation depend on the integral nuclear membrane protein Samp1. *Journal of Cell Science*, *131*(8). https://doi.org/10.1242/jcs.211664

Lavut, A., & Raveh, D. (2012). Sequestration of highly expressed mRNAs in cytoplasmic granules, P-bodies, and stress granules enhances cell viability. *PLoS Genetics*, *8*(2), e1002527. https://doi.org/10.1371/journal.pgen.1002527

Lee, A. Y., St Onge, R. P., Proctor, M. J., Wallace, I. M., Nile, A. H., Spagnuolo, P. A., Jitkova, Y., Gronda, M., Wu, Y., Kim, M. K., Cheung-Ong, K., Torres, N. P., Spear, E. D., Han, M. K. L., Schlecht, U., Suresh, S., Duby, G., Heisler, L. E., Surendra, A., … Giaever, G. (2014). Mapping the cellular response to small molecules using chemogenomic fitness signatures. *Science (New York, N.Y.)*, *344*(6180), 208–211. https://doi.org/10.1126/science.1250217

Lee, M. G., & Nurse, P. (1987). Complementation used to clone a human homologue of the fission yeast cell cycle control gene cdc2. *Nature*, *327*(6117), 31–35. https://doi.org/10.1038/327031a0

Leibundgut, M., Maier, T., Jenni, S., & Ban, N. (2008). The multienzyme architecture of eukaryotic fatty acid synthases. *Current Opinion in Structural Biology*, *18*(6), 714–725. https://doi.org/10.1016/j.sbi.2008.09.008

Lester, R. L., Withers, B. R., Schultz, M. A., & Dickson, R. C. (2013). Iron, glucose and intrinsic factors alter sphingolipid composition as yeast cells enter stationary

phase. *Biochimica Et Biophysica Acta*, *1831*(4), 726–736. https://doi.org/10.1016/j.bbalip.2012.12.012

Li, W., Laishram, R. S., & Anderson, R. A. (2013). The novel poly(A) polymerase Star-PAP is a signal-regulated switch at the 3'-end of mRNAs. *Advances in Biological Regulation*, *53*(1), 64–76. https://doi.org/10.1016/j.jbior.2012.10.004

Li, X., Rivas, M. P., Fang, M., Marchena, J., Mehrotra, B., Chaudhary, A., Feng, L., Prestwich, G. D., & Bankaitis, V. A. (2002). Analysis of oxysterol binding protein homologue Kes1p function in regulation of Sec14p-dependent protein transport from the yeast Golgi complex. *The Journal of Cell Biology*, *157*(1), 63–77. https://doi.org/10.1083/jcb.200201037

Lillie, S. H., & Pringle, J. R. (1980). Reserve carbohydrate metabolism in Saccharomyces cerevisiae: Responses to nutrient limitation. *Journal of Bacteriology*, *143*(3), 1384–1394. https://doi.org/10.1128/JB.143.3.1384-1394.1980

Lin, Y., Qi, Y., Lu, J., Pan, X., Yuan, D. S., Zhao, Y., Bader, J. S., & Boeke, J. D. (2008). A comprehensive synthetic genetic interaction network governing yeast histone acetylation and deacetylation. *Genes & Development*, *22*(15), 2062–2074. https://doi.org/10.1101/gad.1679508

Lindstrom, K. C., Vary, J. C., Parthun, M. R., Delrow, J., & Tsukiyama, T. (2006). Isw1 functions in parallel with the NuA4 and Swr1 complexes in stress-induced gene repression. *Molecular and Cellular Biology*, *26*(16), 6117–6129. https://doi.org/10.1128/MCB.00642-06

Litsios, A., Huberts, D. H. E. W., Terpstra, H. M., Guerra, P., Schmidt, A., Buczak, K., Papagiannakis, A., Rovetta, M., Hekelaar, J., Hubmann, G., Exterkate, M., Milias-Argeitis, A., & Heinemann, M. (2019). Differential scaling between G1 protein production and cell size dynamics promotes commitment to the cell division cycle in budding yeast. *Nature Cell Biology*, *21*(11), 1382–1392. https://doi.org/10.1038/s41556-019-0413-3

Liu, S., & Pellman, D. (2020). The coordination of nuclear envelope assembly and chromosome segregation in metazoans. *Nucleus (Austin, Tex.)*, *11*(1), 35–52. https://doi.org/10.1080/19491034.2020.1742064

Lloyd, A. C. (2013). The regulation of cell size. *Cell*, *154*(6), 1194–1205. https://doi.org/10.1016/j.cell.2013.08.053

Lomakin, I. B., Xiong, Y., & Steitz, T. A. (2007). The crystal structure of yeast fatty acid synthase, a cellular machine with eight active sites working together. *Cell*, *129*(2), 319–332. https://doi.org/10.1016/j.cell.2007.03.013

Longtine, M. S., McKenzie, A., Demarini, D. J., Shah, N. G., Wach, A., Brachat, A., Philippsen, P., & Pringle, J. R. (1998). Additional modules for versatile and economical PCR-based gene deletion and modification in Saccharomyces cerevisiae. *Yeast (Chichester, England)*, *14*(10), 953–961. https://doi.org/10.1002/(SICI)1097-0061(199807)14:10<953::AID-YEA293>3.0.CO;2-U

Lucena, R., Alcaide-Gavilán, M., Schubert, K., He, M., Domnauer, M. G., Marquer, C., Klose, C., Surma, M. A., & Kellogg, D. R. (2018). Cell Size and Growth Rate

Are Modulated by TORC2-Dependent Signals. *Current Biology: CB*, *28*(2), 196-210.e4. https://doi.org/10.1016/j.cub.2017.11.069

Madsen, C. T., Sylvestersen, K. B., Young, C., Larsen, S. C., Poulsen, J. W., Andersen, M. A., Palmqvist, E. A., Hey-Mogensen, M., Jensen, P. B., Treebak, J. T., Lisby, M., & Nielsen, M. L. (2015). Biotin starvation causes mitochondrial protein hyperacetylation and partial rescue by the SIRT3-like deacetylase Hst4p. *Nature Communications*, *6*, 7726. https://doi.org/10.1038/ncomms8726

Maeda, K., Anand, K., Chiapparino, A., Kumar, A., Poletto, M., Kaksonen, M., & Gavin, A.-C. (2013). Interactome map uncovers phosphatidylserine transport by oxysterol-binding proteins. *Nature*, *501*(7466), 257–261. https://doi.org/10.1038/nature12430

Maitra, N., Hammer, S., Kjerfve, C., Bankaitis, V. A., & Polymenis, M. (2021). Translational control of lipogenesis links protein synthesis and phosphoinositide signaling with nuclear division. *BioRxiv*, 2021.01.03.425130. https://doi.org/10.1101/2021.01.03.425130

Maitra, N., He, C., Blank, H. M., Tsuchiya, M., Schilling, B., Kaeberlein, M., Aramayo, R., Kennedy, B. K., & Polymenis, M. (2020). Translational control of one-carbon metabolism underpins ribosomal protein phenotypes in cell division and longevity. *ELife*, *9*. https://doi.org/10.7554/eLife.53127

Manukyan, A., Abraham, L., Dungrawala, H., & Schneider, B. L. (2011). Synchronization of yeast. *Methods in Molecular Biology (Clifton, N.J.)*, *761*, 173–200. https://doi.org/10.1007/978-1-61779-182-6_12

Masui, Y., & Markert, C. L. (1971). Cytoplasmic control of nuclear behavior during meiotic maturation of frog oocytes. *The Journal of Experimental Zoology*, *177*(2), 129–145. https://doi.org/10.1002/jez.1401770202

Mayer, V. W., Goin, C. J., Arras, C. A., & Taylor-Mayer, R. E. (1992). Comparison of chemically induced chromosome loss in a diploid, triploid, and tetraploid strain of Saccharomyces cerevisiae. *Mutation Research*, *279*(1), 41–48. https://doi.org/10.1016/0165-1218(92)90264-z

McCusker, D., & Kellogg, D. R. (2012). Plasma membrane growth during the cell cycle: Unsolved mysteries and recent progress. *Current Opinion in Cell Biology*, *24*(6), 845–851. https://doi.org/10.1016/j.ceb.2012.10.008

McGee, T. P., Skinner, H. B., Whitters, E. A., Henry, S. A., & Bankaitis, V. A. (1994). A phosphatidylinositol transfer protein controls the phosphatidylcholine content of yeast Golgi membranes. *The Journal of Cell Biology*, *124*(3), 273–287. https://doi.org/10.1083/jcb.124.3.273

Mendenhall, M. D., & Hodge, A. E. (1998). Regulation of Cdc28 cyclin-dependent protein kinase activity during the cell cycle of the yeast Saccharomyces cerevisiae. *Microbiology and Molecular Biology Reviews: MMBR*, *62*(4), 1191–1243.

Méndez-López, I., & Worman, H. J. (2012). Inner nuclear membrane proteins: Impact on human disease. *Chromosoma*, *121*(2), 153–167. https://doi.org/10.1007/s00412-012-0360-2

Meseroll, R. A., & Cohen-Fix, O. (2016). The Malleable Nature of the Budding Yeast Nuclear Envelope: Flares, Fusion, and Fenestrations. *Journal of Cellular Physiology*, *231*(11), 2353–2360. https://doi.org/10.1002/jcp.25355

Mitchell, L., Lambert, J.-P., Gerdes, M., Al-Madhoun, A. S., Skerjanc, I. S., Figeys, D., & Baetz, K. (2008). Functional dissection of the NuA4 histone acetyltransferase reveals its role as a genetic hub and that Eaf1 is essential for complex integrity. *Molecular and Cellular Biology*, *28*(7), 2244–2256. https://doi.org/10.1128/MCB.01653-07

Mitchell, S. F., Jain, S., She, M., & Parker, R. (2013). Global analysis of yeast mRNPs. *Nature Structural & Molecular Biology*, *20*(1), 127–133. https://doi.org/10.1038/nsmb.2468

Mitchison, J. M. (2003). Growth during the cell cycle. *International Review of Cytology*, *226*, 165–258. https://doi.org/10.1016/s0074-7696(03)01004-0

Morris, D. R., & Geballe, A. P. (2000). Upstream open reading frames as regulators of mRNA translation. *Molecular and Cellular Biology*, *20*(23), 8635–8642. https://doi.org/10.1128/mcb.20.23.8635-8642.2000

Mortimer, R. K. (1958). Radiobiological and genetic studies on a polyploid series (haploid to hexaploid) of Saccharomyces cerevisiae. *Radiation Research*, *9*(3), 312–326.

Moseley, J. B., Mayeux, A., Paoletti, A., & Nurse, P. (2009). A spatial gradient coordinates cell size and mitotic entry in fission yeast. *Nature*, *459*(7248), 857–860. https://doi.org/10.1038/nature08074

Moser von Filseck, J., Vanni, S., Mesmin, B., Antonny, B., & Drin, G. (2015). A phosphatidylinositol-4-phosphate powered exchange mechanism to create a lipid gradient between membranes. *Nature Communications*, *6*, 6671. https://doi.org/10.1038/ncomms7671

Mousley, C. J., Tyeryar, K., Ile, K. E., Schaaf, G., Brost, R. L., Boone, C., Guan, X., Wenk, M. R., & Bankaitis, V. A. (2008). Trans-Golgi network and endosome dynamics connect ceramide homeostasis with regulation of the unfolded protein response and TOR signaling in yeast. *Molecular Biology of the Cell*, *19*(11), 4785–4803. https://doi.org/10.1091/mbc.e08-04-0426

Mousley, C. J., Tyeryar, K. R., Vincent-Pope, P., & Bankaitis, V. A. (2007). The Sec14-superfamily and the regulatory interface between phospholipid metabolism and membrane trafficking. *Biochimica Et Biophysica Acta*, *1771*(6), 727–736. https://doi.org/10.1016/j.bbalip.2007.04.002

Mousley, C. J., Yuan, P., Gaur, N. A., Trettin, K. D., Nile, A. H., Deminoff, S. J., Dewar, B. J., Wolpert, M., Macdonald, J. M., Herman, P. K., Hinnebusch, A. G., & Bankaitis, V. A. (2012). A sterol-binding protein integrates endosomal lipid metabolism with TOR signaling and nitrogen sensing. *Cell*, *148*(4), 702–715. https://doi.org/10.1016/j.cell.2011.12.026

Murray, A. W., Solomon, M. J., & Kirschner, M. W. (1989). The role of cyclin synthesis and degradation in the control of maturation promoting factor activity. *Nature*, *339*(6222), 280–286. https://doi.org/10.1038/339280a0

Nasmyth, K. (1996). At the heart of the budding yeast cell cycle. *Trends in Genetics: TIG*, *12*(10), 405–412. https://doi.org/10.1016/0168-9525(96)10041-x

Nasmyth, K. (2001). A prize for proliferation. *Cell*, *107*(6), 689–701. https://doi.org/10.1016/s0092-8674(01)00604-3

Neumann, F. R., & Nurse, P. (2007). Nuclear size control in fission yeast. *The Journal of Cell Biology*, *179*(4), 593–600. https://doi.org/10.1083/jcb.200708054

Newman, H. A., Romeo, M. J., Lewis, S. E., Yan, B. C., Orlean, P., & Levin, D. E. (2005). Gpi19, the Saccharomyces cerevisiae homologue of mammalian PIG-P, is a subunit of the initial enzyme for glycosylphosphatidylinositol anchor biosynthesis. *Eukaryotic Cell*, *4*(11), 1801–1807. https://doi.org/10.1128/EC.4.11.1801-1807.2005

Nile, A. H., Tripathi, A., Yuan, P., Mousley, C. J., Suresh, S., Wallace, I. M., Shah, S. D., Pohlhaus, D. T., Temple, B., Nislow, C., Giaever, G., Tropsha, A., Davis, R. W., St Onge, R. P., & Bankaitis, V. A. (2014). PITPs as targets for selectively interfering with phosphoinositide signaling in cells. *Nature Chemical Biology*, *10*(1), 76–84. https://doi.org/10.1038/nchembio.1389

Novick, P., Field, C., & Schekman, R. (1980). Identification of 23 complementation groups required for post-translational events in the yeast secretory pathway. *Cell*, *21*(1), 205–215. https://doi.org/10.1016/0092-8674(80)90128-2

Nurse, P., & Thuriaux, P. (1980). Regulatory genes controlling mitosis in the fission yeast Schizosaccharomyces pombe. *Genetics*, *96*(3), 627–637.

Nurse, P., Thuriaux, P., & Nasmyth, K. (1976). Genetic control of the cell division cycle in the fission yeast Schizosaccharomyces pombe. *Molecular & General Genetics: MGG*, *146*(2), 167–178. https://doi.org/10.1007/BF00268085

Omura, S. (1976). The antibiotic cerulenin, a novel tool for biochemistry as an inhibitor of fatty acid synthesis. *Bacteriological Reviews*, *40*(3), 681–697.

Pardee, A. B. (1974). A restriction point for control of normal animal cell proliferation. *Proceedings of the National Academy of Sciences of the United States of America*, *71*(4), 1286–1290. https://doi.org/10.1073/pnas.71.4.1286

Park, H. Y., Buxbaum, A. R., & Singer, R. H. (2010). Single mRNA tracking in live cells. *Methods in Enzymology*, *472*, 387–406. https://doi.org/10.1016/S0076-6879(10)72003-6

Parrou, J. L., & François, J. (1997). A simplified procedure for a rapid and reliable assay of both glycogen and trehalose in whole yeast cells. *Analytical Biochemistry*, *248*(1), 186–188. https://doi.org/10.1006/abio.1997.2138

Pedruzzi, I., Bürckert, N., Egger, P., & De Virgilio, C. (2000). Saccharomyces cerevisiae Ras/cAMP pathway controls post-diauxic shift element-dependent transcription through the zinc finger protein Gis1. *The EMBO Journal*, *19*(11), 2569–2579. https://doi.org/10.1093/emboj/19.11.2569

Pelechano, V., Wei, W., & Steinmetz, L. M. (2013). Extensive transcriptional heterogeneity revealed by isoform profiling. *Nature*, *497*(7447), 127–131. https://doi.org/10.1038/nature12121

Phillips, S. E., Vincent, P., Rizzieri, K. E., Schaaf, G., Bankaitis, V. A., & Gaucher, E. A. (2006). The diverse biological functions of phosphatidylinositol transfer proteins in eukaryotes. *Critical Reviews in Biochemistry and Molecular Biology*, *41*(1), 21–49. https://doi.org/10.1080/10409230500519573

Polymenis, M., & Schmidt, E. V. (1997). Coupling of cell division to cell growth by translational control of the G1 cyclin CLN3 in yeast. *Genes & Development*, *11*(19), 2522–2531. https://doi.org/10.1101/gad.11.19.2522

Polymenis, M., & Schmidt, E. V. (1999). Coordination of cell growth with cell division. *Current Opinion in Genetics & Development*, *9*(1), 76–80. https://doi.org/10.1016/s0959-437x(99)80011-2

Price, A. C., Choi, K. H., Heath, R. J., Li, Z., White, S. W., & Rock, C. O. (2001). Inhibition of beta-ketoacyl-acyl carrier protein synthases by thiolactomycin and cerulenin. Structure and mechanism. *The Journal of Biological Chemistry*, *276*(9), 6551–6559. https://doi.org/10.1074/jbc.M007101200

Ramachandran, V., Shah, K. H., & Herman, P. K. (2011). The cAMP-dependent protein kinase signaling pathway is a key regulator of P body foci formation. *Molecular Cell*, *43*(6), 973–981. https://doi.org/10.1016/j.molcel.2011.06.032

Reed, S. I. (1980). The selection of S. cerevisiae mutants defective in the start event of cell division. *Genetics*, *95*(3), 561–577.

Ren, J., Pei-Chen Lin, C., Pathak, M. C., Temple, B. R. S., Nile, A. H., Mousley, C. J., Duncan, M. C., Eckert, D. M., Leiker, T. J., Ivanova, P. T., Myers, D. S., Murphy, R. C., Brown, H. A., Verdaasdonk, J., Bloom, K. S., Ortlund, E. A.,

Neiman, A. M., & Bankaitis, V. A. (2014). A phosphatidylinositol transfer protein integrates phosphoinositide signaling with lipid droplet metabolism to regulate a developmental program of nutrient stress-induced membrane biogenesis. *Molecular Biology of the Cell*, *25*(5), 712–727. https://doi.org/10.1091/mbc.E13-11-0634

Ricciardi, S., Manfrini, N., Alfieri, R., Calamita, P., Crosti, M. C., Gallo, S., Müller, R., Pagani, M., Abrignani, S., & Biffo, S. (2018). The Translational Machinery of Human CD4+ T Cells Is Poised for Activation and Controls the Switch from Quiescence to Metabolic Remodeling. *Cell Metabolism*, *28*(6), 961. https://doi.org/10.1016/j.cmet.2018.09.010

Rigby, L., Muscat, A., Ashley, D., & Algar, E. (2012). Methods for the analysis of histone H3 and H4 acetylation in blood. *Epigenetics*, *7*(8), 875–882. https://doi.org/10.4161/epi.20983

Rivas, M. P., Kearns, B. G., Xie, Z., Guo, S., Sekar, M. C., Hosaka, K., Kagiwada, S., York, J. D., & Bankaitis, V. A. (1999). Pleiotropic alterations in lipid metabolism in yeast sac1 mutants: Relationship to "bypass Sec14p" and inositol auxotrophy. *Molecular Biology of the Cell*, *10*(7), 2235–2250. https://doi.org/10.1091/mbc.10.7.2235

Robert, L. (2015). Size sensors in bacteria, cell cycle control, and size control. *Frontiers in Microbiology*, *6*, 515. https://doi.org/10.3389/fmicb.2015.00515

Rubbini, S., Cocco, L., Manzoli, L., Lutterman, J., Billi, A. M., Matteucci, A., & Wirtz, K. W. (1997). Phosphoinositide signalling in nuclei of Friend cells: DMSO-

induced differentiation reduces the association of phosphatidylinositol-transfer protein with the nucleus. *Biochemical and Biophysical Research Communications*, *230*(2), 302–305. https://doi.org/10.1006/bbrc.1996.5950

Saitoh, S., Takahashi, K., Nabeshima, K., Yamashita, Y., Nakaseko, Y., Hirata, A., & Yanagida, M. (1996). Aberrant mitosis in fission yeast mutants defective in fatty acid synthetase and acetyl CoA carboxylase. *The Journal of Cell Biology*, *134*(4), 949–961. https://doi.org/10.1083/jcb.134.4.949

Sanchez-Alvarez, M., Zhang, Q., Finger, F., Wakelam, M. J. O., & Bakal, C. (2015). Cell cycle progression is an essential regulatory component of phospholipid metabolism and membrane homeostasis. *Open Biology*, *5*(9), 150093. https://doi.org/10.1098/rsob.150093

Santos-Rosa, H., Leung, J., Grimsey, N., Peak-Chew, S., & Siniossoglou, S. (2005). The yeast lipin Smp2 couples phospholipid biosynthesis to nuclear membrane growth. *The EMBO Journal*, *24*(11), 1931–1941. https://doi.org/10.1038/sj.emboj.7600672

Scaffidi, P., & Misteli, T. (2006). Lamin A-dependent nuclear defects in human aging. *Science (New York, N.Y.)*, *312*(5776), 1059–1063. https://doi.org/10.1126/science.1127168

Scaglia, N., Tyekucheva, S., Zadra, G., Photopoulos, C., & Loda, M. (2014). De novo fatty acid synthesis at the mitotic exit is required to complete cellular division. *Cell Cycle (Georgetown, Tex.)*, *13*(5), 859–868. https://doi.org/10.4161/cc.27767

Schaaf, G., Ortlund, E. A., Tyeryar, K. R., Mousley, C. J., Ile, K. E., Garrett, T. A., Ren, J., Woolls, M. J., Raetz, C. R. H., Redinbo, M. R., & Bankaitis, V. A. (2008). Functional anatomy of phospholipid binding and regulation of phosphoinositide homeostasis by proteins of the sec14 superfamily. *Molecular Cell*, *29*(2), 191–206. https://doi.org/10.1016/j.molcel.2007.11.026

Scharwey, M., Tatsuta, T., & Langer, T. (2013). Mitochondrial lipid transport at a glance. *Journal of Cell Science*, *126*(Pt 23), 5317–5323. https://doi.org/10.1242/jcs.134130

Schmoller, K. M., Turner, J. J., Kõivomägi, M., & Skotheim, J. M. (2015). Dilution of the cell cycle inhibitor Whi5 controls budding-yeast cell size. *Nature*, *526*(7572), 268–272. https://doi.org/10.1038/nature14908

Schneiter, R., Hitomi, M., Ivessa, A. S., Fasch, E. V., Kohlwein, S. D., & Tartakoff, A. M. (1996). A yeast acetyl coenzyme A carboxylase mutant links very-long-chain fatty acid synthesis to the structure and function of the nuclear membrane-pore complex. *Molecular and Cellular Biology*, *16*(12), 7161–7172. https://doi.org/10.1128/mcb.16.12.7161

Schooley, A., Vollmer, B., & Antonin, W. (2012). Building a nuclear envelope at the end of mitosis: Coordinating membrane reorganization, nuclear pore complex assembly, and chromatin de-condensation. *Chromosoma*, *121*(6), 539–554. https://doi.org/10.1007/s00412-012-0388-3

Schulz, T. A., & Prinz, W. A. (2007). Sterol transport in yeast and the oxysterol binding protein homologue (OSH) family. *Biochimica Et Biophysica Acta*, *1771*(6), 769–780. https://doi.org/10.1016/j.bbalip.2007.03.003

Sha, B., Phillips, S. E., Bankaitis, V. A., & Luo, M. (1998). Crystal structure of the Saccharomyces cerevisiae phosphatidylinositol-transfer protein. *Nature*, *391*(6666), 506–510. https://doi.org/10.1038/35179

Shi, L., & Tu, B. P. (2013). Acetyl-CoA induces transcription of the key G1 cyclin CLN3 to promote entry into the cell division cycle in Saccharomyces cerevisiae. *Proceedings of the National Academy of Sciences of the United States of America*, *110*(18), 7318–7323. https://doi.org/10.1073/pnas.1302490110

Shiber, A., Döring, K., Friedrich, U., Klann, K., Merker, D., Zedan, M., Tippmann, F., Kramer, G., & Bukau, B. (2018). Cotranslational assembly of protein complexes in eukaryotes revealed by ribosome profiling. *Nature*, *561*(7722), 268–272. https://doi.org/10.1038/s41586-018-0462-y

Shulman, R. W., Hartwell, L. H., & Warner, J. R. (1973). Synthesis of ribosomal proteins during the yeast cell cycle. *Journal of Molecular Biology*, *73*(4), 513–525. https://doi.org/10.1016/0022-2836(73)90097-1

Siniossoglou, S. (2013). Phospholipid metabolism and nuclear function: Roles of the lipin family of phosphatidic acid phosphatases. *Biochimica Et Biophysica Acta*, *1831*(3), 575–581. https://doi.org/10.1016/j.bbalip.2012.09.014

Slater, M. L. (1973). Effect of reversible inhibition of deoxyribonucleic acid synthesis on the yeast cell cycle. *Journal of Bacteriology*, *113*(1), 263–270. https://doi.org/10.1128/JB.113.1.263-270.1973

Slater, M. L. (1974). Recovery of yeast from transient inhibition of DNA synthesis. *Nature*, *247*(5439), 275–276. https://doi.org/10.1038/247275a0

Smith, S., & Blobel, G. (1994). Colocalization of vertebrate lamin B and lamin B receptor (LBR) in nuclear envelopes and in LBR-induced membrane stacks of the yeast Saccharomyces cerevisiae. *Proceedings of the National Academy of Sciences of the United States of America*, *91*(21), 10124–10128. https://doi.org/10.1073/pnas.91.21.10124

Snider, C. E., Willet, A. H., Chen, J.-S., Arpağ, G., Zanic, M., & Gould, K. L. (2017). Phosphoinositide-mediated ring anchoring resists perpendicular forces to promote medial cytokinesis. *The Journal of Cell Biology*, *216*(10), 3041–3050. https://doi.org/10.1083/jcb.201705070

Soifer, I., Robert, L., & Amir, A. (2016). Single-Cell Analysis of Growth in Budding Yeast and Bacteria Reveals a Common Size Regulation Strategy. *Current Biology: CB*, *26*(3), 356–361. https://doi.org/10.1016/j.cub.2015.11.067

Soma, S., Yang, K., Morales, M. I., & Polymenis, M. (2014). Multiple metabolic requirements for size homeostasis and initiation of division in Saccharomyces cerevisiae. *Microbial Cell (Graz, Austria)*, *1*(8), 256–266. https://doi.org/10.15698/mic2014.08.160

Sonenberg, N., & Hinnebusch, A. G. (2009). Regulation of translation initiation in eukaryotes: Mechanisms and biological targets. *Cell*, *136*(4), 731–745. https://doi.org/10.1016/j.cell.2009.01.042

Spellman, P. T., Sherlock, G., Zhang, M. Q., Iyer, V. R., Anders, K., Eisen, M. B., Brown, P. O., Botstein, D., & Futcher, B. (1998). Comprehensive identification of cell cycle-regulated genes of the yeast Saccharomyces cerevisiae by microarray hybridization. *Molecular Biology of the Cell*, *9*(12), 3273–3297. https://doi.org/10.1091/mbc.9.12.3273

Spriggs, K. A., Bushell, M., & Willis, A. E. (2010). Translational regulation of gene expression during conditions of cell stress. *Molecular Cell*, *40*(2), 228–237. https://doi.org/10.1016/j.molcel.2010.09.028

Stefan, C. J., Manford, A. G., Baird, D., Yamada-Hanff, J., Mao, Y., & Emr, S. D. (2011). Osh proteins regulate phosphoinositide metabolism at ER-plasma membrane contact sites. *Cell*, *144*(3), 389–401. https://doi.org/10.1016/j.cell.2010.12.034

Steffen, K. K., Kennedy, B. K., & Kaeberlein, M. (2009). Measuring replicative life span in the budding yeast. *Journal of Visualized Experiments: JoVE*, *28*. https://doi.org/10.3791/1209

Storck, E. M., Özbalci, C., & Eggert, U. S. (2018). Lipid Cell Biology: A Focus on Lipids in Cell Division. *Annual Review of Biochemistry*, *87*, 839–869. https://doi.org/10.1146/annurev-biochem-062917-012448

Strahl, T., Hama, H., DeWald, D. B., & Thorner, J. (2005). Yeast phosphatidylinositol 4-kinase, Pik1, has essential roles at the Golgi and in the nucleus. *The Journal of Cell Biology*, *171*(6), 967–979. https://doi.org/10.1083/jcb.200504104

Stumpf, C. R., Moreno, M. V., Olshen, A. B., Taylor, B. S., & Ruggero, D. (2013). The translational landscape of the mammalian cell cycle. *Molecular Cell*, *52*(4), 574–582. https://doi.org/10.1016/j.molcel.2013.09.018

Surana, U., Robitsch, H., Price, C., Schuster, T., Fitch, I., Futcher, A. B., & Nasmyth, K. (1991). The role of CDC28 and cyclins during mitosis in the budding yeast S. cerevisiae. *Cell*, *65*(1), 145–161. https://doi.org/10.1016/0092-8674(91)90416-v

Swenson, K. I., Farrell, K. M., & Ruderman, J. V. (1986). The clam embryo protein cyclin A induces entry into M phase and the resumption of meiosis in Xenopus oocytes. *Cell*, *47*(6), 861–870. https://doi.org/10.1016/0092-8674(86)90801-9

Swinnen, E., Wanke, V., Roosen, J., Smets, B., Dubouloz, F., Pedruzzi, I., Cameroni, E., De Virgilio, C., & Winderickx, J. (2006). Rim15 and the crossroads of nutrient signalling pathways in Saccharomyces cerevisiae. *Cell Division*, *1*, 3. https://doi.org/10.1186/1747-1028-1-3

Takemoto, A., Kawashima, S. A., Li, J.-J., Jeffery, L., Yamatsugu, K., Elemento, O., & Nurse, P. (2016). Nuclear envelope expansion is crucial for proper chromosomal segregation during a closed mitosis. *Journal of Cell Science*, *129*(6), 1250–1259. https://doi.org/10.1242/jcs.181560

Tanenbaum, M. E., Stern-Ginossar, N., Weissman, J. S., & Vale, R. D. (2015). Regulation of mRNA translation during mitosis. *ELife*, *4*. https://doi.org/10.7554/eLife.07957

Tatsuta, T., Scharwey, M., & Langer, T. (2014). Mitochondrial lipid trafficking. *Trends in Cell Biology*, *24*(1), 44–52. https://doi.org/10.1016/j.tcb.2013.07.011

Terasima, T., & Tolmach, L. J. (1963). Growth and nucleic acid synthesis in synchronously dividing populations of HeLa cells. *Experimental Cell Research*, *30*, 344–362. https://doi.org/10.1016/0014-4827(63)90306-9

Thorburn, R. R., Gonzalez, C., Brar, G. A., Christen, S., Carlile, T. M., Ingolia, N. T., Sauer, U., Weissman, J. S., & Amon, A. (2013). Aneuploid yeast strains exhibit defects in cell growth and passage through START. *Molecular Biology of the Cell*, *24*(9), 1274–1289. https://doi.org/10.1091/mbc.E12-07-0520

Tripathi, A., Martinez, E., Obaidullah, A. J., Lete, M. G., Lönnfors, M., Khan, D., Soni, K. G., Mousley, C. J., Kellogg, G. E., & Bankaitis, V. A. (2019). Functional diversification of the chemical landscapes of yeast Sec14-like phosphatidylinositol transfer protein lipid-binding cavities. *The Journal of Biological Chemistry*, *294*(50), 19081–19098. https://doi.org/10.1074/jbc.RA119.011153

Ungricht, R., & Kutay, U. (2017). Mechanisms and functions of nuclear envelope remodelling. *Nature Reviews. Molecular Cell Biology*, *18*(4), 229–245. https://doi.org/10.1038/nrm.2016.153

Urbani, L., Sherwood, S. W., & Schimke, R. T. (1995). Dissociation of nuclear and cytoplasmic cell cycle progression by drugs employed in cell synchronization. *Experimental Cell Research*, *219*(1), 159–168. https://doi.org/10.1006/excr.1995.1216

Vadia, S., Tse, J. L., Lucena, R., Yang, Z., Kellogg, D. R., Wang, J. D., & Levin, P. A. (2017). Fatty Acid Availability Sets Cell Envelope Capacity and Dictates Microbial Cell Size. *Current Biology: CB*, *27*(12), 1757-1767.e5. https://doi.org/10.1016/j.cub.2017.05.076

van Meer, G., Voelker, D. R., & Feigenson, G. W. (2008). Membrane lipids: Where they are and how they behave. *Nature Reviews. Molecular Cell Biology*, *9*(2), 112–124. https://doi.org/10.1038/nrm2330

Vanderperre, B., Lucier, J.-F., Bissonnette, C., Motard, J., Tremblay, G., Vanderperre, S., Wisztorski, M., Salzet, M., Boisvert, F.-M., & Roucou, X. (2013). Direct detection of alternative open reading frames translation products in human significantly expands the proteome. *PloS One*, *8*(8), e70698. https://doi.org/10.1371/journal.pone.0070698

Vattem, K. M., & Wek, R. C. (2004). Reinitiation involving upstream ORFs regulates ATF4 mRNA translation in mammalian cells. *Proceedings of the National Academy of Sciences of the United States of America*, *101*(31), 11269–11274. https://doi.org/10.1073/pnas.0400541101

Verghese, J., Abrams, J., Wang, Y., & Morano, K. A. (2012). Biology of the heat shock response and protein chaperones: Budding yeast (Saccharomyces cerevisiae) as a

model system. *Microbiology and Molecular Biology Reviews: MMBR*, *76*(2), 115–158. https://doi.org/10.1128/MMBR.05018-11

Vietri, M., Schink, K. O., Campsteijn, C., Wegner, C. S., Schultz, S. W., Christ, L., Thoresen, S. B., Brech, A., Raiborg, C., & Stenmark, H. (2015). Spastin and ESCRT-III coordinate mitotic spindle disassembly and nuclear envelope sealing. *Nature*, *522*(7555), 231–235. https://doi.org/10.1038/nature14408

Vietri, M., & Stenmark, H. (2018). Orchestrating Nuclear Envelope Sealing during Mitosis. *Developmental Cell*, *47*(5), 541–542. https://doi.org/10.1016/j.devcel.2018.11.020

Vilela, C., Linz, B., Rodrigues-Pousada, C., & McCarthy, J. E. (1998). The yeast transcription factor genes YAP1 and YAP2 are subject to differential control at the levels of both translation and mRNA stability. *Nucleic Acids Research*, *26*(5), 1150–1159. https://doi.org/10.1093/nar/26.5.1150

Vuaridel-Thurre, G., Vuaridel, A. R., Dhar, N., & McKinney, J. D. (2020). Computational Analysis of the Mutual Constraints between Single-Cell Growth and Division Control Models. *Advanced Biosystems*, *4*(2), e1900103. https://doi.org/10.1002/adbi.201900103

Walters, A. D., Amoateng, K., Wang, R., Chen, J.-H., McDermott, G., Larabell, C. A., Gadal, O., & Cohen-Fix, O. (2019). Nuclear envelope expansion in budding yeast is independent of cell growth and does not determine nuclear volume. *Molecular Biology of the Cell*, *30*(1), 131–145. https://doi.org/10.1091/mbc.E18-04-0204

Walters, A. D., Bommakanti, A., & Cohen-Fix, O. (2012). Shaping the nucleus: Factors and forces. *Journal of Cellular Biochemistry*, *113*(9), 2813–2821. https://doi.org/10.1002/jcb.24178

Walters, A. D., May, C. K., Dauster, E. S., Cinquin, B. P., Smith, E. A., Robellet, X., D'Amours, D., Larabell, C. A., & Cohen-Fix, O. (2014). The yeast polo kinase Cdc5 regulates the shape of the mitotic nucleus. *Current Biology: CB*, *24*(23), 2861–2867. https://doi.org/10.1016/j.cub.2014.10.029

Wang, C., Schmich, F., Srivatsa, S., Weidner, J., Beerenwinkel, N., & Spang, A. (2018). Context-dependent deposition and regulation of mRNAs in P-bodies. *ELife*, *7*. https://doi.org/10.7554/eLife.29815

Wang, Y., Mousley, C. J., Lete, M. G., & Bankaitis, V. A. (2019). An equal opportunity collaboration between lipid metabolism and proteins in the control of membrane trafficking in the trans-Golgi and endosomal systems. *Current Opinion in Cell Biology*, *59*, 58–72. https://doi.org/10.1016/j.ceb.2019.03.012

Webster, M., Witkin, K. L., & Cohen-Fix, O. (2009). Sizing up the nucleus: Nuclear shape, size and nuclear-envelope assembly. *Journal of Cell Science*, *122*(Pt 10), 1477–1486. https://doi.org/10.1242/jcs.037333

Wei, M., Fabrizio, P., Hu, J., Ge, H., Cheng, C., Li, L., & Longo, V. D. (2008). Life span extension by calorie restriction depends on Rim15 and transcription factors downstream of Ras/PKA, Tor, and Sch9. *PLoS Genetics*, *4*(1), e13. https://doi.org/10.1371/journal.pgen.0040013

Wenz, P., Schwank, S., Hoja, U., & Schüller, H. J. (2001). A downstream regulatory element located within the coding sequence mediates autoregulated expression of the yeast fatty acid synthase gene FAS2 by the FAS1 gene product. *Nucleic Acids Research*, *29*(22), 4625–4632. https://doi.org/10.1093/nar/29.22.4625

Whitters, E. A., Cleves, A. E., McGee, T. P., Skinner, H. B., & Bankaitis, V. A. (1993). SAC1p is an integral membrane protein that influences the cellular requirement for phospholipid transfer protein function and inositol in yeast. *The Journal of Cell Biology*, *122*(1), 79–94. https://doi.org/10.1083/jcb.122.1.79

Witkin, K. L., Chong, Y., Shao, S., Webster, M. T., Lahiri, S., Walters, A. D., Lee, B., Koh, J. L. Y., Prinz, W. A., Andrews, B. J., & Cohen-Fix, O. (2012). The budding yeast nuclear envelope adjacent to the nucleolus serves as a membrane sink during mitotic delay. *Current Biology: CB*, *22*(12), 1128–1133. https://doi.org/10.1016/j.cub.2012.04.022

Wood, E., & Nurse, P. (2013). Pom1 and cell size homeostasis in fission yeast. *Cell Cycle (Georgetown, Tex.)*, *12*(19), 3228–3236. https://doi.org/10.4161/cc.26462

Xie, Z., Fang, M., & Bankaitis, V. A. (2001). Evidence for an intrinsic toxicity of phosphatidylcholine to Sec14p-dependent protein transport from the yeast Golgi complex. *Molecular Biology of the Cell*, *12*(4), 1117–1129. https://doi.org/10.1091/mbc.12.4.1117

Xu, Z., Wei, W., Gagneur, J., Perocchi, F., Clauder-Münster, S., Camblong, J., Guffanti, E., Stutz, F., Huber, W., & Steinmetz, L. M. (2009). Bidirectional promoters

generate pervasive transcription in yeast. *Nature*, *457*(7232), 1033–1037. https://doi.org/10.1038/nature07728

Yang, L., Guan, T., & Gerace, L. (1997). Integral membrane proteins of the nuclear envelope are dispersed throughout the endoplasmic reticulum during mitosis. *The Journal of Cell Biology*, *137*(6), 1199–1210. https://doi.org/10.1083/jcb.137.6.1199

Yang, X., Lau, K.-Y., Sevim, V., & Tang, C. (2013). Design principles of the yeast G1/S switch. *PLoS Biology*, *11*(10), e1001673. https://doi.org/10.1371/journal.pbio.1001673

York, J. D., Odom, A. R., Murphy, R., Ives, E. B., & Wente, S. R. (1999). A phospholipase C-dependent inositol polyphosphate kinase pathway required for efficient messenger RNA export. *Science (New York, N.Y.)*, *285*(5424), 96–100. https://doi.org/10.1126/science.285.5424.96

Zach, R., & Převorovský, M. (2018). The phenomenon of lipid metabolism “cut” mutants. *Yeast (Chichester, England)*, *35*(12), 631–637. https://doi.org/10.1002/yea.3358

Zach, R., Tvaružková, J., Schätz, M., Tupa, O., Grallert, B., & Prevorovský, M. (2018). Mitotic defects in fission yeast lipid metabolism “cut” mutants are suppressed by ammonium chloride. *FEMS Yeast Research*, *18*(6). https://doi.org/10.1093/femsyr/foy064

Zaman, S., Lippman, S. I., Zhao, X., & Broach, J. R. (2008). How Saccharomyces responds to nutrients. *Annual Review of Genetics*, *42*, 27–81. https://doi.org/10.1146/annurev.genet.41.110306.130206

Zapata, J., Dephoure, N., Macdonough, T., Yu, Y., Parnell, E. J., Mooring, M., Gygi, S. P., Stillman, D. J., & Kellogg, D. R. (2014). PP2ARts1 is a master regulator of pathways that control cell size. *The Journal of Cell Biology*, *204*(3), 359–376. https://doi.org/10.1083/jcb.201309119

Zatulovskiy, E., Zhang, S., Berenson, D. F., Topacio, B. R., & Skotheim, J. M. (2020). Cell growth dilutes the cell cycle inhibitor Rb to trigger cell division. *Science (New York, N.Y.)*, *369*(6502), 466–471. https://doi.org/10.1126/science.aaz6213

Zhang, D., & Oliferenko, S. (2013). Remodeling the nuclear membrane during closed mitosis. *Current Opinion in Cell Biology*, *25*(1), 142–148. https://doi.org/10.1016/j.ceb.2012.09.001

Zhang, F., Gaur, N. A., Hasek, J., Kim, S., Qiu, H., Swanson, M. J., & Hinnebusch, A. G. (2008). Disrupting vesicular trafficking at the endosome attenuates transcriptional activation by Gcn4. *Molecular and Cellular Biology*, *28*(22), 6796–6818. https://doi.org/10.1128/MCB.00800-08

Zhang, H., & Siede, W. (2004). Analysis of the budding yeast Saccharomyces cerevisiae cell cycle by morphological criteria and flow cytometry. *Methods in Molecular Biology (Clifton, N.J.)*, *241*, 77–91. https://doi.org/10.1385/1-59259-646-0:77

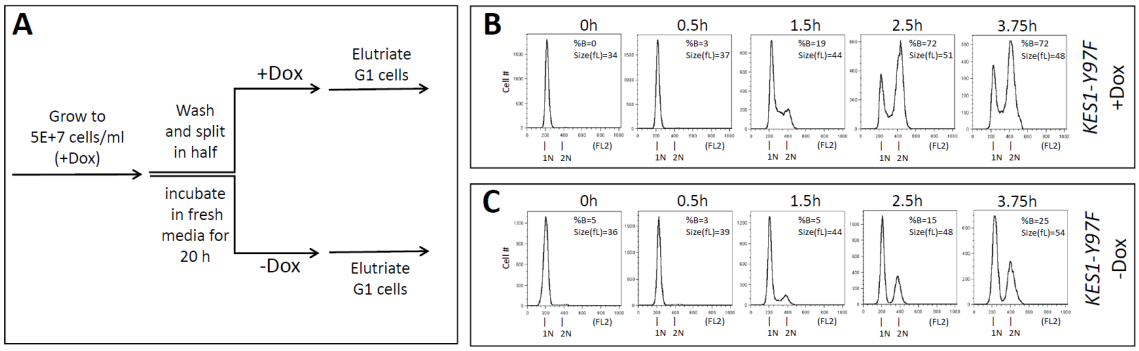

Figure A- 1 Related to Figure 6. Most early G1 cells expressing the gain-of-function *KES1Y97F* allele do not initiate cell division.

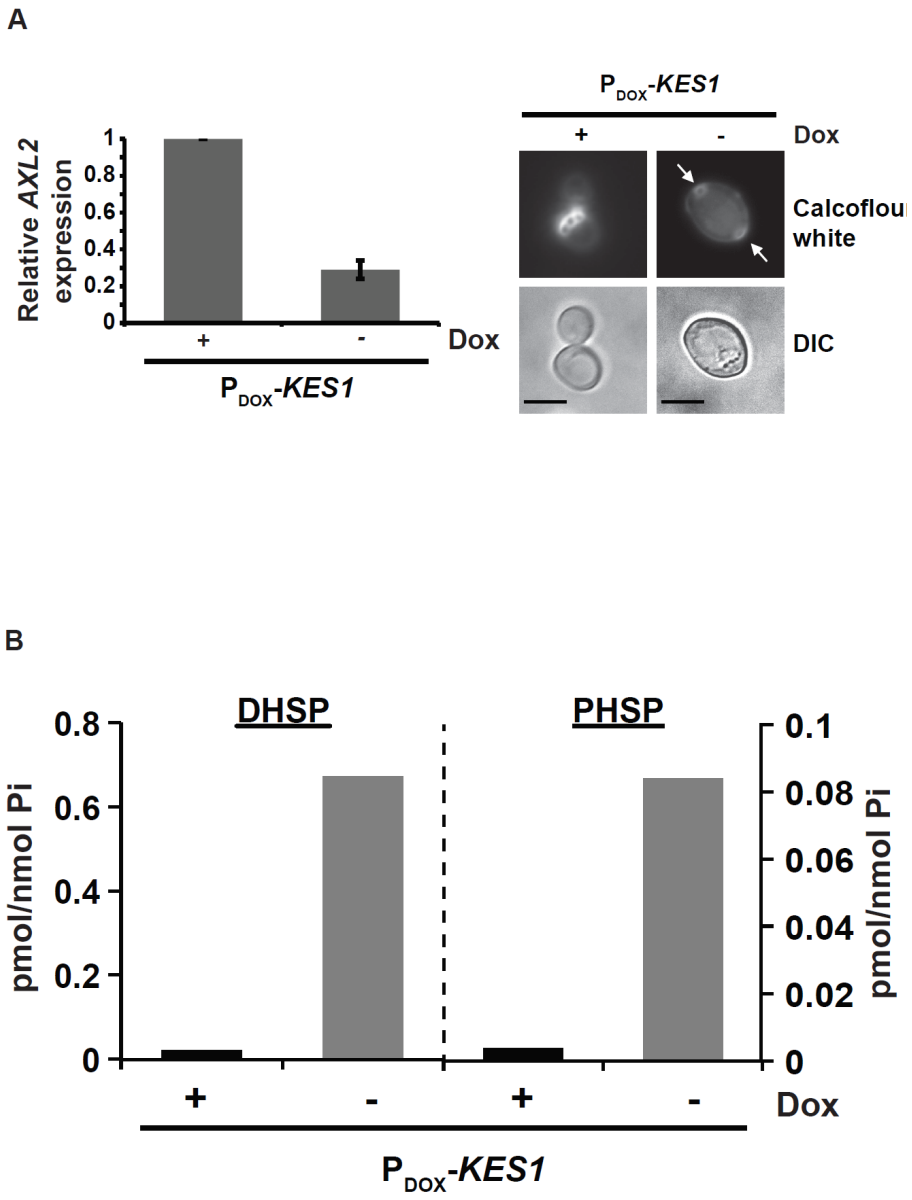

Figure A- 2 Related to Figure 6. Cells with elevated Kes1 activity show signatures of cells activating quiescence programs.

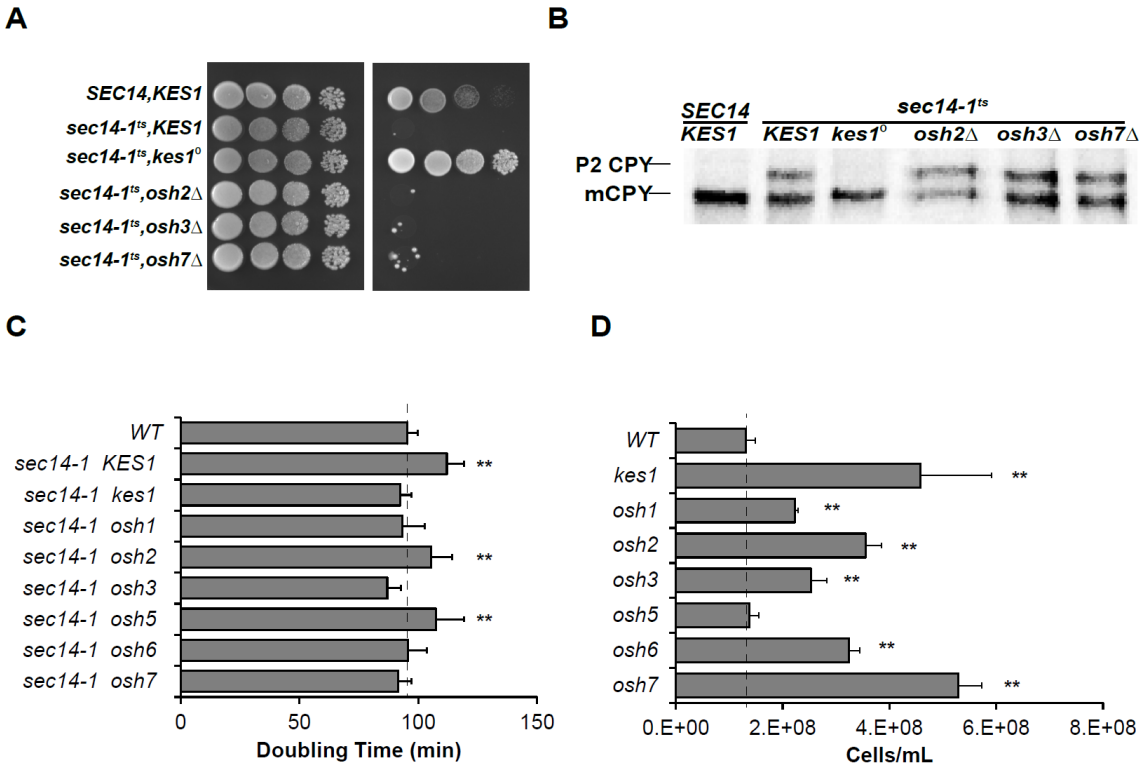

Figure A- 3 Related to Figure 10. Functional specification of yeast ORPs

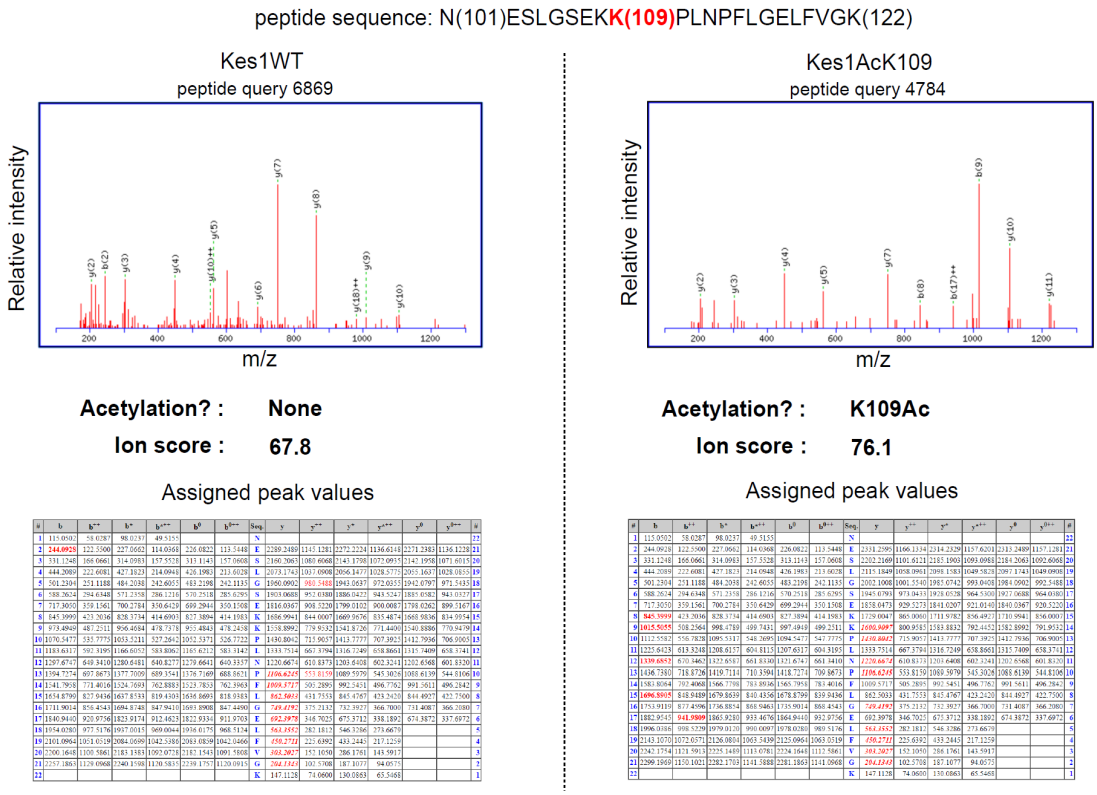

Figure A- 4 Related to Figure 11. Site-specific acetylation of Kes1 residue K109.

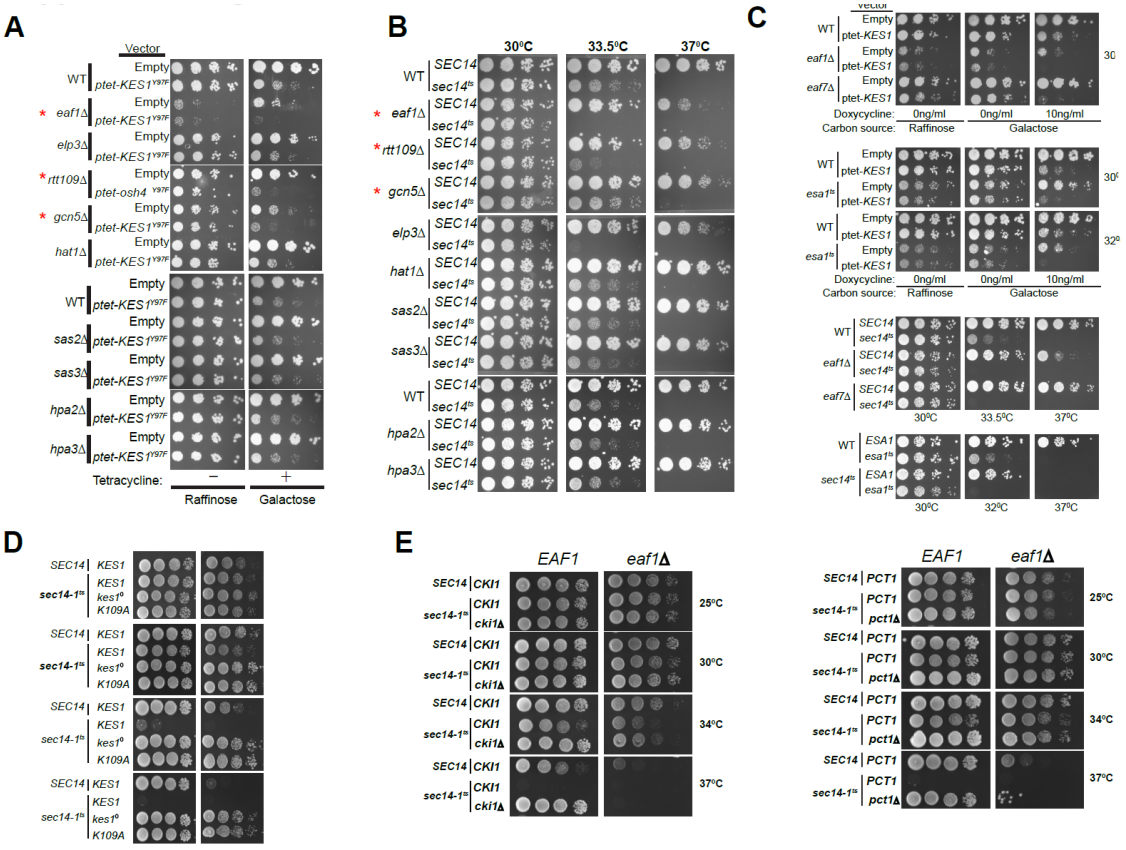

Figure A- 5 Related to Figure 11. Genetic screens for KATs that acetylate Kes1.

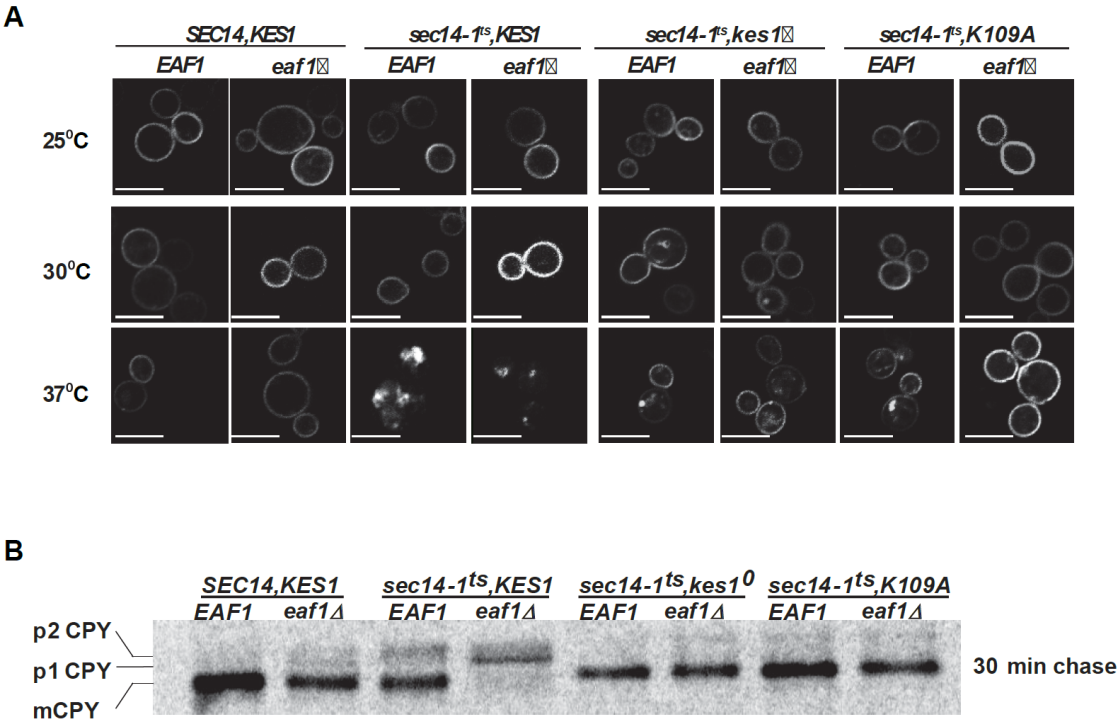

Figure A- 6 Related to Figure 11. NuA4 activity and membrane trafficking.

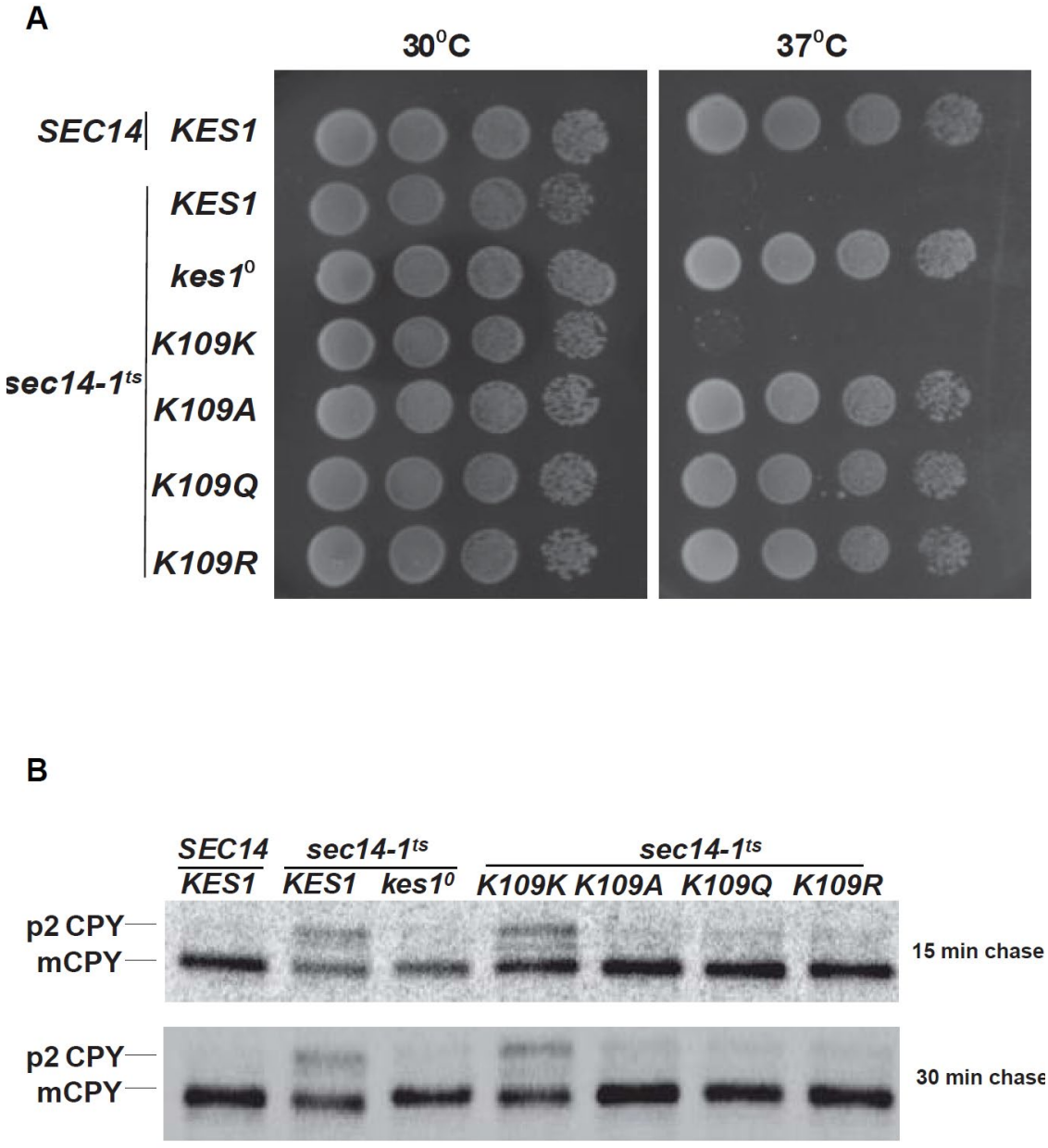

Figure A- 7 Related to Figure 11. K109 missense substitutions and membrane trafficking

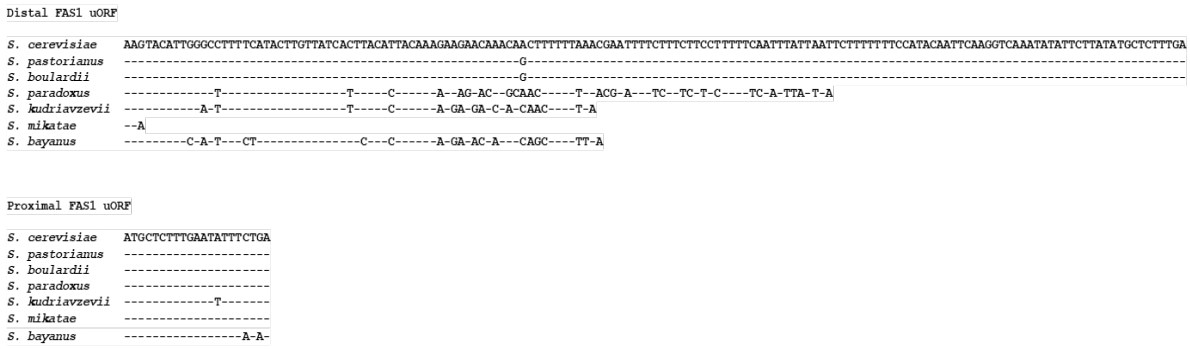

Figure B- 1 Related to Figure 13. Multiple sequence alignment of the *FAS1* uORFs among Saccharomyces species.

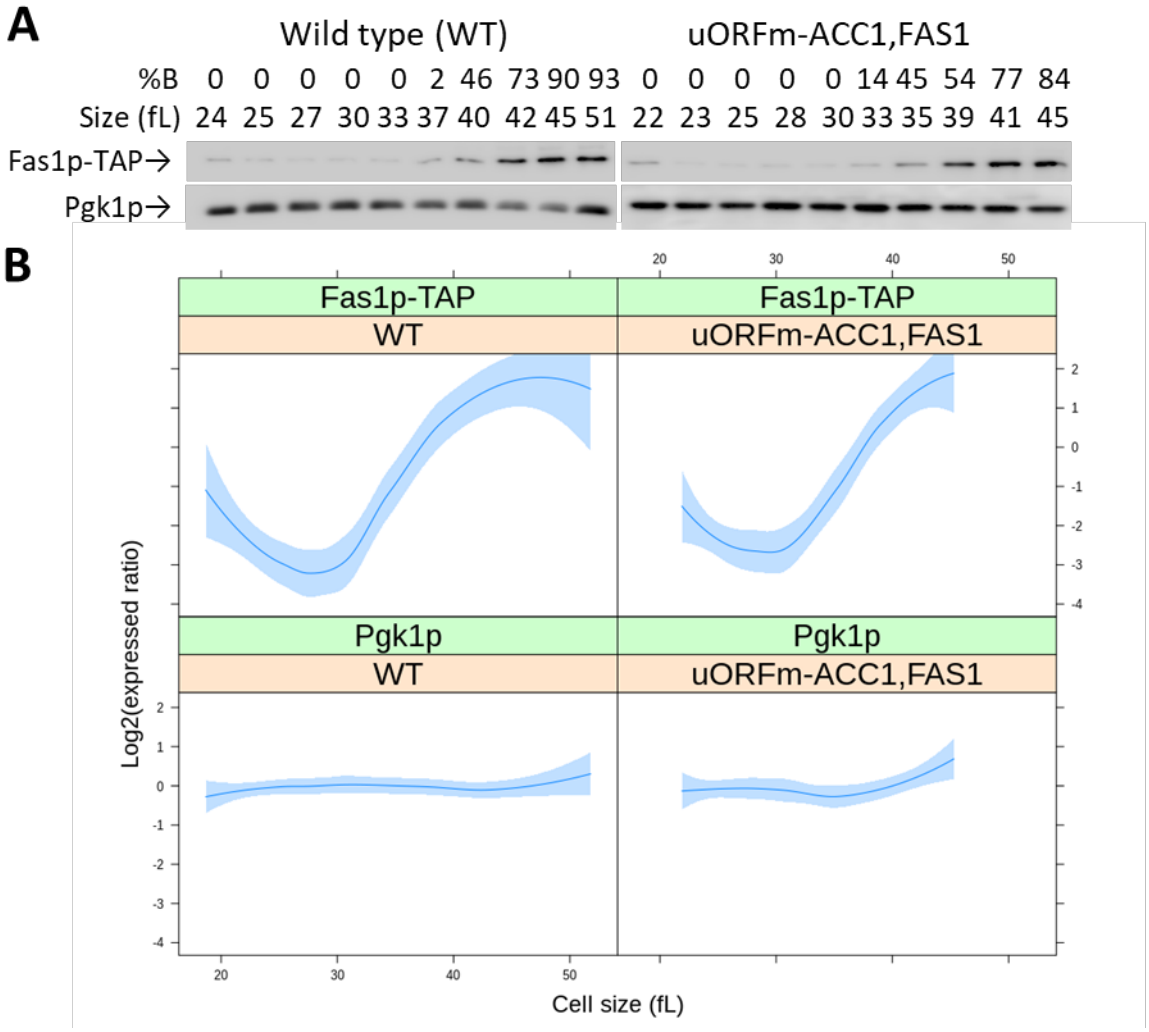

Figure B- 2 Related to Figure 13. Fas1p abundance is periodic in cells lacking the uORFs in *ACC1* and *FAS1*.

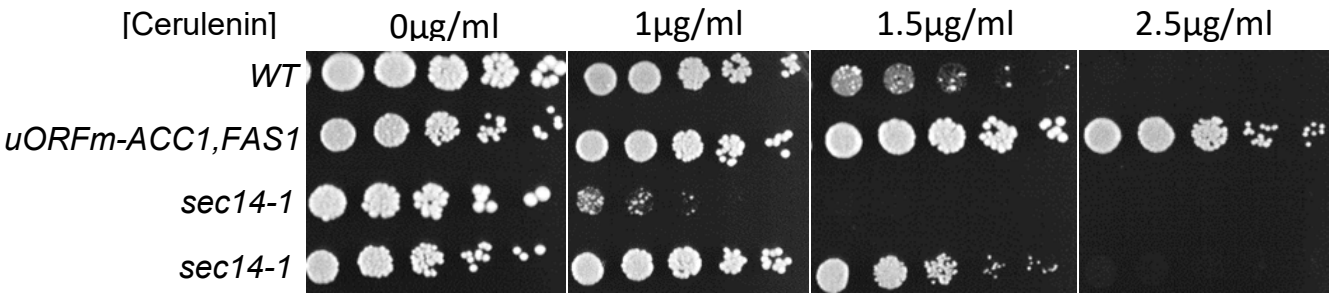

Figure B- 3 Related to Figure 14. Cells lacking the uORFs in *ACC1* and *FAS1* are resistant to cerulenin, a specific FAS inhibitor

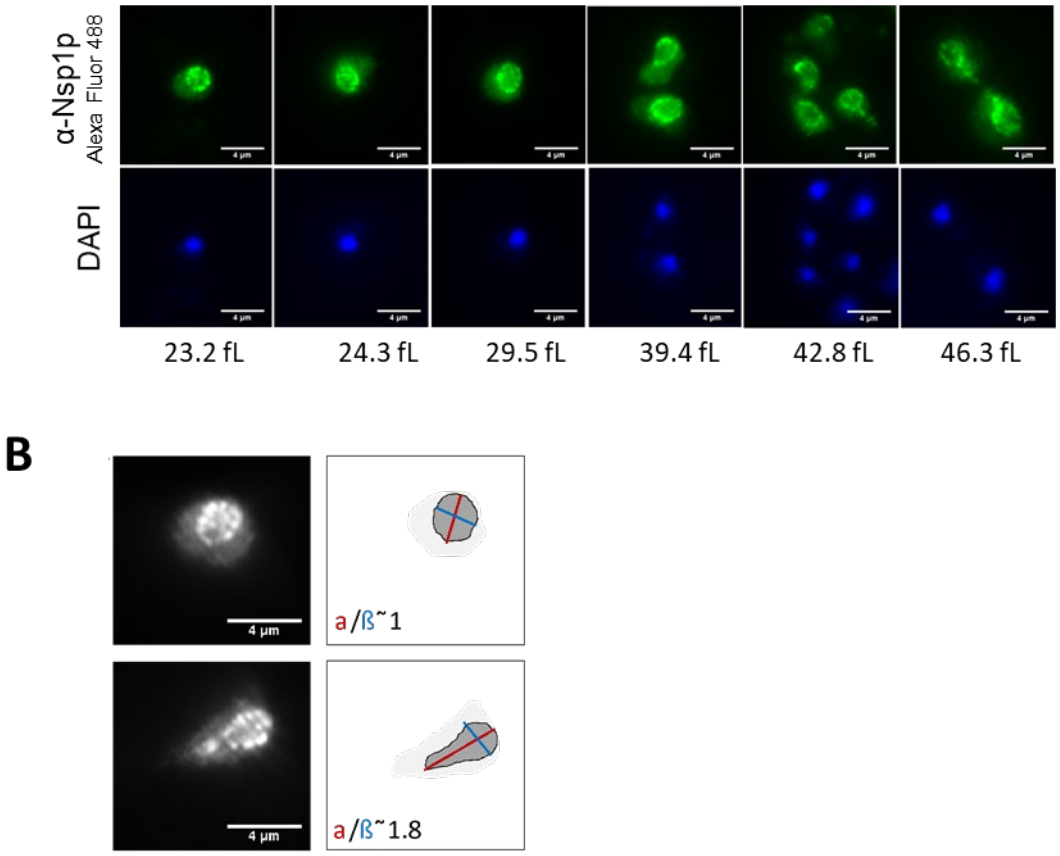

Figure B- 4 Related to Figure 15. Monitoring nuclear morphology

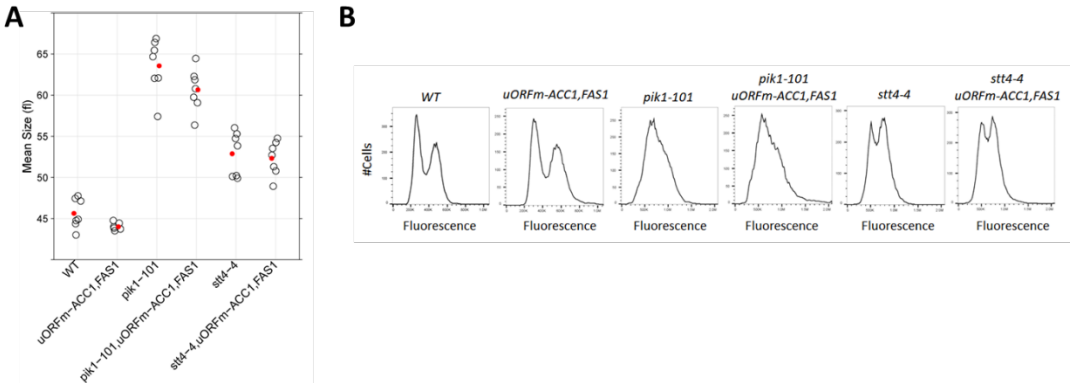

Figure B- 5 Related to Figure 19. Cells lacking Pik1p or Stt4p are large (A) and have a DNA content consistent with a delay in the S-phase (B)

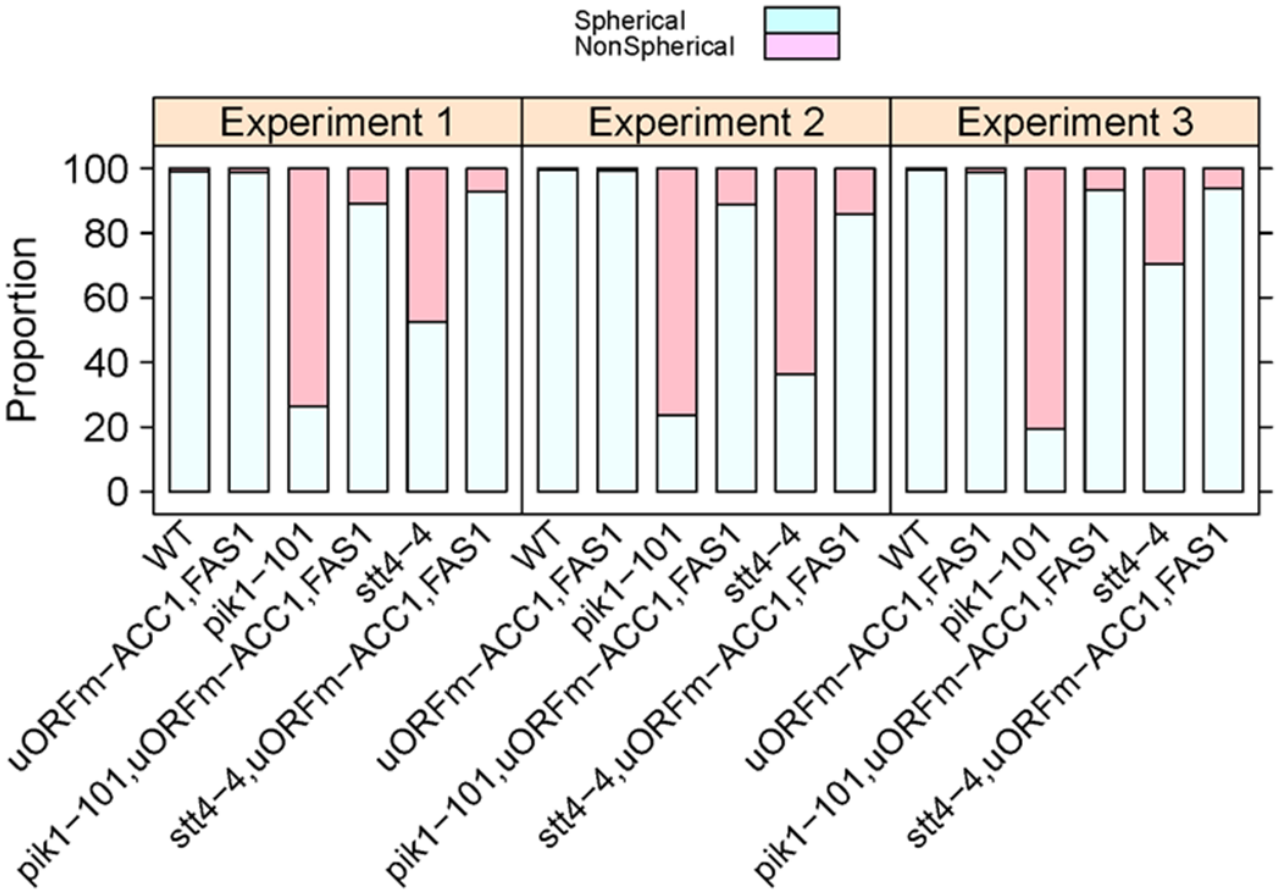

Figure B- 6 Related to Figure 19. Scoring the nuclear shape of PI- 4-kinase mutants, from three independent experiments